The roles of integrin-like proteins, tyrosine phosphorylation and F-actin in hyphal tip growth

A thesis
submitted in partial fulfilment
of the requirements for
the Degree of

Doctor of Philosophy in Biochemistry

in the

University of Canterbury

By

Kanueng Chitcholtan

2005

Table of Contents

Abstract

Tip growth, the mechanism by which hyphae, pollen tubes, root hairs, and algal rhizoids extend, is a complex and dynamic process that is characterised by localised extension at the extreme apex of the cell and morphological polarity. Its complexity suggests that high degree of regulation is needed to ensure that the characteristics of a particular cell type are maintained during growth. Regulation is likely to come about through bidirectional interplay between the cell wall and cytoplasm, although the mechanisms by which such cross-talk might occur are unknown.

Results of this thesis present immunocytochemical data that indicate the presence of, and a close association between β4 integrin subunit-like proteins and proteins containing phosphorylated tyrosine residues in the oomycete *Achlya bisexualis*. When hyphae were plasmolysed, these proteins were present in wall-membrane attachment sites where there was also F-actin. A combination of immunoblots, ELISA, and a coupled enzyme assay suggest that phosphorylation may occur by both autophosphorylation and through the possible action of a tyrosine kinase. Tyrphostins, which are inhibitors of tyrosine kinases, abolished the anti-phosphotyrosine staining, inhibited the kinase activity, slowed tip growth and affected the organisation of the actin cytoskeleton, in a dose-dependent manner. In addition, results show *A. bisexualis* contains proteins epitopically similar to the rod domain of animal talin. However, these proteins do not co-localise with F-actin, and mainly locate at the sub-apical region in hyphae.

For comparative purposes, *Saccharomyces cerevisiae* was also used to investigate the presence of β4 integrin subunit-like proteins and tyrosine phosphorylation. Immunoblotting showed that *S. cereviaise* contains a protein, which is found in the microsomal pellet fraction, that cross reacts with anti-β4 integrin subunit antibody. Furthermore, there are a number of proteins containing phosphotyrosine residues. Immunocytochemistry shows that this anti-β4 integrin staining is at the cortical site but anti-phosphotyrosine residues are distributed throughout cells. On the basis of an ELISA and a coupled enzyme assay, it is suggested that a soluble fraction of *S. cerevisiae* contains tyrosine kinase activity. This activity is strongly inhibited by tyrphostins.

Abbreviations

°C	Degree Celsius
µl	Microlitre
µM	Micromolar
A_{280}	Absorbance at 280 nm
ADP	Adenosine diphosphate
ATP	Adenosine triphosphate
BLAST	Basic Local Alignment Search Tool
BSA	Bovine serum albumin
DMSO	Dimethyl sulphoxide
DTT	Dithiothreitol
EDTA	Ethylenediaminetetraacetic acid
EGTA	Ethylene glycol-bis (β-aminoethyl ether) N, N, N, N,-tetraacetic acid
ELISA	Enzyme-Linked Immunosorbent Assay
g	Grams
HEPES	4-(2-Hydroxyethyl)piperazine-1-ethanesulfonic acid
IgG	Immunoglobulin G
kDa	Kilodalton
L	Litre
mg	Milligram
mins	Minutes
mL	Millilitres
mM	Millimolar
mV	Millivolt
NADH	Nicotinamide adenine dinucleotide
nm	Nanometres
nM	Nanomolar
PAGE	Polyacrylamide gel electrophoresis
PBS	Phosphate buffer saline
PIPES	Piperazine-N,N′-bis(2-ethanesulfonic acid)
PMSF	Phenylmethylsulfonyl fluoride

PYG	Peptone-Yeast extract-Glucose
rpm	Revolutions per minute
S.D.	Standard deviation
SDS	Sodium dodecyl sulfate
v/v	Volume/volume
w/v	Weight/volume
YPD	Yeast extract- Peptone- Dextrose

Acknowledgements

For all his tremendous understanding, supporting, and guidance on many aspects relating to this project, and my life in the present and in the future, I would like to say a big thank you to my supervisor, Ashley Garrill. I also thank Sandra Jackson for contributing her knowledge to this thesis and assisting with confocal microscopic techniques.

I would also like to thank my partner David Anderson for emotional, physical and financial supporting throughout my study.

I would like to thank sexy Craig Galilee for ordering chemicals and many things that I can not remember. Also, this thesis would not be completed without assistance of the spunky Manfred Ingerfeld for helping me with microscopic techniques, so thank you spunky. I also thank Matt Walter for his tremendous assistance and guidance of printing.

Also, this thesis can not be completed without a supporting from my good friends, Sophie Walker, Andy Cox, Nick Cuming, Tracy Putoczki , Hemma Nair, Shane Welsh, Fergus, Sandi, and to all my friends who I can not remember your names.

Chapter 1 : General introduction

1.1 Mechanism of tip growth and cell polarity

Tip growth is a major form of cell growth, characteristic of fungal and oomycete hyphae and plant cells such as root hairs and pollen tubes. The tip growth mechanism is complex and dynamic and includes localised expansion of the apical cell wall and plasma membrane (PM), the migration of the cytoplasm to keep up with the advancing tip, the movement of both organelles and exocytotic vesicles through the apical cytoplasm and the production and maintenance of polarised distributions of membrane proteins such as cell-wall fibril synthases and ion channels (Heath, 2000), (Heath and Skalamera, 2001). These processes lead to a highly polarised cell structure as depicted in Error! Reference source not found.. which shows a hyphal tip of *Achlya bisexualis*. Wall vesicles accumulate at the extreme tip of hyphae. Mitochondria are distributed at just behind the hyphal apex and nuclei are present in more subapical regions.

The hyphal growth of oomycetes, fungi and plant cells is driven by the internal hydrostatic pressure called turgor pressure, the pressure exerted on the plastic wall at the tip causing deformation and thus localised extension at this site. Ray et al., (1972) stated that cell expansion is driven by turgor in the sense that the wall yields to the force exerted by the internal hydrostatic pressure. Turgor pressure is commonly defined as being the pressure exerted on the cell by the turgid protoplasm which is brought about the difference in the osmotic potential of the protoplasm and the external environment (Money, 1997). Hyphal organisms such as oomycetes and fungi encounter and must adapt to variation in the external osmotic potential when they grow in diverse environments. This can affect their ability to take up water during cellular expansion and maintain their internal turgor.

Turgor pressure is a common property of fungi and oomycetes but turgor does not appear to be essential for hyphal growth. Some oomycetes such as *A. bisexualis* and *Saprolegnia ferax* do not regulate turgor after hyperosmotic treatment (Money and Harold, 1992; Lew et al., 2004; Money et al., 2004). In *S. ferax* a variety of structural and developmental events are unaffected by turgor loss. Furthermore, the distribution of F-actin in hyphal apices is not influenced by turgor reduction, nor is hyphal sensitivity to a range of compounds that disrupt the cytoskeleton and cyst germination occurs with normal frequency (Harold et al., 1996). Furthermore, the discovery of a wall-less amoeboid variant of *N. crassa* suggests that even ascomycetes have the innate ability to grow in the absence of turgor (Emerson, 1963), although *N. crassa* can regulate turgor pressure after hyperosmotic treatment. Thus it appears that the true fungi but not oomycetes are able to regulate turgor pressure. This difference may reflect their habitats representing two extremes in terms of osmotic challenge. *N. crassa* is a terrestrial fungus whereas *A. bisexualis* and *S. ferax* are present in fresh water. Thus data would suggest a single model of tip growth driven by turgor pressure may not be sufficient to explain hyphal extension in oomycetes and/or wall-less *N. crassa*.

If the turgor pressure plays a non-essential role in hyphal growth in oomycetes then there may be other processes that function along side turgor pressure. One alternative pathway that hyphae of oomycetes may utilise is the polymerisation of actin. Hyphae of oomycetes and fungi have enrichments of actin located at their extreme tips. Error! Reference source not found.**.B** shows F-actin in the apex of *A. bisexualis* hyphae. This has been used to suggest that actin polymerisation may generate a protrusive force.

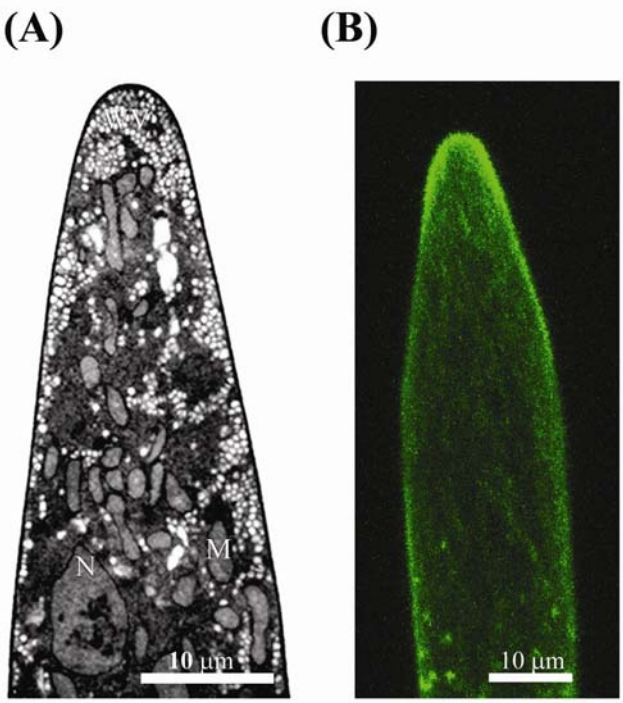

Figure 1.1. Transmission electron micrograph of a chemically fixed hypha of *A. bisexualis* (A). Wall vesicles (WV) are accumulated at the tips. Mitochondria (M) are distributed at the apical region and the nucleus (N) is located in the sub-apical region. The distribution of F-actin in hypha of *A. bisexualis* (B). An actin cap locates at the extreme tip and actin plaques are found in the sub-apical region.

Actin polymerisation is a major force generating system in the expansion of animal cells. The best example is the movement of lamellipodium. **Figure 1.1.** shows the process of ameboid movement that involves the coordination of several components including F-actin, actin-binding proteins, integrins and signalling molecules, such as Ca^{2+}. When animal cells grow on a solid substrate, they are able to move by extension of the leading edge. Actin assembles predominantly at the leading edge because the concentration of uncapped barbed end is high in this region and can be rate limiting for polymerisation (Chen et al., 2000). The uncapped barbed ends can be generated by *de novo* nucleation, severing of existing filaments and removal of barbed ends capping proteins. The actin related protein 2/3 (Arp2/3) plays a crucial role in movement of lamellipodium. The location of the Arp2/3 complex to the leading edge helps to provide the spatial organisation necessary for locomotion. The Arp2/3 complex is activated for actin nucleation by binding to proteins in the Wiscott-Aldrich Syndrome protein family, which are in turn activated by Cdc42 (Chen et al., 2000; Pantaloni et al., 2001). The details of actin polymerisation are addressed further in chapter 4.

Several lines of evidence suggest that the growing hyphal tip may have some similarity with lamellipodia/amoeboid movements in animal cells. Some oomycete zoospore appear to escape from their sporangia by an amoeboid process (Gay and Greenwood, 1966). When secondary zoospores of *Saprolegnia* leave the germ tubes of the primary cysts, they seem to do so by amoeboid movement against the germ tube wall (Holloway and Heath, 1977a). Probably the most compelling argument for amoeboid based tip growth studies in the *slime* mutants of the fungus *Neurospora*. This mutant fails to produce a cell wall and thereby is devoid of turgor but they can proliferate in osmotically buffered media as protoplasts. The protoplasts can move across solid substrate like amoebae by producing tubular pseudopodia (Trevithick and Galsworthy, 1977). In common with lamellipodia/amoeboid movement this movement depends on substrate adhesion. The process is thus likely to involve adhesion molecules such as integrins, located at the plasma membrane.

(A)

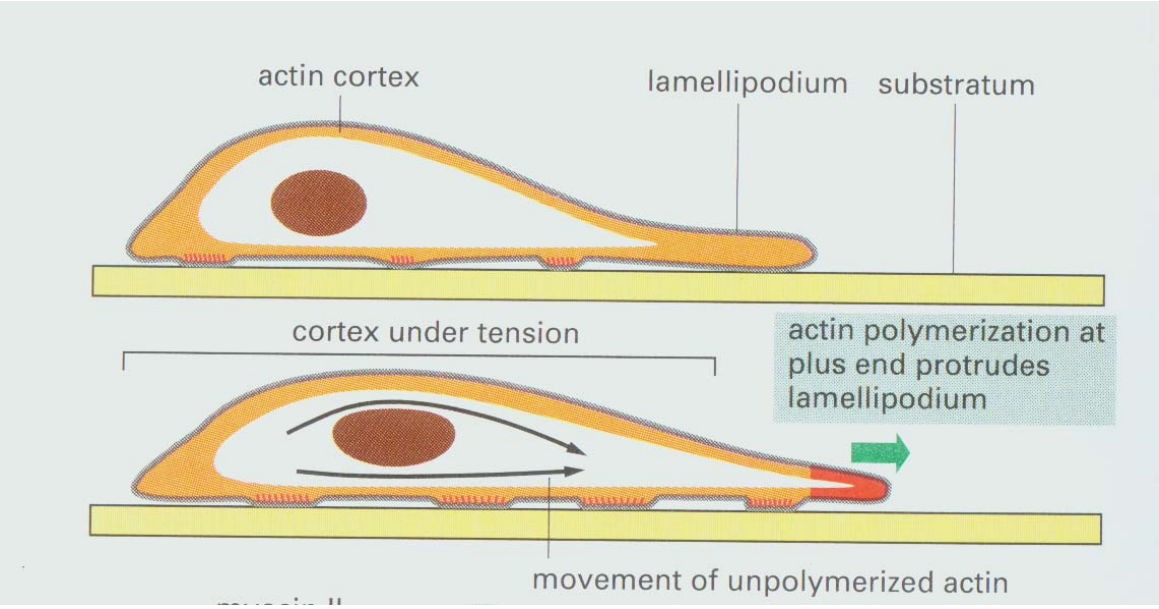

(B)

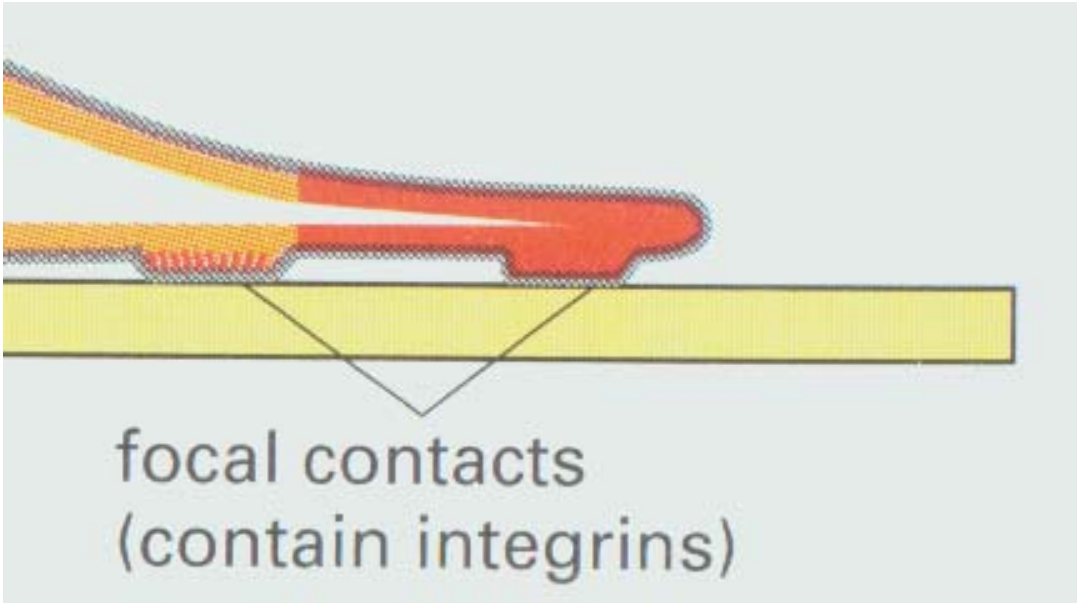

Figure 1.1. Representation of involvement of F-actin and integrins in movement of lamellipodium (from Alberts et al., 2004, Molecular Biology of the Cell 4th Edition).

1.2 Integrins

Integrins are heterodimers of α and β subunits that consist of an extracellular domain that is responsible for ligand binding and a cytoplasmic domain that plays a vital role in signalling processes and protein-protein interactions at focal contacts and hemidesmosomes. Each individual subunit has a large amino terminal consisting of more than 700 residues forming the extracellular domain, and a cytoplasmic domain that in most cases consists of 20-70 residues. One exception is the cytoplasmic domain of the β4 subunit that contains 1000 amino acid residues (Error! Reference source not found.**.** A and B). Integrins play a vital role in many processes including cell adhesion, cell migration, the control of cell differentiation, proliferation and programmed cell death. They are able to convey signals from the outside of the cell to the inside and conversely from the inside to the outside. These phenomena referred to as bidirectional signalling.

1.2.1 *Structure of integrins*

There are 8 known β subunits and 18 known α subunits that are combined to form 24 distinct integrins. A hallmark of the integrins is the ability of individual family members to recognise multiple ligands. Error! Reference source not found.**.** summarises the members of integrins and the ligands that they interact with. The list includes a large number of extracellular matrix proteins reflecting the primary function of integrins in cell adhesion to extracellular matrices (Plow et al., 2000). Integrin-ligand interactions are determined by several factors. One major determinant of ligand binding specificity is the subunit composition of an integrin. One half of the integrin α subunits contain an extra von Willebrand factor A-type domain (αA or I domain) and are known as αA domains see Error! Reference source not found.**B** (Arnaout et al., 2002). A single bound divalent cation is found at the apex of αA, coordinated by oxygen containing side chains from three loops, one containing an Asp-X-Ser-X-Ser motif (where X is any amino acid), the second an invariant threonine and the third an invariant aspartic acid. These residues are referred as the metal-ion-dependent adhesion site (MIDAS) motif (Emsley et al., 2000).

In αA lacking integrins, ligand binding is mediated by a predicted β-propeller domain from the α subunit and a predicted αA-like domain (βA) from the β subunit (Humphries et al., 2003).

The MIDAS motif of αA binds Mn^{2+} or Mg^{2+} with high (micromolar) affinity and Ca^{2+} with low (millimolar) affinity. Three additional metal-binding regions were predicted in the extracellular segment of integrins: one in βA, another in the EF-hand-like sequence at the bottom of the propeller and the third in the propeller's central core (Arnaout et al., 2002). The β subunit contains eight domains. A βA domain contacts the top of the subunit's propeller, thus forming the αβ heterodimers. The βA projects from an I-set immunoglobulin-like "hybrid" domain. Both the βA and hybrid domains contribute to the head region (Liddington, 2002). The β leg section is formed of six domains: an amino terminal PSI (plexins, semaphorins and integrins) domain lies at the base of the hybrid domain and is probably linked to the first of four epidermal growth factor (EGF) domains by a disulfide bond. PSI, EGF1 and EGF2 domains are disordered. EGF3 and EGF4 each contains a core of six cysteine residues linked in a Cys1-Cys3, Cys2-Cys4, Cys5-Cys6 pattern (Arnaout et al., 2002). The structure determined by Xiong et al., (2001) was obtained in a Ca^{2+} buffer and lacked bound ligand. This condition usually produces inactive integrins. Subsequent structures obtained after diffusing cycloRGDF and Mn^{2+} into the crystal showed cycloRGDF bound at the αβ interface with the arginine residue binding the propeller domain of the α subunit and the aspartate joining the coordination sphere of a Mn^{2+} ion bound at the MIDAS site (Xiong et al., 2002).

Table 1.1. Combinations of possible integrin subunits and their protein ligands (Plow et al., 2000)

	Subunits	Ligands
β1	α1	Collagens, Laminins
	α2	Collagens, Laminins
	α3	Laminins, Fibronectin, Thrombospondin
	α4	Fibronectin, VCAM
	α5	Fibronectin
	α6	Laminins
	α7	Laminins
	α8	Fibronectin, Tenascin
	α9	Tenascin
	α10	Collagens
	α11	Collagens
	αv	Fibronectin, Vitronectin
β2	αL	ICAMs
	αM	Fibrinogen, ICAMs, iC3b
	αX	Fibrinogen, ic3B
	αD	VCAM, ICAMs
β3	αIib	Collagens, Fibronectin, Vitronectin, Fibrinogen, Thrombospondin
	αv	Fibronectin, Vitronectin, Fibrinogen, Thrombospondin
β4	α6	Laminins
β5	αv	Vitronectin
β6	αv	Fibronectin, Tenascin
β7	α4	Fibronectin, VCAM, MAdCAM
	αE	E-cadherin
β8	αv	Collagens, Laminins, Fibronectin

(A)

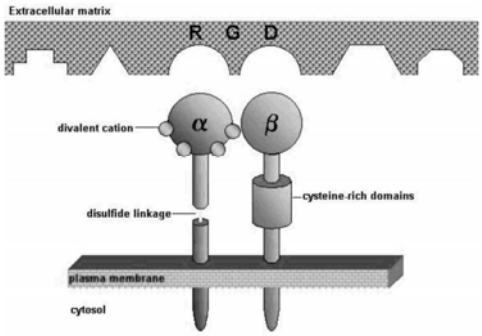

(B)

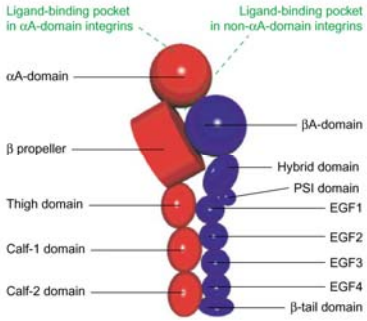

Figure 1.3. Integrins are composed of non-covalent linked α and β subunits that extend out of the plasma membrane (A) (White et al, 2004). Schematic representation of the straightened form of an integrin (B). The α subunit is in red and the β subunit is in blue. The α subunit comprises a β propellar at the top, followed by three β-sandwich modules. Half of the 18 different integrin α subunits contain an A-domain inserted between blades 2 and 3 of the seven-blades β propellar. The β subunit comprises a PSI domain, an A-domain, followed by a β-sandwich hybrid domain, four repeats and a β-tail domain (Humphries et al., 2003).

1.2.2 *Integrin activation: Current model of outside-in and inside-out signalling*

Xiong et al. (2001, 2002) suggested that the bent form is the active form of the integrin. However, others have argued that it is more likely to be an inactive state, based on the details of the conformation of the β-I/A domain and the fact that it was crystallised in the absence of ligand (Shimaoka et al., 2000; Liddington and Ginsberg, 2002). By mapping epitopes for activation specific monoclonal antibodies to specific residues in I-EGF repeats 2 and 3, it has been shown that these residues would be buried in the bent form of the integrin (Beglova et al., 2002). Beglova et al, (2002) proposed that the bent form represents the inactive state and that activation occurs by a "switch-blade" opening of the integrin into an extended shape and a separation of the legs. Such a conformational change could expose the epitopes for activation-specific antibodies, many of which are known to bind to the I-EGF repeats or to the PSI domain.

(Takagi et al., 2002) showed that integrins clamped in the inactive state predominantly adopt a bent shape as seen by electron microscopy (EM), whereas integrins activated by Mn^{2+} or by cycloRGDF were predominantly in an extended form. They showed that the claimed bent form did not bind ligand, whereas the activated extended form did. Finally they presented evidence that integrins on cell surfaces can be trapped in a bent and inactive state by an engineered disulfide bond that when released, allows their activation. These results confirm well with the idea that the bent form seen in the crystal represents the inactive state of the integrin and that activation comprises straightening and separation of the legs. These concepts are schematised in Error! Reference source not found.**.** , which shows two ways in which the bent form might be related to the membrane. These differ in the orientation of the membrane-proximal "ankles" of the legs relative to the membrane; this is unknown at present. In the switch-blade or "flick-knife" model, the "calves" of each leg are perpendicular to the membrane and the head domain is very close to the cell surface. In a variant "angle-poise" model, the legs are bent over closer to the membrane and extend like an angle-poise lamp during activation. The latter model would place the head domain in a better position to interact with macromolecular ligand (Hynes, 2002).

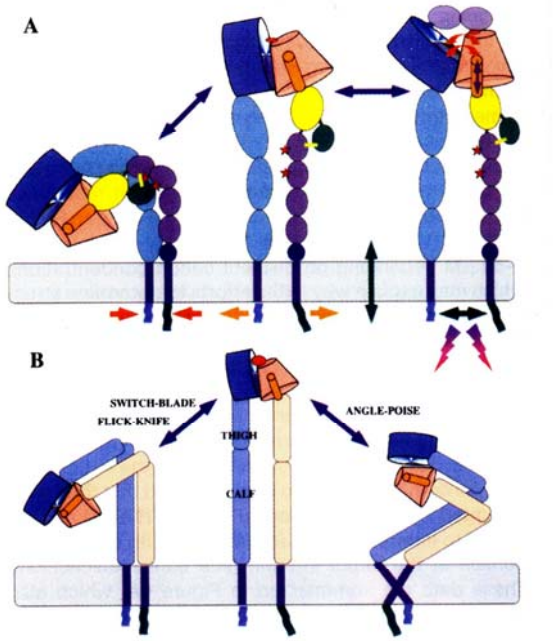

Figure 1.4. Models for long-range allosteric changes giving birectional signaling by integrins. (A) Integrin in its bent form is presumed to be inactive. Activation can occur either by ligand binding or by effect on the cytoplasmic domains, leading to straightening and separation of the legs. Alterations in the orientation of the propeller and I/A domains are coupled to changes in the hybrid domain (yellow) by movement of the C-terminal helix of the I/A domain (orange). The hybrid domain, in turn, is linked to the I-EGF domains (purple) via the PSI domain (green), which is disulfide bonded (yellow line) to the first I-EGF domain. Straightening and separation of the legs exposes activation epitopes in the I-EGF domains (red stars) and in the PSI domain (not shown) Separation of the cytoplasmic domains is accompanied by conformational changes in them, allowing binding of cytoplasmic proteins and signaling. (B) Two models for the proposed straightening up of integrins during activation. The switch-blade or flick-knife model and an alternative angle-poise model differ in the way in which the C termini of the legs relate to the transmembrane segments. The angle-poise model incorporates the possibility that the transmembrane helices may be especially long and could change orientation and/or move in and out of the membrane during activation. The angle-poise model would place the ligand binding site in a more accessible position for macromolecule ligands.

For some time, it has been suggested that the interaction of αβ tails of integrins lead to altered states of integrin activation. (Lu et al., 2001b) replaced the cytoplasmic domains of αL and β2 with acidic and basic peptides that form an α-helical coiled-coil heterodimers, thus clasping the integrin tail region together (**Error! Reference source not found..a**). Expression of these mutated integrin subunits on the surface of cells resulted in cell adhesion molecule 1 (ICAM-1), unless activated externally. If, however, both subunits were expressed with basic coiled-coil domains that do not interact, the cells constitutively bound ligand. A similar approach was taken to study the effect of C-terminal opening on soluble α5β1 activation in the absence of cellular factors (Takagi et al., 2001). This study used integrin that was truncated N-terminally to the transmembrane domain and clasped with the acid-base coiled-coil heterodimeric system (Error! Reference source not found.**.b)**. Enzymatic cleavage of the constraint led to increased fibronectin binding to the soluble integrin, compared with the clasped integrin. In addition, it was shown that activation of integrin by unclasping correlated with an approximate 14 nm separation of the integrin leg regions (Takagi et al., 2001; Travis et al., 2003). This suggests that conformational changes in integrins can account for major affinity changes in integrin irrespective of integrin clustering or avidity changes. These two studies therefore demonstrate that releasing the C-terminal constraint on integrins can mimic 'inside-out' signalling, and suggest that the mechanism of inside-out activation involves the spatial separation of the cytoplasmic and/or transmembrane domains.

A number of intracellular proteins have been reported to bind to integrin cytoplasmic domains, with many influencing integrin function. Such molecules have been implicated in both outside-in and inside-out signaling processes. Several molecules including calcium- and integrin- binding protein (CIB), β3-endonexin, cytohesin-1 and talin, have been shown to bind to integrin β-subunit cytoplasmic tails resulting in activation of the integrin. (O'Toole et al., 1991; O'Toole et al., 1994) have shown that the short cytoplasmic domain of αIIb acts as a negative regulator of activation. A constitutively active integrin could be produced if the entire domain or the highly conserved sequence was deleted. O'Toole et al., (1994) also suggested that the interaction of the cytoplasmic domain of integrins with proteins at focal adhesion sites was a central control point in the

activation process. (Horwitz et al., 1986) found that the talin co-localizes with integrins at focal adhesion sites and possibly forms a link between integrins and the actin cytoskeleton.

(Vinogradova et al., 2002) have proposed a model for the activating properties of talin, which was previously demonstrated to bind to the β3 tail through its N-terminal head domain, leading to integrin activation. (Vinogradova et al., 2002) verified that a fragment of talin could activate αIIbβ3 and also demonstrated that it disrupted the αβ complex observed using NMR. Furthermore, the substantial transferred nuclear overhauser effects (NOEs), which detect protein-protein interactions through space, for the αIIb-β3 mixture was lost in the presence of talin.

The authors concluded that talin effectively competed with the αIIb tail for binding to the β3 tail, thereby disrupting the interaction between the two tails. This mechanism could be controlled at the level of talin because its integrin binding site is masked in the whole molecule. Binding of talin to inositol phospholipids or proteolytic cleavage of talin resulted in unmasking of this integrin binding site (Calderwood et al., 1999; Martel et al., 2001; Yan et al., 2001). The authors therefore suggested a model in which one of a series of agonist signals would result in a conformational change in talin, leading to exposure of its integrin binding site. Subsequent binding of talin to the β3 tail would in turn lead to separation of the integrin tails and integrin activation (Error! Reference source not found.**.**) A recent study has determined the crystal structure of interacting fragments of talin and β3 cytoplasmic domain. The phosphotyrosine binding (PTB)-like domain of talin was found to interact directly with a central motif of the β3 tail, encompassing the NPLY motif (Hynes, 2002).

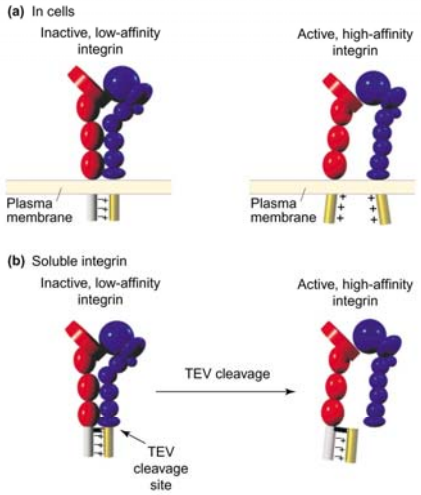

Figure 1.5. Production of integrin constructs that mimic closed and open cytoplasmic domain conformations. (a) The cytoplasmic domains of the αL and β2 subunit were replaced by negative (grey) and positively (gold) charged coiled-coil regions, respectively. This mimicked close proximity of the integrin tails, resulting in an inactive, low-affinity integrin. To open up the complex, the negatively charged coiled-coil region was replaced by a positively charged coil. Electrostatic repulsion mimicked an opening of the cytoplamic domains, resulting in an active, high-affinity integrin.
(b) The transmembrane and cytoplamic of integrin α5β1 were removed to produce a secreted, soluble heterodimer. C-terminal negatively and positively charged coiled-coil regions were used as in (a) but were clasped together by a disulfide bond within this region. A tobacco etch virus (TEV) cleavage site that was introduced above the β1 positive coil allowed release of the coil restraint, mimicking an opening of the cytoplasmic domains. The α- and β-subunit are shown in red and blue, respectively.
For clarity, the A domain of the αL subunit has been omitted (Travis et al., 2003).

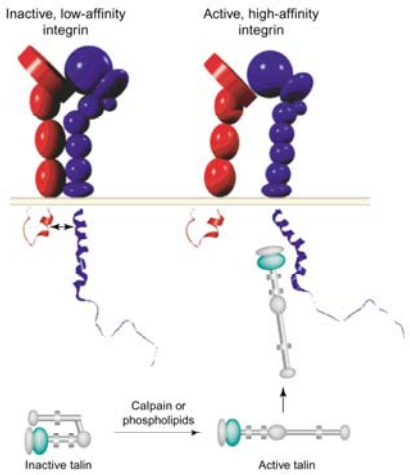

Figure 1.6. Putative model of integrin activation by talin. The inactive integrin has low affinity for the ligand as a result of electrostatic and hydrophobic interactions between the cytoplasmic tails (double-headed arrow). The integrin binding site of talin (green sphere) in the head domain is masked until activation by calpain or phospholipids. Activated talin has a higher affinity for the integrin β3 tail than the αIIb tail and therefore binds to the β3 tail. This disrupts the interactions between the αIIb and β3 tails, leading to integrin separation. The resulting conformational changes in between the integrin subunits lead to integrin activation and integrin ligand binding. The αIIb and β3 subunits are shown in red and blue, respectively (Travis et al., 2003).

1.2.3 *Integrin-like proteins in oomycete and fungi*

The presence of proteins with epitopic similarity to metazoan integrins in oomycetes, fungal and plant cells has been suggested by their cross-reactivity to antibodies raised against animal integrins, so the term of "integrin-like protein" has been used in oomycetes, fungi and plant literature (**Table 1.1.**).

(Kaminskyj and Heath, 1995) found that the filamentous oomycete *Saprolegnia ferax* has integrin-like proteins that are located at the tip. Western blots cross reacted with β_1-integrin antibody and a protein band at 120 kDa was obtained under reducing conditions. However, the failure of RGD-containing peptides to disrupt growth and adhesion in *S. ferax* suggests that either this protein is insensitive to RGD-containing proteins or that it does not play a role in growth or adhesion (Bachewich and Heath, 1997). Preliminary data with *A. bisexualis* however suggests that RGD-containing peptides do inhibit tip extension and affect tip morphology.

Fungi such as *Uromyces* and *Mucor rouxii* have been shown to be sensitive to RGD-containing peptides (Correa et al., 1996; Pereyra et al., 2003). (Degousee et al., 2000) investigated integrin-like proteins in the filamentous ascomycete *N. crassa*, immunofluorescence showed that integrin-like proteins are located at the plasma membrane/cell wall and are enriched at the extreme tip; with more punctuate staining in the subapical region. These authors also found that in western blots a protein band at ~63 kDa cross reacted with the anti-β_1 integrin antibody, presumably corresponding to a fragment of the reduced form of the protein or an integrin homologue. The bean rust *Uromyces appendiculatus* has also been shown to contain integrin-like proteins, which were detected by two different β1 antibodies, one from chicken and the other from human, a similar 95 kDa band was obtained.

With respect to studies on non-filamentous fungi, (Marcantonio and Hynes, 1988) found that anti-integrin β1 directed against the COOH-terminal domain of chicken cross reacted with a 95 kDa protein present in a membrane extract from *C. albicans*, but not from *S. cerevisiae*. (Gale et al., 1996) isolated a gene encoding a putative integrin-like protein in

C. albicans by screening a genomic library with conserved sequences from the transmembrane and cytoplasmic domains of the human αM. These authors found the predicted polypeptide (αInt1p) of 188 kDa which contains several motifs common to αM and αX: a putative I domain, two EF-hand divalent cation-binding site, a transmembrane domain and a cytoplasmic tail with a single tyrosine residue. More recent evidence showed that *C. albicans* has αvβ3 and αvβ5 integrin-like proteins, which recognise vitronectin in vitro. Moreover, the engagement of such integrin-like proteins consequently activates protein tyrosine phosphorylation (Santoni et al., 2002).

Table 1.1. Integrin-like proteins found in fungi and oomycetes.

Species	Antibodies used	Detected molecular weight (kDa)	References
Saccharomyces cerevisiae	β1	none	Marcantonio et al,1988
Candida albicans	β_1	95	Marcantonio et al,1988
Neurospora crassa	β_1	63, 120	Degousée et al,2000
Uromyces appendiculatus	β_1	95	Corrêa et al,1996
Saprolegnia ferax	β_1	120, 178	Kaminskyj et al,1995

1.2.4 *Integrin-like proteins in plants*

In plants, it is apparent that the cell wall plays a key role in both cell-cell communication and the maintenance cell shape. A large number of proteins-associated with the cell wall have been investigated these include WAK-like kinases, cellulose synthases, glucanases, arabinogalactan proteins (AGPs), pectin and glycine-rich protein (GRP) all of which are candidates as wall membrane linkers that could function in cell wall/cytoplasmic communication (Kohorn, 2000). Recently, several lines of evidence have emerged suggesting that plants also contain integrin-like proteins which could also fulfil such a role. Furthermore, integrin-like proteins found in plants have a range of molecular weight similar to those found in animal cells (**Table 1.2**).

(Sun et al., 2000) used confocal microscopy to image antibodies against the αv, β3, and β_1 integrin subunits. These gave prominent staining at the tips of pollen tube in lily and tobacco. These authors previously showed that antibodies raised against the human VnR and against the β_3, and αv integrin subunits cross reacted with proteins in the PM fractions of *Hemerocallis citrina* (Sun et al., 1998). Sun et al (2000) also found that anti-β3, anti-αv and anti-VnR antibodies all recognised a ~150 kDa band in western blots in both *H. citrina* Baroni and in *L. davidii* Duch under non-reducing conditions. However, under reducing condition the anti-β3 antibody also cross reacted with a minor band at 95-97 kDa in *H. citrina* Baroni in addition to a major 150 kDa band.

Other groups have identified putative integrin-like proteins of 100, 58, and 84-116 kDa in plasma membrane fractions from *Arabidopsis*. There appears to be a high concentration of integrin-like protein in the root of *Arabidopsis*. In onion cells, (Gens et al., 1996) have described an integrin-like protein using monoclonal antibody against the cytoplasmic domain of β_1 integrin in animal cells. Gens et al., (1996) found two protein bands of 105-110 and 115-125 kDa that cross reacted with the β1 integrin antibody. These authors concluded that the protein bands from onion cells very likely represent protein antigenically analogous to β_1 integrin from animal cells. (Lynch et al., 1998) showed the presence of a similar β_1 integrin-like protein localised inside amyloplast of

tobacco NT-1 suspension culture, callus cells and whole-root caps. A distinct band at 110 kDa in western blots suggested size homology with the known β_1 integrin from chicken embryo crude extract.

With respect to RGD sensitivity, (Labouré et al., 1999) found that when maize calluses were grown in the presence of the RGD peptide, important morphological changes were observed indicating the presence of a putative RGD-binding receptor. Immunoblotting showed a protein band at 120 kDa under reduced conditions using the anti-β1 antibody and protein bands at 30 and 60 kDa using anti-αIIbβ3 antibody. Only the 60 kDa was observed when using anti-β3 antibodies.

Table 1.2. Integrin-like proteins of plant species.

Plant Species	Antibody used	Detected molecular weights (kDa)	References
Arabidopsis	β_1	58, 84-116,100	Katembe et al 1997, Swatzell et al,1999
Onion Cells	β_1	105-125	Gens et al,1996
Nicotiana tabacum	β_1	110	Lynch et al,1998
Lilium davidii	β_3	150	Sun et al,2000
	αv	150	
Hemerocallis citrina	β_3	95-97, 150	Sun et al,2000
	αv	150	
Pisum sativum	β_1	60,74,86	Kiba et al,1998
Maize calluses	β_1	120	Labouré,1999
	β_3	60	
	αIIb β_3	30,60	

1.3 Relationship of integrins and tyrosine phosphorylation

Protein phosphorylation regulates a variety of cellular processes and is known to be involved in both eukaryotes and prokaryotes. In eukaryotes, signal transduction involving phosphorylation is generally initiated from the cell surface to the nucleus for development and function of cells (Nakashima et al., 2005). The signal is transferred through the cell in a cascade of threonine/serine and tyrosine phosphorylation events. In many cases these events lead to altered gene expression.

1.3.1 *Hemidesmosomes and focal adhesion sites in animal cells*

In animal cells, adhesive interactions between cells and the surrounding extracellular matrix (ECM) proteins via integrins plays a vital role in cell migration, cell proliferation and differentiation, cell survival, blood clotting and inflammatory responses. Some of the integrin-mediated signal transduction pathways such as tyrosine phosphorylation have been shown to be initiated at cell junctions such as hemidesmosomes and focal adhesion sites (**Error! Reference source not found.**).

1.3.1.1 *Presence of β4 integrin in hemidesmosomes*

The β4 integrin subunit associates exclusively with the α6 subunit and is a receptor for the laminins (Plow et al., 2000). The β4 cytoplasmic domain is distinct both in size (approximately 1000 amino acid residues) and structure from any other integrin subunit. From a functional prospective, it is known that α6β4 is essential for the organisation and maintenance of epithelial architecture. In many epithelia, α6β4 mediates the formation of stable adhesives structures termed hemidesmosomes on the basal cell surface that link the intermediate filament cytoskeleton with laminins in the basement membrane (Green and Jones, 1996) (Error! Reference source not found.**.** A). A significant breakthrough was the finding that α6β4 can also associate with F-actin and is localised at the leading edges of

invasive carcinoma cells (Mercurio et al., 2004). Moreover, α6β4 mediates the migration of such cells through its ability to associate with the actin cytoskeleton and promotes the formation and stabilisation of filopodia and lamellipodia (Mercurio and Rabinovitz, 2001).

A link between α6β4-stimulation of invasion and signal transduction is though to activate phosphoinositide 3-OH kinases (PI3-K), a key signalling molecule and that activity of PI3-K is essential for invasion (Mercurio et al., 2004) One important function of PI3-K with respect to invasion appears to be its ability to regulate actin dynamics via the Rho-family of GTPases (Mercurio and Rabinovitz, 2001).

1.3.1.2 *Presence of integrins in focal adhesion sites*

Unlike the β4 integrin subunit, the β1 integrin subunit, which has formed the basis for a number of studies in oomycetes, fungi and plants, can associate with several α subunits. It typically associates with the ligand fibronectin and forms a major component of focal adhesion sites, which mediate cell to ECM adhesion (Hynes, 1992). The aggregation of actin stress fibers and associated intracellular proteins at these sites are thought to contribute to the spreading and migration of cells. The physical interaction of the cytoplasmic tail of integrins and proteins at focal adhesion sites indirectly links to the actin cytoskeleton via actin-binding proteins. Talin is a major structural element of focal adhesions and it is also the first actin binding protein that was shown to directly interact with the cytoplasmic domain of an integrin (Horwitz et al., 1986). However, both hemidesmosomes and focal adhesion sites play more than a structural role in anchoring the cell to the ECM, as ligand binding of integrin leads to the activation of a range of biochemical signalling events, including elevation of intracellular pH and Ca^{2+}, activation of protein kinases, changes in lipid metabolism and ultimately, changes in gene expression.

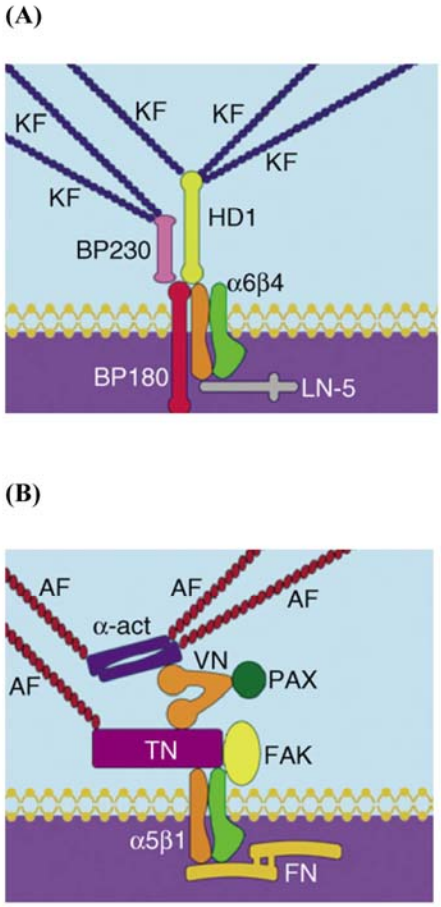

Figure 1.7. Schematic representations of hemidesmosomes (A) and focal contacts (B). Abbrevations: FN, fibronectin; TN, talin; VN, vinculin; FAK, focal adhesion kinase; PAX, paxillin; α-act, α-actinin; AF, actin filament; LN-5; laminin-5; BP180 and BP230, bullous pemphigoid antigens 180and 230; HD1, hemidesmosome 1 antigen; KF, keratin filament (Suzuki et al. 2003).

Talin consists of an NH_2-terminal about 47 kDa globular head domain and about 196 kDa, COOH-terminal (Ree et al., 1990). The talin head domain has a band 4.1, ezrin, radixin, meosin homology (FERM) domain and this domain also can activate integrins

(Calderwood et al., 1999; Calderwood et al., 2002). Talin also binds to actin thus indirectly providing a linkage between integrins and the actin cytoskeleton. The binding of integrins to other families of actin-binding proteins such as α-actinin has also been well characterized. Like talin, α-actinin co-localises with integrins in focal adhesions by interacting with β cytoplasmic domain tails (Cattelino et al., 1999). However, the binding affinity of α-actinin to the β domain of integrin is less than that of talin (Goldmann, 2000). Additionally, integrins bind indirectly to several proteins at focal adhesion sites, these include vinculin, filamin, paxillin, actin and tensin (Calderwood et al., 2000; Critchley, 2000).

Integrin-β-tails do not only provide a link to the actin cytoskeleton but they also regulate outside-in and inside-out signalling. However, integrins themselves have no enzymatic activity in their cytoplasmic tails. This suggests that for integrins to mediate a signal, they require direct binding of signalling proteins. A focal adhesion kinase (FAK) has been reported to bind to the integrin β domain (Vuori, 1998; Parsons, 2003) and indeed FAK appears to play a central role in integrin-mediated signal transduction in animal cells. This kinase is tyrosine phosphorylated and its tyrosine kinase activity is enhanced upon integrin engagement (Parsons., 2003). FAK also binds to several signalling molecules that include paxillin, Grb2-SOS protein complex, phosphoinositide 3-kinases (PI 3-kinase) phospholipase C (PLC), Grb 7, CAS, ASAP/GRAF and Src (Schaller, 2001).

1.3.2 *The presence of tight adhesions in oomycetes, fungi and plants*

Recent evidence suggests that oomycetes and fungi have a membrane skeleton linking to cell wall polymers forming tight adhesions, which can be detected following plasmolysis. The adhesions are found abundantly in regions of active wall expansion at the growing hyphal tips. In oomycetes such as *S. ferax* and *A. bisexualis* and fungi such as *N. crassa*, the apical cytoplasm often remains firmly attached to the apical walls

following plasmolysis as the rest of the protoplasm retracts sub apically (Heath, 1987; Kaminskyj and Heath, 1995; Bachewich and Heath, 1997).

It has been suggested that such attachments may be analogous to focal contacts in animal cells (Heath and Steinberg, 1999). Such adhesion sites in oomycetes and fungi have been found to contain actin and integrin-like proteins, it can thus be hypothesised that signal transduction processes common to focal adhesions, such as tyrosine phosphorylation, might also occur at hyphal tips. Evidence is accumulating to support the hypothesis that a tip-high Ca^{2+} gradient is generated and maintained in fungi internally by IP3. Alteration of IP3 results in the reduction of tip morphogenesis and growth (Silverman-Gavrila and Lew, 2002). For the oomycete *S. ferax* hyphal tip growth was correlated with the difference between tip-localised Ca^{2+} and basal Ca^{2+} although in this organism the tip high Ca^{2+}-gradient may be generated by localised mechanosensitive ion channels (Garrill et al., 1993). Other signalling molecules such as GTPases (e.g. Cdc42, Rac, and Rho) and G-protein subunits are key regulators in the signalling pathway that links extracellular growth signals to the assembly and organisation of the actin cytoskeleton, and these are found in several filamentous fungi (Raudaskoski et al., 2001). These signalling molecules are down stream molecules, which are regulated by tyrosine phosphorylation in animal cells.

Tyrosine kinases such as Wee1 or Swe1p have been found in *S. cerevisiae* (Parker et al., 1993) The cell cycle delay that is induced by the morphogenesis checkpoint requires Swe1p. Checkpoint control of mitosis in *S. cerevisiae* is regulated by tyrosine phosphorylation of Cdc2 by Swe1p and dephosphorylation by a Cdc25-related phosphatase (McMillan et al., 1999). In this organism it has also been (Dailey et al., 1990) shown that p40 is a protein kinase with features that resemble known protein-serine kinase, which has tyrosine kinase activity toward an exogenous tyrosine containing peptide such as poly(Glu:Tyr $_{4:1}$). In addition, (Santoni et al., 2002) recently showed that *Candida albicans* expresses a focal adhesion kinase (Fak)-like protein that is antigenically related to the animal Fak^{p125}.

With regard to hyphal tip growth, there is as yet no direct evidence showing the involvement of tyrosine kinases and/or tyrosine phosphorylation in this process. However, we can not rule out the possible role of such kinases and it is interesting to note recent evidence shows that tyrosine kinase inhibitors alter the development of fucoid algae including the genus *Fucus* and *Pelvetia* (Corellou et al., 2000). Furthermore,

several signalling molecules, especially Ca^{2+} play a role in the tip growth process (Fowler and Quatrano, 1997).

In plants, several kinases that regulate many different aspects of metabolism growth and division have been isolated and characterised (Stone and Walker, 1995). Although protein phosphorylation seems to occur less abundantly on tyrosine than on serine or threonine residues and although conventional tyrosine kinases do not appear in sequence data from higher plants, tyrosine phosphorylation and tyrosine kinase activities have been reported in several plant species such as pea (Torruella et al., 1985; Håkansson and Allen, 1995), alfalfa (Duerr et al., 1993), tobacco (Zhang et al., 1996), maize (Trojanek et al., 1996), and coconut (Islas-Flores et al., 1998).

1.3.3 *Protein cytoskeleton: actin and actin - binding proteins*

Filamentous organisms grow in a highly polarised fashion and give rise to tubular hyphae. Cytoskeletal elements in particular actin microfilaments are organised to support such growth. The current understanding of cytoskeletal organisation during polarised cell growth has greatly benefited from studies on the budding and the fission yeasts (Sawin, 1999). However, the growth pattern of filamentous growth differs from those of budding or fission yeast in that polarised growth has to be maintained (Xiang and Plamann, 2003).

Actin is one of the most abundant proteins in all eukaryotes. Under physiological conditions, actin, a 43-kDa globular protein, polymerises itself into polar, helical filaments in which subunits are connected by a 167° rotation and 2.7 nm axial rise (Pantaloni et al., 2001). Irreversible hydrolysis of the bound ATP associated with polymerisation is at the origin of treadmilling and destabilises the filament. Treadmilling plays a crucial role in the function of actin in motility.

1.3.4 *Actin and cell polarity*

The budding yeast *S. cerevisiae* has proven a useful model system for investigating the molecular mechanisms involved in cell polarisation. The mechanisms underlying polarised morphogenesis highlights several important features that are likely to apply to filamentous organisms as well.

In *S. cerevisiae*, cortical landmark proteins that generate a positional signal such as Bud3p, Bud4p and Axl2p or a bipolar budding pattern such as Bud8p, Bud9p and Rax2p have been well characterised and are summarised in Error! Reference source not found.. (Harris and Momany, 2004). The published genomes of filamentous species shows that these markers are poorly conserved in those species (e.g. *Aspergillus nidulans*) (Harris and Momany, 2004). The lack of strong positional marker homologues might indicate that filamentous fungi do not use landmark proteins. In *S. cerevisiae*, once a positional landmark is established, it is transduced via the Cdc42 Rho GTPase module to the morphogenetic machinery. The active Cdc42-GTP transduces signals to multiple downstream effectors that in turn signal to the actin cytoskeleton. Among the best-characterised effectors are the p21-activated kinases (PAKs), Ste20p, and Cla4p, which among other functions may control actin cytoskeletal organisation by regulating the polarisome (Goehring et al., 2003). Cdc42 module proteins are highly conserved in *A. nidulans* and other filamentous fungi (Harris and Momany, 2004) and deletion of CDC42 is lethal in other fungi (Bassilana et al., 2003).

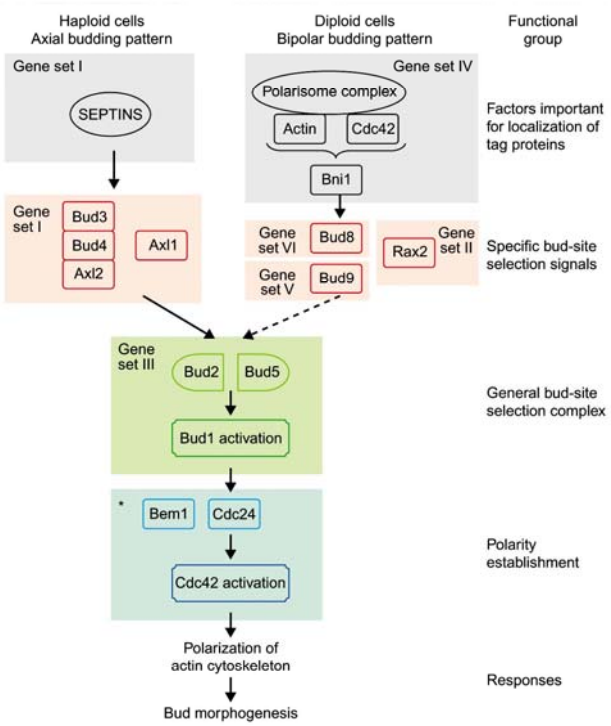

Figure 1.8. Summary of processes of establishment and regulation of cell polarity in yeast cells (Harris and Momany, 2004).

1.3.5 *Actin and tip growth*

Actin is thought to play a major role in tip growth of oomycetes, fungi, pollen tubes, and root hairs. In the oomycetes, growing tips contain a fine network of fibrils most concentrated at the extreme tip which become less abundant and more widely separated sub-apically (Heath, 1987). These apical fibrils (which have been called an F-actin cap) are oriented parallel to the long axis of the hyphae and lie exclusively adjacent to the plasma membrane. In non-growing tips, the actin cap is replaced by PM-associated plaques similar to those found in sub-apical regions of all hyphae. Conversely, the actin cap assembles prior to new tip formation when branches are produced (Bachewich and Heath, 1998).

This pattern of actin is seen when hyphae are fixed with formaldehyde then stained with fluorochrome-labeled phalloidin. An alternative procedure has been used involving the introduction of rhodamine-labeled phalloidin (RP) into living hyphae in both *S. ferax* and *Phytophthora sporangia* (Jackson and Heath, 1990a, 1993a; Jackson and Hardham, 1998). However, this method is not thought to reveal all actin. Recently, hyphae of the oomycete *A. bisexualis* fixed with combinations of formaldehyde and methylglyoxal, showed an actin-depleted zone within the actin caps (Yu et al., 2004). This may suggest that in the growing tips of oomycetes there may be a discontinuity in the actin cap, which may reflect sites of vesicles accumulation.

In the eufungi, there are no reports of an apical fibrillar cap in hyphal tips. Instead, the actin is always seen to be concentrated into peripheral plaques. In some species these occur over the entire apex, being most concentrated at the extreme apex (Heath, 1990; Heath and Skalamera, 2001), but in some species such plaques are absent from the extreme apex but become most abundant about 5 μm back from the apex (Srinivasan et al., 1996; Torralba et al., 1998). In *N. crassa*, the presence of a structure that is rich in vesicles and F-actin, the Spitzenkörper staining is only seen in growing hyphae where the plaques are absent from the extreme tip (Degousee et al., 2000), however, plaques reoccur when Spitzenkörper is absent.

In fact the SpitzenkÖrper appears to be a part of the actin cytoskeleton and also is highly motile (Lopez-Franco and Bracker, 1996). It might also suggest that there are other undetected populations of actin in the apices of the eufungi. The presence of actin as either filaments or plaques at tips suggests that it plays critical functions in the tip growth process including the control of surface expansion and protrusion, the regulation of exocytosis, the direction of vesicle and organelle motility, an involvement in cytoplasmic migration and the regulation of plasma membrane protein distribution (Heath, 2000). Disruptions of actin by phalloidin, cytochalasins and latrunculins alters the morphogenesis of tips and terminates tip extension (Heath, 2000).

1.3.6 *Actin-binding proteins (ABPs)*

The elongation of actin towards a growing tip is analogous to the distribution shown in motile structures of animal cells such as lamellipodia, filopodia, phagosomes and pinosomes. These cells require the assembly of actin filaments at the leading edge of the cell. Actin polymerisation is regulated and maintained by actin-binding proteins. Many actin-binding proteins have been identified and studied, and have been isolated from organisms across the evolutionary spectrum. ABPs regulate filament assembly and disassembly (e.g. profilin, thymosin β4, ADF/cofilin, gelsolin, capping protein), de novo nucleation of actin filaments (e.g. Arp2/3, WASP), cross-link or bundle actin filament (e.g. fimbrin, filamin, villin, α-actinin) or are involved in the formation of focal adhesions (e.g. vinculin, talin, paxillin, integrin). These ABPs are found in animal cells although not all of these ABPs are found in oomycetes, fungi and plants.

The treadmilling of actin filaments is maintained by the actin depolymerising factor (ADF)/cofilin. ADF/cofilin is an 18 kDa, ubiquitous, conserved actin-binding protein, which is responsible for the rapid turnover of actin filaments in the cell. ADF/cofilin interacts preferentially with G-actin and F-actin in the ADP bound form (Carlier et al., 2003). ADF accelerates pointed end depolymerisation, which is the rate limiting step in the treadmilling ATPase cycle (Pantaloni et al., 2001). As a result, a higher steady-state concentration of monomeric ATP-actin is established that supports faster barbed end growth, balancing faster pointed-end depolymerisation (**Figure 1.2.**).

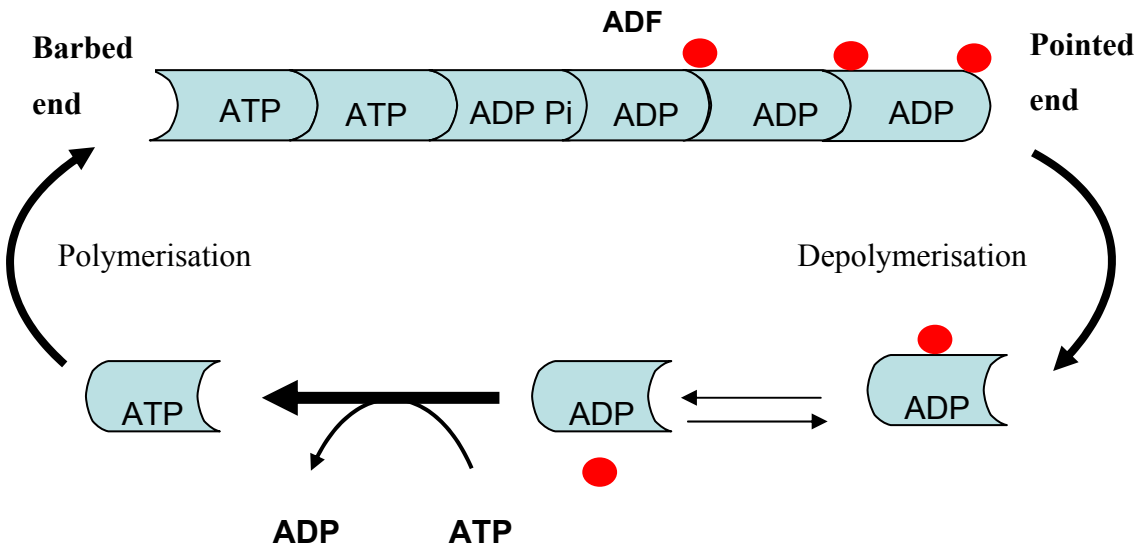

Figure 1.2. Schematic diagram for the general activity of ADF/cofilin. ADF/cofilin servers actin filaments and enhances the disassociation of actin monomers from the pointed end and provides monomers for assembly at the barbed end of an actin filament.

Plant ADF/cofilin family members share approximately 30 % amino acid identity with the vertebrate family members (Danyluk et al., 1996). ADF/cofilin has been found in pollen tubes and root hair of maize (Hussey et al., 2002) , tobacco (Chen et al., 2002), *Arabidopsis* (Hussey et al., 2002) and yeast (Du and Frieden, 1998). The oomycetes *Phytophthora infestans* and *Phytophthora sojae* have nucleotide sequences of ADF analogous to those found in *Lilium longiflorum* and *A. thaliana*. (http://www.pfgd.org).

Profilin is an actin-binding protein, with functions that cooperate with those of ADF. Profilin specifically interacts with ATP-G actin. The profilin-actin complex productively associates with barbed ends (Carlier et al., 2003). It enhances the process of the treadmilling of actin filaments and improves actin-based motility. The actin related protein (Arp2/3) is a complex of actin-binding proteins, which is responsible for branching of actin filaments. The Arp2/3 complex is the downstream target of a variety of signalling pathway leading to actin polymerisation. Early studies provided evidence that the Arp2/3 complex was required for the motility and integrity of *S. cerevisiae* actin patches (Winter et al., 1997). Recently, genetic studies suggest that plant Arp2/3 complexes have similar functions to those of mammals (Millard et al., 2004). The key components of actin patch formation also include the Wiscott-Aldrich syndrome protein (WASP) family and Cdc42, which is a small GTPase. These actin regulators including the WASP homologue Las17/Bee1p and myosin Myo3p, have been found in yeast (Harris and Momany, 2004). Las17p is necessary for actin assembly in permeabilised cell assays, which is though to reflect a role in patch assembly (Weaver et al., 2003).

1.4 Aims of Thesis

The aims of the research described in the thesis were to firstly identify the presence of β4 integrin subunit-like proteins in the oomycete *Achlya bisexualis*. Also, the relationship between these integrin-like proteins, F-actin and tyrosine phosphorylation and their role in tip growth were examined using immunocytochemistry, immunoblotting, ELISA, and coupled enzyme assays. Preliminary work was also carried out looking for similar proteins in yeasts with a view to creating a platform for future studies of their roles in budding and pseudohyphal growth.

Chapter 2 : Immunocolocalisation of integrin-like proteins and phosphotyrosine containing proteins in *A. bisexualis* and *S. cerevisiae*

2.1 Introduction

Tip growth, the mechanism by which hyphae, pollen tubes, root hairs and algal rhizoids extend, is a complex and dynamic process that is characterised by localised extension at the extreme apex of the cell and morphological polarity (Geitmann et al., 2001). Its complexity suggestions that a high degree of regulation is needed to ensure that the characteristics of a particular cell type are maintained during growth. Regulation is likely to come about through bidirectional interplay between the cell wall and cytoplasm, although the mechanisms by which such cross-talk might occur are unknown. There have been suggests that this may involve proteins with functional similarity to the integrins of the metazoan (Heath and Steinberg, 1999).

2.1.1 *Integrin-like proteins in oomycetes, fungi and plants*

With respect to the above, the α6β4 integrin is of particular interest in that it plays a role in cell adhesion and given the appropriate signal can function in cell migration. The α6β4 is primarily concentrated at the basement membrane zone and is a component of hemidesmosomes (Watt, 2002). The α6β4 binds with cytoskeleton proteins such as intermediate filaments and F-actin. One of the mechanisms by which α6β4 promotes migration is through the activation of phophatidylinositol 3-kinase (PI3-K) and signalling via tyrosine phosphorylation and the mitogen activated protein kinase (MAPK) pathway (Watt, 2002). As detailed in chapter 1 and at greater length below, the presence of proteins with epitopic similarity to metazoan integrins in oomycete, fungal and plant cells

has been suggested by their cross-reactivity to antibodies raised against animal integrins although none of these studies have addressed the α6 or β4 integrin subunits.

There are also a number of investigations that show an inhibitory effect of RGD-containing peptides on cell growth and development in many plant and fungal species (Santoni et al., 1994; Santoni et al., 1995; Correa et al., 1996; Gil et al., 1996; Canut et al., 1998; Faik et al., 1998; Kiba et al., 1998; Labouré et al., 1999; Pereyra et al., 2003). Evidence for the presence of integrin-like proteins in filamentous organisms is mostly derived using antibodies from animal integrins. Using immunoblotting or immunocytochemistry, it has been suggested that oomycetes, filamentous fungi, yeasts, and plants have integrin-like proteins that may be located at the plasma membrane- cell wall adhesion sites.

In the oomycete *S. ferax*, immunoblotting showed that a polypeptide of about 178 kDa that had cross reactivity with the anti-β1 antibody. This integrin-like protein is located in the plasma membrane and at cell wall adhesion sites (Kaminskyj and Heath, 1995). However, RGD-containing peptides did not affect tip extension and tip morphology in this organism (Bachewich and Heath, 1997). Using a human αM cDNA as a probe, (Gale et al., 1996) detected a *C. albicans* DNA sequence expressing an integrin-like domain. The full length of gene, the termed "*INT1"* was detected and encoded a protein with a molecular weight of about 188 kDa (Gale et al., 1996). However, the amino acid sequence identity was low in comparison to animal integrin amino acid sequences.

A putative fibronectin receptor molecular weight of about 120 kDa expressed by *C. albicans* was recognised by anti-β1 antibody (Santoni et al., 1995) and a protein with a molecular weight about 84 kDa has been recognised by anti β5 antibody (Santoni et al., 1998). In *S. cerevisiae* a gene termed *USO1* was identified by immunoscreening of an expression library of an integrin-I domain that is conserved in animal integrins. However, the biological function of USO1 protein appears to be in intracellular transport and it is mainly present in cytosolic rather than plasma membrane fractions (Sapperstein et al., 1996). A peptide of 95 kDa from the filamentous fungus *Uromyces appendiculatus* was recognised by an anti-β1 antibody (Correa et al., 1996) and under reducing condition a peptide of about 63 kDa identified from PM fractions of *N. crassa* treated with the anti-

β1 antibody. However, immunoblotting of an unboiled PM extract showed a band at about 120 kDa (Degousee et al., 2000).

A cDNA clone, *AtELP1* (*Arabidopsis thaliana* EGF receptor-like protein) from *A. thaliana* has similarity to a highly conserved region of animal β-integrins (Laval et al., 1999). Immunoblotting analysis showed that a protein of 60 kDa from *A. thaliana* cross reacts with an anti-β3 antibody. (Faik et al., 1998; Kiba et al., 1998) found that plasma membrane proteins from *Pisum sativum* at molecular weight at 60-, 74- and 86- kDa were recognised by anti-β1 antibody.

2.1.2 *The existence of adhesion sites in oomycetes, fungi and plants*

In oomycetes and fungi, there are a number of pieces of evidence that indicate the presence of adhesion sites and that these are more abundant or are stronger in the hyphal tips. Firstly, plasmolysis leaves remnants of the plasma membrane and actin attached to the cell wall. These remnants are greater in number at the tips than sub-apical Hechtian strands. Furthermore, plasmolysis draws the cell wall inward in a region just behind the apex, where the plasma membrane remains attached to the wall via very broad adhesions (Kaminskyj and Heath, 1995; Bachewich and Heath, 1997). In addition, any contractions of cytoplasm are predominantly unidirectional towards the tips indicating potential sites of attachment.

In fungi, it is possible that these attachments contain integrins or integrin-like proteins as fungal cell walls contain proteins with putative integrin-binding sites, comparable to those of animal ECM molecules (Laurent et al., 1999). This is also supported by the observed effects of RGD peptides on growth or differentiation in several fungi (Correa et al., 1996; Hostetter, 2000; Mellersh and Heath, 2001; Pereyra et al., 2003). In addition F-actin is often concentrated in the apical region of hyphae and associated with the apical plasma membrane (Kaminskyj and Heath, 1995). The data above are consistent with structures in walled cells that are comparable to focal adhesions of animal cells.

In plants, physical connections between the cell wall and the plasma membrane have been observed in a number of ways including electron microscopy of cells showing the

appression of PM against the cell wall (Roberts, 1990). In plants, it is assumed that turgor pressure is largely responsible for appression, as disruption of turgor by osmotic shock induces plasmolysis and results in separation of the membrane from the cell wall (Roberts, 1990). The exact nature of the contact site is unknown, although there have been suggestions of homology between these and focal adhesion sites in animal cells. This suggestion is supported by the observed effects of treatment with RGD-containing peptides which can influence several physiological events in plants (Schindler et al., 1989; Wayne et al., 1992). Significantly these include a loss of plasma membrane-cell wall adhesion in plasmolysed *Arabidopsis* cells and a loss of the thin Hechtian strands that form during onion cell plasmolysis (Canut et al., 1998). A similar loss of localised plasma membrane-cell wall adhesions in plasmolysed zygotes of the alga *Pelvetia* after RGD-containing peptide treatments indicate that this type of interaction may not just be restricted to plants (Henry et al., 1996).

More recently, two proline-rich cell wall proteins from bean, that were up-regulated during osmotic stress, were shown to interact with the plasma membrane in a manner that was disrupted specifically by RGD-containing peptides, even though these cell wall proteins apparently lack an RGD motif (García-Gómez et al., 2000). This may suggest that although the molecules involved in plasma membrane-cell wall/ECM interactions in plants and animal may differ in their exact structure, plant may possess functionally analogous cell wall/ECM proteins that contain an RGD-like configuration.

2.1.3 *Tyrosine phosphorylation in hyphae and plants*

The formation of polarised cells such as hyphae requires the specification of growth sites, followed by the recruitment of morphogenetic machinery for localised the cell wall deposition. Once established, polarity must be strictly maintained during hyphal extension. Polarity maintenance implies the existence of novel regulatory molecules that include the Ras- related GTPases (Cdc42p), G-proteins, calcium, actin and actin-binding proteins and also the involvement of protein phosphorylation. One such type of phosphorylation, tyrosine phosphorylation is still to be shown in hyphae and indeed is still a controversial area in oomycete, fungal and plant biology (see chapter 3). There are

indications that numerous phosphorylations may be present in growing fungal tips. These include the elevated levels of Ca^{2+} and IP3, phospholipase C (PLC), the presence of other protein kinases, actin and actin-binding proteins (Foissner et al., 2002; Silverman-Gavrila and Lew, 2002; Harris and Momany, 2004). Recent evidence also suggests that tyrosine phosphorylation may be important with respect to embryogenesis in zygotes of fucoid algae (Corellou et al., 2000).

It is worth noting that tyrosine phosphorylation has been less well reported than phosphorylation of serine or threonine residues and conventional tyrosine kinases do not appear in the sequence data from higher plants (Luan et al., 2001; Luan, 2002). There is however evidence of tyrosine phosphorylation in a number of plant species such as pea (Torruella et al., 1985; Håkansson and Allen, 1995), alfalfa (Duerr et al., 1993), tobacco (Zhang et al., 1996), maize (Trojanek et al., 1996), and coconut (Islas-Flores et al., 1998).

2.1.4 *Adhesion sites in animal cells*

In animal cells, focal adhesion sites play a vital role in integrin mediated signalling pathways. Many of the signalling proteins regulated by integrins occur at focal adhesion sites and also are involved in signal transduction pathways. Engagement of integrins with their cognate ligands at these sites induces a number of signalling events within the cell, including changes of pH and intracellular Ca^{2+} concentration, stimulation of tyrosine phosphorylation of a number of cellular proteins, and induction of gene expression.

Protein phosphorylation is one of the earliest events detected in response to integrin stimulation. Tyrosine phosphorylation has been shown to be a common and perhaps ubiquitous response to integrin engagement in many cell types. Several proteins that associate with integrin-nucleated protein complexes contain a domain termed Src homology 2 (SH2) and 3 (SH3), that specifically mediates protein-protein coupling. The SH2 domain binds to proteins through interactions with specific peptide motifs containing phosphotyrosine, whereas SH3 domains bind to short proline-rich region on their protein targets.

The focal adhesion kinase (FAK) appears to play a central role in integrin-mediated signal transduction. This kinase is tyrosine-phosphorylated, and its tyrosine kinase activity is enhanced upon integrin engagement. Integrin-induced phosphorylation of FAK requires the cytoplasmic domain of the β integrin subunits. The targeting of FAK to focal adhesions appears to involve multiple binding interactions. The N-terminal of FAK binds to cytoplasmic domains of integrin, whereas the C-terminal provides the binding site for the cytoskeletal protein paxillin and in turn, several proteins bind to paxillin through SH2 and SH3 domains (Vuori, 1998). The identification of the cytoskeletal proteins paxillin and tensin as substrate for tyrosine kinases suggests a possible mechanism for the assembly and regulation of integrin-mediated signalling complexes and pathways (DeMali et al., 2003). Many signalling proteins that contain the SH2 and SH3 domains carry additional catalytic domains. These include Grb2, mSOS1, a guanine nucleotide exchange factor (GNEF), Crk, and C3G.

The involvement of Grb2 and mSOS1 with FAK suggests that integrins may regulate the Ras-MAP kinase pathways. The activation of this pathway subsequently regulates cytoskeleton change and gene expression. In addition, MAP-kinase phosphorylates and activates cytoplasmic phospholipase A_2 ($cPLA_2$) to yield arachidonic acid and lysophospholipid. Integrin-FAK complexes also regulate the association of phosphatidylinositol (PI)-3 kinase, which phosphorylates either PI(4)phosphate (PIP) to generate $PI(3,4)P_2$ or PI(4,5)bisphosphate (PIP_2) to generate $PI(3,4,5)P_3$. The production of PIP_2 by the engagement of integrins could be important for actin polymerisation via the regulation of actin-binding proteins such as profilin. In addition, phospholipase C (PLC) uses PIP_2 as substrate to generate the important secondary messenger diacylglycerol (DAG) and inositol triphosphate (IP_3) which in turn enhances the activity of protein kinase C (PKC). The activation of PKC regulates cell spreading and tyrosine phosphorylation of FAK (Clark and Brugge, 1995).

In addition, a link between α6β4-stimulation of invasion and signal transduction at hemidesmosome is thought to activate phosphoinositide 3-OH kinase (PI3-K), a key signalling molecule and that activity of PI3-K is essential for invasion (Mercurio et al., 2004) One important function of PI3-K with respect to invasion appears to be its ability

to regulate actin dynamics via the Rho-family of GTPases (Mercurio and Rabinovitz, 2001).

Due to the limited evidence for the presence of integrin-like proteins and tyrosine phosphorylation in oomycete organisms, experiments were carried out to investigate the presence of these in the oomycete *A. bisexualis*. For comparative purpose, experiments were also carried out on cells of the yeast *S. cerevisiae*. The antibody that was used in these experiments was raised against amino acid residues at 28 to 128 of the N- terminal of the human integrin β4 subunit. Unlike integrin β1 subunits, the integrin β4 subunit forms with only one alpha subunit, α6, and specifically binds with laminins at a conserved RGD sequence. The cytoplasmic domain of the β4 subunit is composed of about 1000 amino acid residues which compares with about 50 amino acids in most of the other β subunits (Hynes, 2002). A comparison of the amino acid residues at 28 to 128 between β4 and β1 subunits using BLATP programme, which is available at www. ncbi.nlm.nih.gov/ shows 30% identity.

This chapter shows that the oomycete *A. bisexualis* and yeast *S. cerevisiae* contain proteins that are epitopically related to the β4 subunit of animals. Preliminary data is presented regarding the size of these proteins. Results in this chapter also show the presence of adhesion sites which may be analogous to focal adhesions of animal cells. This is supported by the co-localisation of the integrin-like protein and F-actin in cell wall/plasma membrane adhesion of plasmolysed hyphae of *A. bisexualis*. Furthermore, phosphotyrosine containing proteins are present in both apical and sub-apical regions and these proteins co-localise with integrin-like proteins. Finally, immunoblotting identified several proteins extracted from hyphae of *A. bisexualis* that contained phosphotyrosine residues.

2.2 Materials and Methods

2.2.1 *Cell cultures and antibodies*

A. bisexualis: Stock cultures of a female strain of *A. bisexualis* Coker, isolated in New Zealand from *Xenopus laevis* dung were grown on PYG (3 g/L glucose, 1.25 g/L Bacto Peptone, 1.25 g/L Yeast extract) agar and maintained at 20 °C in the dark. Prior to experiments, hyphae were sub-cultured on PYG agar over laid with cellophane (Hallmark brand) sheets and allowed to grow at 20 °C for 5 days. Cellophane sheets were boiled 3 times and then were autoclaved prior to culturing. This was necessary to remove any manufacturing residues.

S. cerevisiae: Yeast cells (strain SY1129(F131)) were kept in 50 % glycerol and stored at -80 °C. Prior to use, cells were subcultured on YPD (20 g/L glucose, 20 g/L Bacto Peptone, 10 g/L Yeast extract) agar at 30 °C overnight.

Antibodies

Mouse monoclonal IgG_1 antibody raised against amino acids 28-128 of the integrin β4 subunit of human origin was purchased from Santa Cruz Biotechnology, Inc and was used as a primary antibody. Alexa™ 488 goat anti-mouse IgG (H+L) conjugate was purchased from Molecular Probes and used as secondary antibody. Rabbit IgG polyclonal antibody raised against phosphotyrosine was purchased from Santa Cruz Biotechnology, Inc, and chicken anti-rabbit poly IgG antibody conjugated with Texas Red was purchased from Sigma. A mouse monoclonal IgG1 antibody raised against phosphotyrosine purchased from Sigma was used for immunoblotting. Actin was stained using Texas red-phalloidin (Molecular probes).

2.2.2 *Co-localisation of β4 integrin-like protein and phosphotyrosine containing proteins*

A. bisexualis: Prior to experiments, hyphae were grown for 5 days and then cut 1 cm behind the growing margin and allowed to grow in PYG media for 60 mins to enable recovery. For plasmolysis experiments, mycelial sheets were incubated with 0.5-0.7 M sorbitol for 20-30 mins. Plasmolysed hyphae were visualised under the light microscope. Mycelial sheets were fixed in 4% formaldehyde, 0.5 % methylglyoxal in saline buffer containing 60 mM PIPES pH 6.8, 2 mM EGTA, 2 mM $MgCl_2$, 137 mM NaCl, and 0.268 mM KCl for 45 mins at room temperature. Fixed mycelial sheets were rinsed for 4 times for 5 mins with a washing solution (0.05% v/v Tween-20 in saline) then the cell wall was digested for 15 mins in 10 mg/ml Driselase (Sigma) and membranes were permeabilised in 0.1% (v/v) Triton X-100 (Biorad) for 20 mins. The mycelial sheets were again rinsed in the washing solution 2 times for 5 mins and blocked for 30-45 mins in blocking solution containing 2.5 % (w/v) skimmed milk powder (BioRad) and 5% (w/v) BSA (Sigma) in saline and washed 4 times for 5 mins after blocking.

The mycelial sheets were incubated with a 1:100 dilution of the primary mouse monoclonal IgG_1 antibody raised against the integrin β4 subunit, and rabbit IgG polyclonal antibody raised against phosphotyrosine, at 4 °C overnight. The mycelial sheets were rinsed 5 times for 5 mins and incubated with a 1:1000 dilution of secondary antibody Alexa™ 488 goat anti-mouse IgG (H+L) conjugate. After washing twice, they were then incubated with a 1:500 dilution of chicken anti-rabbit poly IgG antibody conjugated with Texas Red. Both secondary antibodies were incubated for 90 mins at room temperature and washed with 20 ml of washing buffer and this was repeated 3 times for 15 mins. Before microscopic examination, anti-fading solution (containing 0.1 % (w/v) of *p*-phenylenediamine dihydrochloride) was added to prevent photo bleaching.

S. cerevisiae: Yeast cells strain (SY1129(F131)) were streaked onto a YPD agar plate and incubated overnight at 30 °C, from this an isolated colony was selected and cultured in 10 ml YPD media overnight at 30 °C. Cells were centrifuged at 5,000 g for 30 mins

and the pellet was washed twice with ice-cold 40 mM PBS pH 7.0. Yeast cells were fixed in fixing solution as described previously for *A. bisexualis*. After washing with the saline buffer, fixed cells were incubated in KS solution (containing 100 mM KPO_4 buffer pH 7.0, 1.2 M sorbitol) at 4°C overnight. The cell wall was digested with 10 mg/ml Driselase in KS solution containing 0.5 % (v/v) β-mercapthoethanol for 30 mins at room temperature. Cells were centrifuged and resuspended in 0.5 % v/v Triton-X in 100 mM KPO_4 buffer pH 7.0 and incubated at room temperature for 20 mins. Cells were washed and fixed to slides by incubating at 45°C for 30 mins. The slide was then washed 3 times and blocked with blocking solution (containing 1% w/v BSA, 0.05 % v/v Tween-20 and 40 mM PBS pH 7.0) for 45 mins at room temperature then the slides were washed 5 times for 5 mins and incubated with primary antibodies and secondary antibodies as described previously for *A. bisexualis*. Anti-fading solution was added prior to visualisation under the microscope.

2.2.3 *Co-localisation of β4 integrin-like protein and F-actin in A. bisexualis*

The procedure was similar to the above except that only the β4-integrin antibody was used in the overnight incubation. Furthermore, after incubation with the secondary antibody conjugated with Alexa 488 and washing, hyphae were incubated in the dark, with Texas red-phalloidin made in buffer containing 60 mM PIPES pH 6.8, 2 mM EGTA, 2 mM $MgCl_2$, 137 mM NaCl, and 0.268 mM KCl for 30 mins at room temperature and washed as described above.

2.2.4 *Immunoblotting of Integrin-like proteins*

A. bisexualis: Forty plates of *A. bisexualis* grown on PYG overlaid with cellophane were cut 1 cm from the margin of mycelia and frozen with liquid nitrogen, then ground. The powder was then re-suspended in buffer containing 50 mM Tris-HCl pH 6.2, 10 mM NaF, 7 mM EDTA, 2 mM DTT, 20 % glycerol, 7 mM β-mercaptoethanol, 2 mM PMSF, 250 mM sucrose and centrifuged at 10,000 g for 45 mins and further centrifuged with Backman L8-M ultracentrifuge SW28 rotor at 100,000 g for 2 hrs. The microsomal

pellet was re-suspended with the same buffer. Soluble crude fractions before and after centrifugation at 100,000 g and microsomal fraction were then precipitated on ice by addition of trichloroacetic acid (TCA) to a final concentration of 10% for 30 mins.

After centrifugation the precipitates were mixed with 5x Laemmli buffer and heated for 5 mins in a boiling water bath. Proteins were separated on a 5% stacking gel and 12% separating polyacrylamide gel. After SDS/PAGE, proteins were transferred to a nitrocellulose membrane in a buffer containing 15.6 mM Tris-Base and 120 mM glycine and the transfer was run at 30 V at 4 °C overnight. Transferred proteins were stained with 0.1% w/v Ponceau red to check for homogeneity of the transfer. The nitrocellulose blots were then blocked in 10 mM PBS containing 5 % BSA and 0.05 % Tween-20 for 2 hours at room temperature then washed with Tris- Buffer saline (TBS) 2 times for 20 mins. The nitrocellulose membrane was incubated overnight at 4 °C with a 1:250 dilution of mouse monoclonal IgG_1 antibody raised against the integrin β4 subunit as primary antibody. The membrane was visualised by Western Breeze™, (Western Immunodetection System, Invitrogen).

S. cerevisiae: Yeast cells (strain SY1129(F131)) were streaked onto a YPD agar plate and incubated overnight at 30 °C, from these, an isolated colony was selected and cultured in 10 ml YPD media overnight at 30 °C. Then, 10 ml of the overnight culture was poured into 1 L YPD media and further incubated at 30 °C overnight on an orbital shaker. Cells were centrifuged at 5,000 g for 30 mins and the pellet was washed twice with ice-cold 40 mM PBS pH 7.0. The pellet was then re-suspended with buffer as described for *A. bisexualis* and vortexed with pre-chilled ice cold glass beads for 20 mins (1 min vortexing and 1 min on ice) and then further sonicated for 30 mins on ice. Lysed cells were then centrifuged at 10,000 g for 30 mins and then further centrifuged at 100,000 g to obtain the microsomal pellet. The microsomal pellet was then re-suspended in buffer as described for *A. bisexualis*. Electrophoresis and immunoblotting was carried out as described for *A. bisexualis*.

2.2.5 *Immunoblotting of phosphotyrosine containing proteins*

***A. bisexualis*:** The growing edge of *A. bisexualis* mycelia were cut, quick frozen with liquid nitrogen, ground and extracted with extraction buffer containing 30 mM Tris-HCl, pH 7.1, 20 mM NaF, 5 mM EGTA, 7 mM EDTA, 2 mM DTT, 50 mM KCl, 2 mM Na_3VO_4, 2 mM PMSF, 20% glycerol. The extract was centrifuged at 10,000 g for 30 mins, the supernatant was then applied to a phosphocellulose column (1cm X 15 cm) that had been equilibrated with extraction buffer. The column was washed with washing buffer containing 30 mM Tris-HCl, pH 7.1, 7 mM EDTA, 6 mM 2-mercapthoethanol, 10 % glycerol and 1 mM Na_3VO_4 until the A_{280} of the elutent was below 0.1, and the column was then eluted with a gradient of 0 to 1 M NaCl in eluting buffer containing 40 mM Hepes pH 7.0, 7 mM EDTA, 2 mM Na_3VO_4, 20 % glycerol, 2 mM DTT. Fractions of 2 ml were collected.

S. cerevisiae: Yeast cells (strain SY1129(F131)) were streaked onto a YPD agar plate and incubated overnight at 30 °C, from this an isolated colony was selected and cultured in 10 ml YPD media overnight at 30 °C. Then, 10 ml of the overnight culture was poured into 1 L YPD media and further incubated at 30 °C overnight on an orbital shaker. Cells were centrifuged at 5,000 g for 30 mins and the pellet was washed twice with ice-cold 40 mM PBS pH 7.0. The pellet was then re-suspended in the extraction buffer as above and vortexed with pre-chilled iced cold glass beads for 20 mins and further sonicated for 30 mins. Lysed cells were then centrifuged at 10,000 g for 30 mins. The soluble crude fraction was partially purified with a phosphocellulose column as described above.

Each fraction was tested for protein content using a Bradford assay (Deutscher, 1990). Fractions containing proteins were then pooled. One ml of pooled fractions was precipitated on ice by addition of trichloroacetic acid (TCA) to a final concentration 10% for 30 mins. After centrifugation the precipitates were mixed with 5x Laemmli buffer, heated 5 mins in a boiling water bath. Proteins were separated on a 5% stacking gel and 12% separating polyacrylamide gel. After SDS-PAGE, proteins were transferred to a nitrocellulose membrane in a buffer containing 15.6 mM Tris-Base and 120 mM glycine and the transfer run at 30 V at 4 °C overnight. Transferred proteins were stained with

0.1% w/v Ponceau red to check for homogeneity of the transfer. The nitrocellulose blots were then blocked in 10 mM PBS containing 5 % BSA and 0.05 % Tween-20 for 2 hours at room temperature then washed with Tris- Buffer saline (TBS). The renaturation of transferred proteins was carried out as described by (Trojanek et al., 1996). The nitrocellulose membranes were incubated with 50 μM of ATP for 60 mins at room temperature to look for auto-phosphorylation and washed with TBS. The membrane was incubated with a 1:2000 dilution of mouse monoclonal IgG1 anti-PY antibody (Sigma) as primary antibody and visualised by Western Breeze^{TM}, (Western Immunodetection System, Invitrogen).

2.2.6 *Immunoblotting of phosphotyrosine-containing proteins in the microsomal pellet fraction from A. bisexualis*

A. bisexualis: culturing, microsomal pellet extraction, SDS-PAGE, and protein blotting were as described in section 2.2.4. After blocking the nitrocellulose membrane, the membrane was incubated overnight at 4 °C with a 1/2000 dilution of mouse monoclonal IgG1 anti-phosphotyrosine antibody purchased from Sigma. Phosphotyrosine containing proteins were then visualised by Western Breeze^{TM}, (Western Immunodetection System, Invitrogen).

2.3 Results

2.3.1 *Immunocytochemistry of integrin-like protein and phosphotyrosine containing proteins in A. bisexualis*

Hyphae of *A. bisexualis* stained with anti- β4 integrin antibody showed two distinctive staining patterns. In approximately 45 % of hyphae (15 out of 33 hyphae) staining was highly visible at the extreme apex (Error! Reference source not found.**.** A). The remaining 55% (18 out of 33) had no obvious tip high concentration and staining was more common in the sub apical regions (Error! Reference source not found.**.** B). Control hyphae were exposed to secondary antibody only and showed no fluorescence.

If integrin-like proteins form connections between the cytoplasm and cell wall, then after hyphae are plasmolysed with sorbitol, the cytoplasmic remnants that remain attached to the wall should contain integrin-like proteins. Typically when *A. bisexualis* hyphae are plasmolysed, the protoplasm does not pull cleanly away from the cell wall and there are distinct wall-membrane attachment sites. When plasmolysed hyphae were stained again two discrete patterns were observed with wall membrane fragments and associated staining present predominantly at the tips (46% of hyphae, n= 100) (Error! Reference source not found.**.** A) or in more sub apical regions (54% of hyphae, n=100) (Error! Reference source not found.**.** B). These wall-membrane fragments were also found to contain F-actin, which co-localised with the β4 integrin-like protein in both intact and plasmolysed cells (**Error! Reference source not found..**). F-actin may thus form the cytoplasmic continuum of the wall-membrane attachments.

In both intact and plasmolysed hyphae simultaneous staining with antisera directed against integrin and phospholated tyrosine residues and merging of the respective images indicated that integrin-like proteins and phosphotyrosine co-localise (**Error! Reference source not found..** and **Error! Reference source not found..**). This was perhaps not surprising given the abundance of staining in some cells (**Error! Reference source not found.** A), but it was also the case when staining occurred in more discrete spots (**Error! Reference source not found.** B).

Some integrin-like protein patches did not show co-localisation with phosphorylated tyrosine and conversely some phosphotyrosine staining was not associated with integrin like staining (**Error! Reference source not found..** B).

2.3.2 *Immunocytochemistry of Integrin-like protein and phosphotyrosine containing proteins in S. cerevisiae*

Using the anti-β4 antibody to detect integrin-like proteins in *S. cerevisiae* cells, immunofluorescence of integrin-like proteins was localised to the cortical regions of cells (Error! Reference source not found.**.** β4-integrin). This may suggest that a polypeptide which is responsible for the staining may associate with the cell wall/plasma membrane. Unlike staining of integrin-like protein, staining of phosphotyrosine containing proteins are located throughout cells (**Error! Reference source not found..** p-Tyr). This may suggest that at least some of the phosphotyrosine containing proteins are soluble proteins. However, some of the phosphotyrosine containing proteins may also be located at the cell wall/plasma membrane (**Error! Reference source not found..** arrows Merged). Controls were carried out by incubating cells with secondary antibody only and these showed no staining.

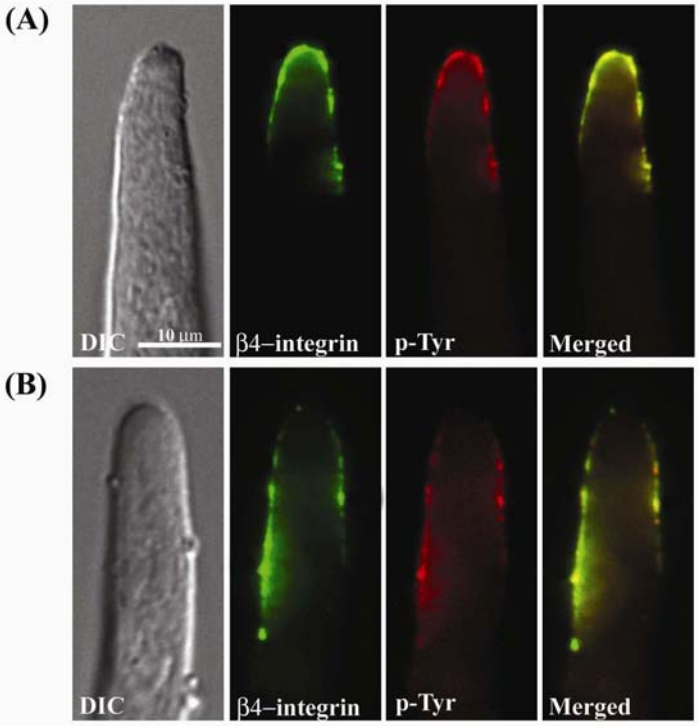

Figure 2.1. β4 integrin-like proteins and phosphotyrosine residues co-localise in hyphae of the oomycete *A. bisexualis*. Two distinct patterns of staining were observed, one in which staining was most prominent at the hyphal tip (A) and one in which staining was more prominent subapically (B).

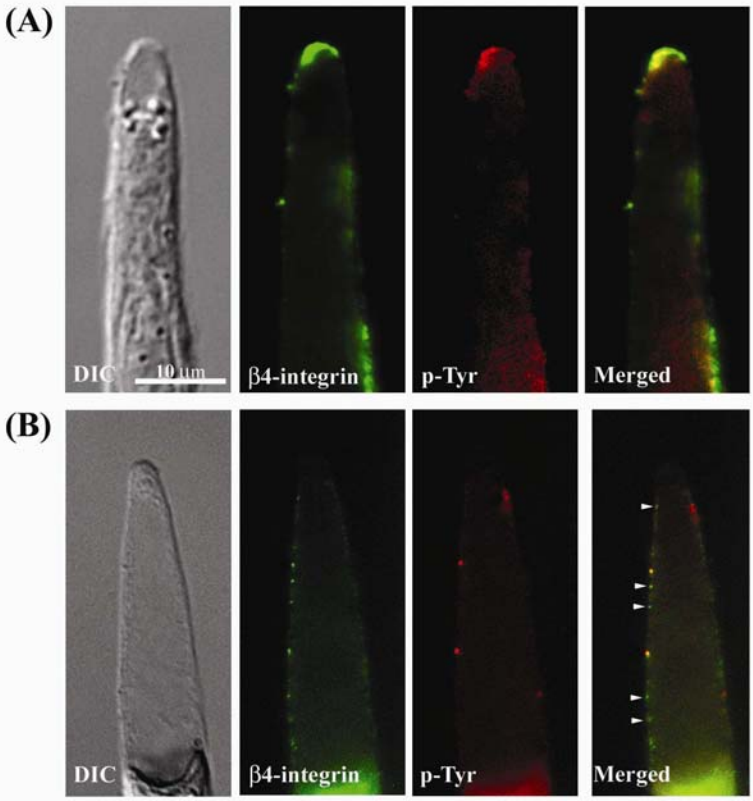

Figure 2.2. β4 integrin-like proteins and phosphotyrosine residues co-localise in cytoplasmic fragment that remain attached to the wall in plasmolysed hyphae of *A. bisexualis*. Again, two distinct types of staining were observed with staining predominantly in fragment at the tip of the cell (A), or in subapical fragments (B). The arrowheads in (B) indicate areas of β4 integrin staining that do not co-localise with phosphotyrosine staining.

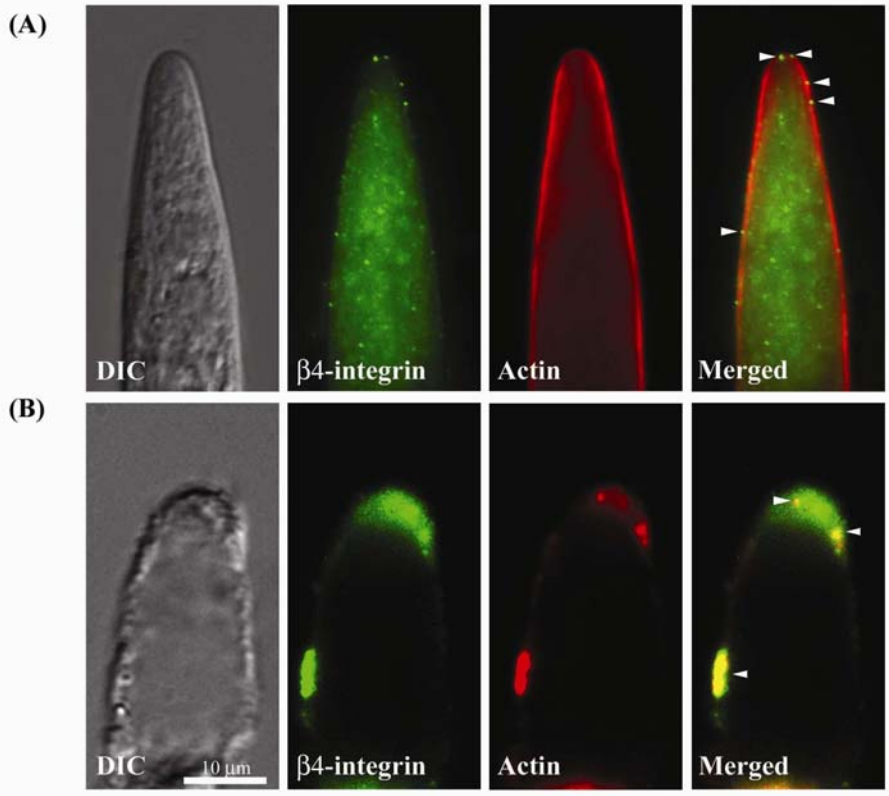

Figure 2.3. β4 integrin-like proteins and F-actin co-localise in hyphae of *A. bisexualis*. In non-plasmolysed hyphae, β4 integrin-like protein patches are co-localised with F-actin (A). In plasmolysed hyphae, β4 integrin-like protein and F-actin co-localise in cytoplasmic fragments that remain attached to the wall (B).

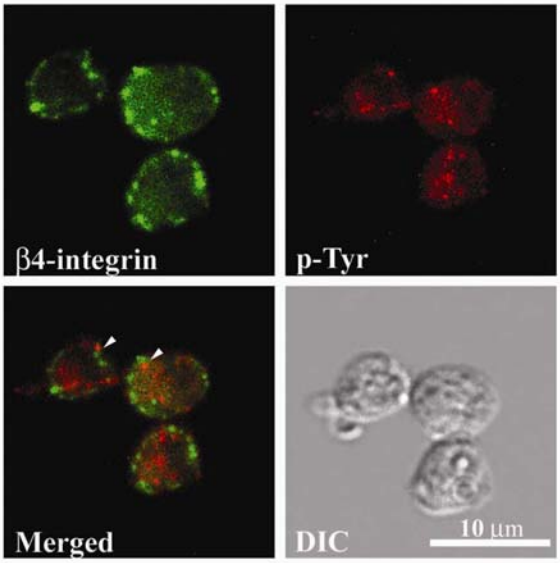

Figure 2.4. β4 integrin-like proteins and phosphotyrosine residues do not appear to co-localise in *S. cerevisiae*. β4 integrin-like protein staining is predominently localised at the cortical region, whereas, phosphotyrosine staining is distributed throughout cells.

2.3.3 *Immunoblotting of Integrin-like protein in A. bisexualis*

Proteins were extracted from *A. bisexualis* hyphae, and were subjected to ultracentrifugation to obtain microsomal pellets. Extractions were carried out in both the presence and absence of DTT and β-mercapthoethanol. Only two polypeptide bands that showed cross reactivity with anti-β4 antibody were present and these were present with or without the reducing compounds. A soluble fraction obtained after the 10,000g centrifugation contained polypeptides with molecular weights of 65 kDa and 85 kDa (Error! Reference source not found.. Lane A). However, after the soluble fraction was further centrifuged at the 100,000 g to obtain microsomal pellets, only the 85 kDa was found (Error! Reference source not found.. Lane B). This indicates that the 85 kDa polypeptide may be plasma membrane associated. The 65 kDa remained in the soluble fraction after centrifugation at the 100,000g (Error! Reference source not found.. Lane C).

2.3.4 *Immunoblotting of integrin-like protein in S. cerevisiae*

Immunoblotting showed that only one polypeptide of about 45 kDa that cross reacted with anti-β4 antibody was present in the microsomal fraction *S. cerevisiae* (Error! Reference source not found.). The crude fraction obtained centrifugation after at 10,000g and after 100,000 g was also subjected to immunoblotting. However, there were no polypeptides that were recognised by the antibody in these (Data not shown).

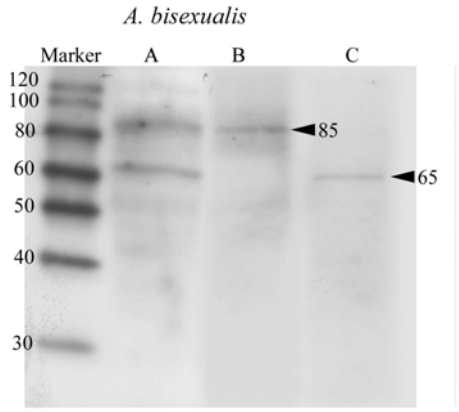

Figure 2.5. Immunoblotting of integrin-like protein from crude proteins obtained from *A. bisexualis* hyphae.
Lane A = crude fraction after centrifugation at 10,000g
Lane B = microsomal pellet fraction after centrifugation at 100,000g
Lane C = crude fraction after centrifugation at 100,000g

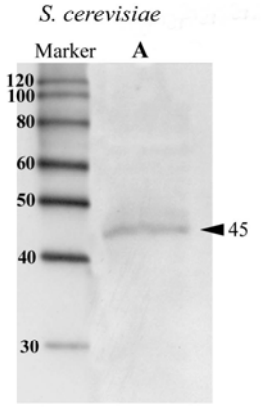

Figure 2.6. Immunoblotting of integrin-like protein from microsomal fraction proteins of *S. cerevisiae* cells.
Lane A = microsomal pellet fraction after centrifugation at 100,000 g

2.3.5 *Immunoblotting of phosphotyrosine containing proteins in A. bisexualis and S. cerevisiae*

Soluble fractions of proteins obtained from *A. bisexualis* hyphae and *S. cerevisiae* cells were separated with SDS-PAGE and then tested for phosphorylation of tyrosine residues by immunoblotting, using the monoclonal anti-phosphotyrosine antibody. In the absence of ATP, four major bands at 26, 46, 60, and 85 kDa from *A. bisexualis* were present (Error! Reference source not found.. A). To verify autophosphorylation of these proteins, experiments were carried out in which nitrocellulose membranes were incubated with ATP prior to staining with the anti-phosphotyrosine antibody. The immunoblotting analysis shows that the intensity of these four protein bands was greater in the presence of ATP. Similar results were also obtained from immunoblotting analysis of yeast proteins (**Error! Reference source not found..** B). With yeast extracts, in the absence of ATP, there were three major bands at about 35, 60, and 90 kDa that contained phosphotyrosine residues and again these proteins show greater staining intensity in the presence of ATP (Error! Reference source not found.. B).

To evaluate tyrosine phosphorylation of integrin-like proteins in *A. bisexualis*, the soluble crude fraction was subjected to ultracentrifugation at 100,000g for 2 hours to obtain a microsomal pellet fraction. Then proteins from the microsomal pellet were immunobloted with anti-phosphotyrosine antibody. The 85 kDa protein from the crude fraction (Error! Reference source not found.. (C), lane A) contains phosphotyrosine residues. Moreover, the 85 kDa band still appears in the microsomal pellet fraction but the intensity of the band is weak (Error! Reference source not found.. (C), lane B). This could be a breaking down of plasma membrane containing proteins during separation by SDS-PAGE.

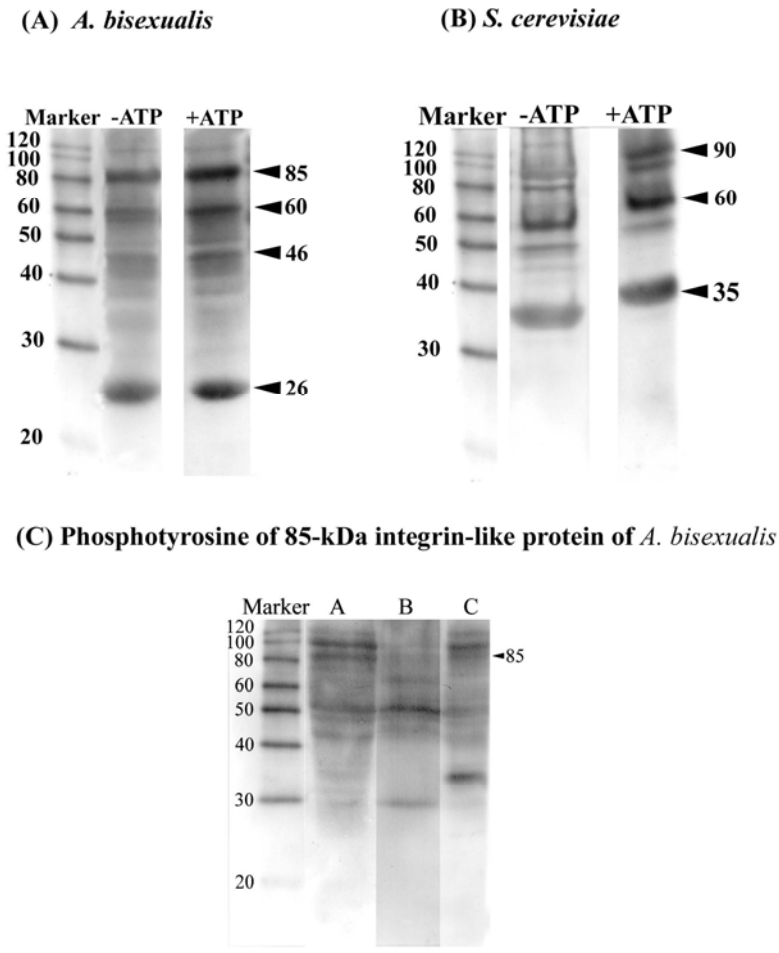

Figure 2.7. Immunoblot analysis of phosphotyrosine containing proteins from *A. bisexualis* **(A)** and *S. cerevisiae* **(B)**. Partially purified proteins (by a phosphocellulose column) were immuno-detected using the anti-phosphotyrosin antibody with or without the presence of ATP. In (C), the band at 85-kDa is a phosphotyrosine containing protein. Lane A is crude fraction, lane B is microsomal pellet and lane C is crude fraction after centrifugation at 100,000g.

2.4 Discussion

The presented results indicate that hyphae of the oomycete *A. bisexualis* and yeast *S. cerevisiae* contain proteins that are epitopically similar to the integrin β4 subunit of human. Specifically this similarity is between amino acid residues 28-128. In *A. bisexualis*, these integrin-like proteins co-localise with phosphotyrosine containing proteins but this does not appear to be the case for *S. cerevisiae*.

Integrin-like proteins stain in hyphae of *A. bisexualis* in both apical region and sub-apical regions. After plasmolysis, the staining was present at wall-membrane attachment sites suggesting a role in wall-membrane attachment. This staining is very similar to that in the oomycete *S. ferax* that was treated with antibody raised against the integrin β1 cytoplasmic domain subunit (Kaminskyj and Heath, 1995). In *S. ferax*, this integrin-like protein also appeared to mediate attachment between the cytoskeleton and the cell wall. This conclusion was supported by the peripheral location of the integrin patches, the strong resistance to plasmolysis in integrin-rich sporangial tips relative to hyphal tips, the formation of integrin-like proteins and actin-rich cytoplasmic remnants that attach to the cell walls following plasmolysis and finally the colocalisation of actin and integrin-like proteins in hyphal and sporangial tips. Integrin-like proteins may therefore function in tip morphogenesis, since this is one suggested role for F-actin. This is supported by preliminary data suggesting that the peptide RGDS, which affects integrin-extracellular matrix interactions in animal cells, interferes with growth and morphology in *A. bisexualis* hyphae.

The appearance of integrin-like protein staining and its co-localisation with F-actin in *A. bisexualis* also fits the above model. In around one half of hyphae (Error! Reference source not found.. A), the antibody staining is highly concentrated at the extreme tip and located at the cell wall/plasma membrane sites. Similar staining is found in the fungus *Neurospora crassa*, in which the anti-β1-integrin antibody showed fine PM-associated spots which were tip-high and tended to fuse into almost continuous caps at the extreme tips, with more separated sub apical staining (Degousee et al., 2000). In plasmolysed hyphae, staining was present in patches located at the cell wall and remnants of cytoplasm (Error! Reference source not found.. A and B).

Immunoblotting has identified candidate proteins responsible for the above staining. The β4-integrin antibody cross reacted with protein bands at about 65 and 85 kDa regardless of the presence/absence of reducing agents. These polypeptide masses differ from similar proteins identified in *S. ferax* using the anti β1-integrin antibody. However, the same molecular weight proteins would be surprising. This is because different antibodies were used, the β4- integrin is bigger than β1-integrin in animal cells, and there is diversity in the sizes of β1-integrin-like proteins in fungi. The 85 kDa protein is however close in weight to the 95 kDa proteins detected with anti β1-integrin antibody in *Candida albicans* (Marcantonio and Hynes, 1988). Western blot analysis with antibody specific to the αv or β5 subunit detected a heterodimer of 130/84 kDa (Santoni et al., 1998). The protein bands found in *A. bisexualis* are also close to the weights of 80 kDa found in *Chara* and 84 kDa *Arabidopsis* (Katembe et al., 1997).

(Marcantonio and Hynes, 1988) investigated the degree of cross-reactivity to integrin antibodies in yeast cells. Immunoblotting experiments showed no specific bands in membrane extracts of *S. cerevisiae* using an antibody raised against the cytoplasmic domain of chicken integrin β1 subunit. Furthermore, there is an absence of integrin sequence in the yeast genome database (http://www.yeastgenome.org). The result from immunoblotting and immunofluorescence in the presence study indicates that *S. cerevisiae* contains a polypeptide that cross-reacts with anti-β4 integrin antibody. A protein of about 45 kDa present in a microsomal pellet fraction was recognised by the antibody. Immunofluorescent images indicate that this protein is located mainly in cortical regions. Using the amino acid sequence at position 28 to 128 of the human β4-integrin as the bait to detect any proteins from the yeast protein sequence database, eight protein profiles have been found (**Table 2.1.**)

Table 2.1. Proteins in the *S. cerevisiae* database that show sequence similarity to the human β4 integrin.

Sequence names	Sequence identities (%)	Protein molecular weight (kDa)	Protein
YMR178W	29	31.1	Hypothetical protein
YBR150C	32	126.9	Probable Zinc-finger protein
YNL267W	31	119.9	Phosphatidylinositol 4-kinase
YLR098C	22	74.4	Zinc-finger protein
YDR272W	32	31.3	Glyoxalase (Glo2p)
YGL116W	25	67.3	Cdc20
YLR030W	36	29.9	Unknown protein
YDR047W	39	41.3	Uroporphyrinogen decarboxylase (Hem12)

Of these only one protein is a transmembrane protein that has a mass close to 45 kDa. This protein is called Hem12p. Hem12p is composed of 362 amino acid residues and has a molecular mass of 41.349 kDa. It contains a transmembrane domain between positions 67 to 93. These amino acid sequences in the transmembrane domain have 39 % identity to the β4-integrin between residues 75-110. The *hem12* gene encodes uroporphyrinogen decarboxylase which catalyses the sequential decarboxylation of the four acetyl side chains of uroporphyrinogen to yield coproporphyrinogen, an intermediate in protoheme biosynthesis (Garey et al., 1992). As such, Hem12 does not appear to play a role in morphogenesis.

One integrin-like gene, *uso1*, has been isolated from *S. cerevisiae* by screening an expression library with two antibodies against leukocyte integrins αX and αM (Hostetter et al., 1995). However, USO1 is a cytosolic rather than plasma a membrane associated protein and has been shown to play a role in intracellular transport of vesicles (Sapperstein et al., 1996). Another integrin-like gene, *int1*, from *Candida albicans* encodes a protein of about 188 kDa. Again, the INT1 protein has limited similarity to vertebrate integrins (Gale et al., 1996). However, it localises to the cell surface and has been shown to be involved in adhesion of yeast to human epithelial cells and in filamentous growth (Hostetter, 1999).

Tyrosine phosphorylation plays an important role in cell signal transduction, regulation of growth and development in animals (Vuori, 1998; Watt, 2002). The relationship between tyrosine phosphorylation and cell polarity in filamentous organisms are still unknown. This thesis presents the first evidence that suggests tyrosine phosphorylation occurs in oomycete hyphae. This tyrosine phosphorylation appears to occur at or close to integrin-like proteins and can occurs at the apex of the hyphae. This may suggest that integrin-like protein itself might have phosphotyrosine residues. This data is consistent with the observation that the cytoplasmic tail of integrins have conserved tyrosine residues that can be phosphorylated and these play a vital role in signalling pathways in animal cells (Calderwood et al., 1999; Calderwood et al., 2002).

Tip growth of hyphae, pollen tubes and root hairs is an example of polarised cell growth. Polarity establishment presumably requires the specification of growth sites,

followed by the recruitment of the morphogenesis machinery necessary for localised cell wall deposition and once polarity is established, it must be maintained during tip extension. The mechanisms underlying polarised morphogenesis have been extensively characterised in the yeasts *S. cerevisiae* and *S. pombe* (Palmieri and Haarer, 1998; Verde, 2001). There are several types of signalling molecules involved in polarisation, these include G-protein, Cdc42p, Cdc24p, Rho GTPase, Rac, Ras, actin, and actin-binding proteins (Harris and Momany, 2004). In animal cells, all these signalling molecules are down regulated by integrin- tyrosine phosphorylation regulation (Clark and Brugge, 1995). Furthermore, actin dynamics are regulated either by reversible tyrosine phosphorylation or by phosphorylation of actin-binding proteins (Kameyama et al., 2000),

Other secondary signalling molecules such Ca^{2+} also play a vital role in tip polarity. Elevation of Ca^{2+} levels have been found in several hyphae (Lew, 1999; Silverman-Gavrila and Lew, 2002). Accordingly, Ca^{2+}-dependent protein kinases are required for germination and pollen tube growth and are co-localised with F-actin in pollen tubes (Putnam-Evans et al., 1989; Estruch et al., 1994). Since, the growing tip of *A. bisexualis* contains by F-actin, there should be actin-binding protein coordination with maintenance of F-actin in the growing tip.

Even though, tyrosine phosphorylation is still unknown in filamentous organisms such as in oomycetes and fungi, recent reports showed that in the dimorphic fungus *C. albicans*, integrin-like proteins and tyrosine phosphorylation co-localised at cortical regions of the yeast cells and a reduction of tyrosine phosphorylation was observed when yeast cells were incubated with tyrosine kinase inhibitors (Santoni et al., 2002). Furthermore, embryogenesis of the fucoid algae *Fucus* and *Pelvetia* requires tyrosine phosphorylation and the germination of embryos were prevented by tyrosine kinase inhibitors (Corellou et al., 2000).

The data from this study also suggests that there are several cytosolic proteins that have proteins containing phosphotyrosine residues. Immunoblot analysis shows partially purified soluble fractions of protein from hyphae of *A. bisexualis* have four such proteins of 26, 46, 60, and 85 kDa. Also these proteins are able to be autophosphorylated in the

presence of ATP. The 26 kDa protein is interesting as it appears to be the predominant band and mostly comes out when the phosphocellulose column is used for purification. However, it does not have any tyrosine kinase activity, and this will be discussed further in the Chapter 3.

Phosphotyrosine-containing proteins have been reported in several plant species. The 26 kDa protein in *A. bisexualis* has a protein mass close to that of phosphotyrosine-containing proteins found in pea mitochondria in respiratory redox signalling (Håkansson and Allen, 1995). The proteins at 46 and 60 kDa found in *A. bisexualis* are close in mass to those found in transformed roots of *Catharanthus roseus* (Rodriguez-Zapata and Hernández-Sotomayor, 1998) and in maize seedlings that contain a group of proteins ranging from 45 to 60 kDa (Trojanek et al., 1996). Recently, proteins at 38, 39, 48, and 75 kDa that are tyrosine phosphorylated have been found during phytohormone-stimulated cell proliferation in *Arabidopsis* hypocotyls (Hang et al., 2003). The data also shows that the 85 kDa protein is phosphotyrosine-containing protein with or without ATP. It is very interesting that this protein band is approximately the same size as the integrin-like protein band. To evaluate the 85 kDa phosphotyrosine-containing protein, the microsomal pellet obtained after ultracentrifugation was used to detect phosphotyrosine residues. Immunoblotting shows that the microsomal pellet has a band but it is weaker than that from the crude and there is high back ground signal. This may be explained by the fact that there may be breakage of plasma membrane during separation by SDS-PAGE. However the data is consistent with the integrin-like protein and the phosphotyrosine containing protein being the same protein.

Results also showed that *S. cerevisiae* contains phosphotyrosine proteins and these are distributed throughout the cell. However, no co-localisation between integrin-like proteins and phosphotyrosine containing proteins was observed in *S. cerevisiae*. There is an absence of integrin sequence in a yeast sequence database but phosphotyrosine containing proteins have been found in yeast. In fungi, the mitogen-activated protein (MAP) kinases are known to play major roles in regulating growth and differentiation processes (Xu, 2000). Although no conventional tyrosine kinases exist in *S. cerevisiae*, tyrosine phosphorylation has been shown to be essential in controlling the activity of MAP kinases in yeast. MAP kinase activation requires phosphorylation on

tyrosine and threonine residues catalysed the dual-specificity MAP kinase kinase (MAPKK)(Cobb and Goldsmith, 1995). MAPKKs such as Wee1 or Swe1p have tyrosine kinase activity (Parker et al., 1993). The cell cycle delay induced by the morphogenesis checkpoint requires Swe1p. Checkpoint control of mitosis in *S. cerevisiae* is regulated by the tyrosine phosphorylation of Cdc2 by Swe1p and dephosphorylation by Cdc25-related phosphatase (McMillan et al., 1999).

Chapter 3 : The presence of protein tyrosine kinase activities in *A. bisexualis* and *S. cerevisiae*

3.1 Introduction

Signal transduction regulates cellular processes in response to external/internal stimuli and is vital for the growth and development of all organisms. It is thought that the reversible phosphorylation of proteins is a crucial component of almost all signalling pathways in living cells. Protein phosphorylation is regulated through the concerted action of kinases and phosphatases. Most protein phosphorylation in cells occurs on residues of serine and threonine with a minor proportion at residues of tyrosine. Despite this tyrosine phosphorylation is very important in animal systems. The introduction of chapter will address the possible existence of tyrosine kinases in oomycetes, fungi, and plants. This will be followed by a consideration of tyrosine kinases found in animal cells.

3.1.1 *Presence of protein tyrosine kinases in oomycetes, fungi, and plants*

The previous chapter suggested the presence of proteins that are epitopically similar to the β4 integrin subunit and an association between this and phosphorylated tyrosine residues. This suggests that *A. bisexualis* may contain a tyrosine kinase. While there is no sequence data available for *A. bisexualis*, the oomycete *Phytophthora sojae* shows nucleotide sequences that resemble tyrosine kinases found in *Dictyostelium discoideum*, *Caenorhabditis elegans*, *Homo sapiens*, *Rattus norvegicus*, and *Mus musculus* (http://cogeme.ex.ac.uk). Although the protein products of these sequences in *Phytophthora* have not yet been characterised, it raises the possibility that oomycetes may have tyrosine kinases (**Table 3.1.).**

Table 3.1. DNA sequences of the oomycete *P. sojae* resemble sequences of tyrosine kinases found in various eukaryotic organisms. Amino acid residues 481-1052 of the human focal adhesion kinase (FAK) were used to detect nucleotide sequences from oomycete and fungal databases, which are available at http://cogeme.ex.ac.uk.

Sequences of *Phytophthora sojae*	**Sequence identities (%)**	**Protein**
Ps31050460	40	Putative tyrosine kinase-like protein from *D. discoideum*
Ps9834403	38	Tyrosine kinase family member (kin-24) from *C. elegans*
Ps30499946	35	Src-related kinase lacking C-terminal regulatory N-terminal myristylation sites from *Homo sapiens*
Ps30499946	34	Src-related kinase lacking C-terminal regulatory N-terminal myristylation sites from *R. norvegicus*
Ps30499946	34	Tyrosine –specific protein kinase from *M. musculus*

Unlike the *Phytophthora* genome, analysis of the budding yeast genomic sequence indicates that this organism may lack true tyrosine kinases. However, some serine/threonine kinases in *S. cerevisiae* such as Swe1 (Wee1), Ste7, Rad53, and Mck1 also have tyrosine kinase activity. For instance, Swe1 (Wee1 in the fission yeast) phosphorylates a conserved tyrosine on Cdc28p (Cdc2 in the fission yeast), thereby preventing cells entry into mitosis until cells reach a critical size (Harvey and Kellogg, 2003). In the yeast mating pathway, the Ste7 which is the MAPKK, phosphorylates two MAPKs (Kss1 and Fus3) on conserved serine and tyrosine (Kusari et al., 2004) and this results in the fusion of two haploid cells opposite mating types to produce a diploid cell (Pan et al., 2000; Maleri et al., 2004). Mck1 kinase functions in a variety of processes including the cell cycle delay by Ca^{2+}, segregation of mitotic chromosome, and diploid cells for expression a gene encoding an early meiotic activator (Mizunuma et al., 2001). Furthermore the Ser/Thr kinases represent virtually all of the kinases described in filamentous fungi. These play a role in MAPK pathways that are very important in filamentous fungi, controlling pathways control diverse growth and differentiation processes and survival and pathogenesis in fungal pathogens (Xu, 2000).

In plants, mitogen-activated protein kinase (MAPK) is a serine/threonine kinase that plays a major role in various physiological, developmental and hormonal responses. The activation of MAPK correlates with stimulatory treatments such as pathogen infection, wounding, low temperature, drought, hyper- and hypo-osmolarity, high salinity, touch and exposure to reactive oxygen species (Munnik and Meijer, 2001; Romeis, 2001; Ichimura and Shinozaki, 2002; Rakwal and Arawal, 2003). *Arabidopsis* shares components of conserved MAPK with human and yeast. MAPK cascades are minimally composed of three kinase modules, MAP kinase kinase kinase (MAPKKK), MAP kinase kinase (MAPKK), and MAP kinase (MAPK), which are linked in various ways to upstream receptors and downstream targets. MAPKKKs are serine/threonine kinases and activate MAPKKs through the phosphorylation of serine and threonine residues. Importantly with respect to the present study, MAPKKs are dual-specificity kinases that phosphorylate MAPKs on threonine and tyrosine residues. Activated MAPKs can phosphorylate a variety of substrates, including transcription factors, protein kinases and cytoskeleton proteins (Jonak et al., 2002).

In *Arabidopsis*, there are 417 genes that have been referred to as receptor kinases (Cock et al., 2002). The structures of plant receptor kinases (PRKs), which consist of an extracellular domain, a single membrane-spanning domain and a cytosolic kinase domain, resemble those of the receptor tyrosine kinase and receptor serine/threonine kinase families in metazoans. A common feature of the receptor kinase families in plants and those of animals is that the kinase domains are homologous although, in contrast, the extracellular domains can be highly diverse. Recent studies indicate that PRKs can autophosphorylate in response to ligand binding both in vitro and in vivo and there is evidence that phosphorylation can occur within receptor oligomers (Cock et al., 2002).

Even though, the presence of true tyrosine kinases in plants remains controversial, there is evidence suggesting the presence of tyrosine kinase activity in plant species such as pea (Torruella et al., 1985; Håkansson and Allen, 1995), alfalfa (Duerr et al., 1993), tobacco (Zhang et al., 1996), maize (Trojanek et al., 1996), and coconut (Islas-Flores et al., 1998). Recent evidence also shows that tyrosine kinase inhibitors alter the development of fucoid algae such as *Fucus* and *Pelvetia* (Corellou et al., 2000). However, the question still remains to be answered as to whether this activity is due to an actual tyrosine kinase or a dual-specificity kinase such as MAPKK.

3.1.2 *Tyrosine kinases in animal cells*

There are two types of tyrosine kinases in animal cells; the transmembrane tyrosine kinase receptors, and the non-receptor tyrosine kinases. Receptor tyrosine kinases include the epidermal growth factor receptor (EGFR), insulin receptors, platelet-derived growth factor (PDGF), insulin-like growth factor 1 (IGF-1) and colony-stimulating factor 1 (CSF-1). All of the receptor tyrosine kinases are induced by binding of specific ligand and it appears that ligand-induced activation of the kinase domains and its signalling potential are mediated by receptor oligomerisation. Receptor oligomerisation permits the transmission of a conformation change from the extracellular domain to the cytoplasmic domain without requiring alterations in the positioning of amino acid residues within the transmembrane domain.

Receptor tyrosine kinases catalyse the phosphorylation of exogenous substrate as well as tyrosine residues within their own polypeptide chains. Most of receptor tyrosine kinases share common domains, which include extracellular, transmembrane, juxtamembrane, tyrosine kinase and carboxy-terminal tail domains. The extracellular domains of the insulin receptor and EGFR share homologous cysteine- rich sequence repeat domains, but the extracellular ligand binding domains of the PDGF receptors have an immunoglobulin-like structure. The transmembrane domain functions in anchoring the receptor in the plane of the plasma membrane; thereby it connects the extracellular environment with internal compartments of the cell. The juxtamembrane domain is involved in modulation of receptor functions by heterologous stimuli or known as receptor transmodulation (Chuen Wong and Guillaud, 2004).

The tyrosine kinase domain is the most conserved portion of all receptor tyrosine kinase molecules. The conserved region contains a consensus sequence, GlyXGlyXXGlyX(15-20)Lys that functions as an ATP- binding site. Replacement of the lysine residue of the ATP- binding site in the EGFR, insulin and PDGF receptors completely abolishes their kinase activities. The carboxy-terminal tail is among the most divergent between all known receptor tyrosine kinases. Several autophosphorylation sites have been identified in the EGFR and in the insulin receptor. Tyrosine residues are conserved in the carboxy-terminal tails within each receptor tyrosine kinase subclass. The autophosphorylation of conserved tyrosine residues at the carboxy-terminal tails plays a role in maintaining the activated state of the insulin kinase activity. EGFR autophosphorylation sites are clustered at the carboxy-terminal tail and appear to modulate the interaction of activated EGFR with substrates and other proteins. Furthermore, the autophosphorylation sites of EGFR compete with exogenous substrate for the substrate binding site of the kinase domain. Hence, autophosphorylation appears to release an internal constraint by establishing a conformation of the receptor that is competent to interact with and phosphorylated cellular substrates (Grandis and Sok, 2004).

As mentioned above other types of tyrosine kinases are non-receptor tyrosine kinases. Several non-receptor tyrosine kinases have been found in animal cells and one which has received particular interest is sarcoma protein (Src), a non-receptor tyrosine kinase.

Src is expressed ubiquitously; however, brain, osteoclasts, and platelets express higher levels of this protein than most other cells. There are 11 members of the Src-family kinases in humans. These include Blk, Brk, Fgr, Frk, Fyn, Hck, Lck, Lyn, Src, Srm, and Yes. Src, Fyn, and Yes are expressed in all cell types. Srm is found in keratinocytes, and Blk, Fgr, Hck, Lck, and Lyn are primarily found in hematopoietic cells. Frk occurs chiefly in bladder, brain, breast, colon, and lymphoid cells. Brk occurs in colon, prostate and the small intestine (Roskoski, 2004).

3.1.3 *Conservative domains of SH2 and SH3 in tyrosine kinase and signaling proteins*

Both receptor and non-receptor tyrosine kinases select their targets by the identification of a conserved protein module of approximately 100 amino acids in the Src homology 2 (SH2) domain and of about 60 amino acids in the Src homology 3 (SH3). These SH2 and SH3 domains are found in a remarkably diverse group of cytoplasmic signalling proteins (Pawson and Gish, 1992). SH2 domains bind to distinct amino acid sequences C-terminal to the phosphotyrosine where as SH3 binds to sequences of proline rich regions (Lee, 2005). Src tyrosine kinase, SH2 and SH3 domains have four important functions. First, they constrain the activity of the enzyme via intracellular contacts. Second, proteins that contain SH2 and SH3 ligands can bind to the SH3 and SH3 domains of Src and attract them to specific cellular location. Third, as a result of displacing the intracellular SH2 and SH3 domains, proteins can activate Src activity. Finally, proteins containing SH2 and SH3 ligands can enhance their ability to function as substrates for Src tyrosine kinase (Roskoski, 2004).

As a result of the tyrosine phosphorylation events, Src tyrosine kinase and the docking proteins residing in focal adhesions form a network of protein-protein interactions that connect to multiple downstream biochemical signalling pathways (**Figure 3.1.**). There are a number of biochemical pathways that can be activated downstream of Src. These include signalling components that are well known from the field of growth factor receptor signalling; the PI3-kinase, PLCγ and MAP kinase pathways (Schaller, 2001).

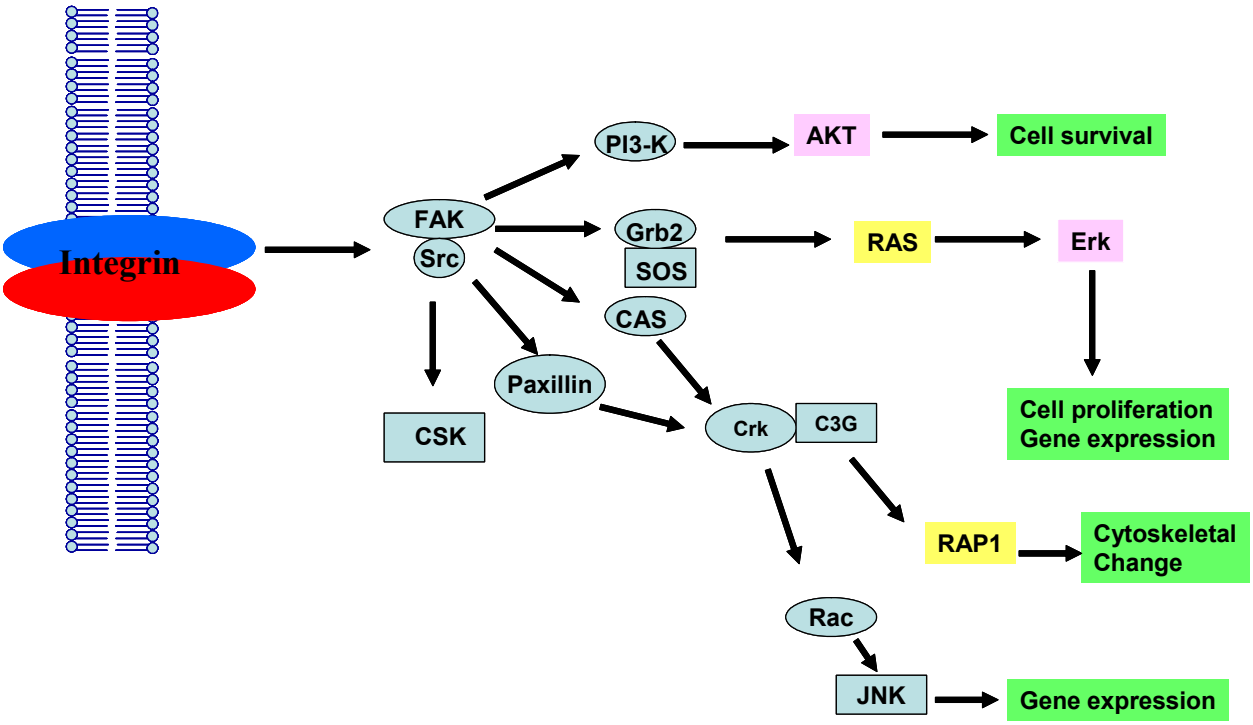

Figure 3.1. Cellular dependent pathways that occur as a result of focal adhesion kinase (FAK) and Src interaction (Vuori, 1998).

3.1.4 *Tyrosine kinase Inhibitors*

Based on animal models, the crucial role of tyrosine phosphorylation by protein tyrosine kinases therefore presents an attractive target for developing an inhibitor. The compounds quercetin, genistein, lavendustin A, erbstatin, and herbimycin A, are tyrosine kinase inhibitors that exhibit broad specificity in micromolar range (Levitzki and Gazit, 1995). Derivatives of quercetin inhibit only tyrosine kinases. Genistein and lavendustin A are competitive inhibitors of ATP in the kinase reaction and compete non-competitively with the protein substrates. These compounds are broad-spectrum tyrosine kinase inhibitors, probably because the ATP binding domain is highly conserved among tyrosine kinases (Levitzki and Gazit, 1995). Synthetic inhibitors such as tyrphostins have been made that are effective both *in vivo* and *in vitro*. The structures of some of these compounds are shown in **Figure 3.2**.

Tyrphostins are tyrosine kinases inhibitors, have been used extensively for the last decade. They specifically bind to the binding site of tyrosine but not the site of ATP binding (Levitzki, 1990). Tyrphostins can inhibit EGFR, the insulin receptor, and PDGF receptor. Tyrphostins also block tyrosine phosphorylation of host cells, in which lipopolysaccharides of gram-negative bacteria cause the development of sepsis (septic shock) (Levitzki and Gazit, 1995). Furthermore, tyrphostins inhibit the EGF induced Ca^{2+} mobilisation concomitant with the inhibition of phosphatidylinositol bisphosphate breakdown to inositol phosphates (Levitzki, 1990). In this study, tyrphostins and genistein were employed to investigate presence of *in vivo* and *in vitro* tyrosine kinase activity in whole cells and cell fractions of *A. bisexualis*.

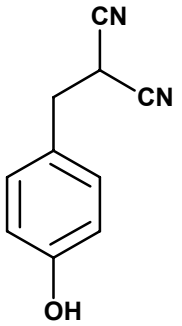

Tyrphostin 63

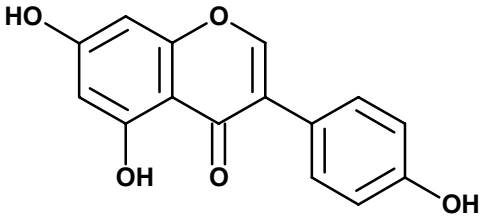

Genistein

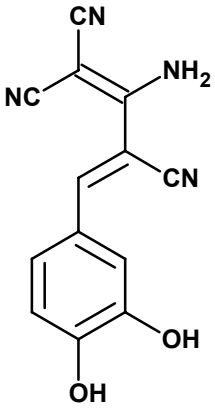

Tyrphostin 25

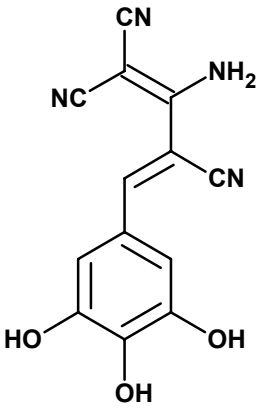

Tyrphostin 51

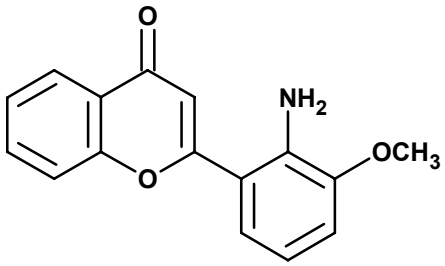

PD098059

Figure 3.2. Structure of tyrosine kinase inhibitors

This chapter firstly shows that tyrosine phosphorylation in hyphae of *A. bisexualis* is reduced by tyrphostin 63. Using various biochemical techniques, the presence of tyrosine kinase activities in crude and partially purified fractions obtained from *A. bisexualis* hyphae and *S. cerevisiae* were identified. These activities were strongly inhibited by tyrphostin 25 and tyrphostin 51. Mycelial growth as well as extension of individual hyphae was reduced by tyrphostin 63 and tyrphostin 25.

3.2 Materials and Methods

Tyrosine kinase assay kits, phosphocellulose powder, and poly(Glu:Tyr)$_{4:1}$ were purchased from Sigma. The Centriprep desalting column was purchased from Amicon Bioseparation, Millipore.

3.2.1 *Immunocytochemistry of phosphotyrosine containing protein of A. bisexualis hyphae in the presence of tyrphostin 63*

Methods were as described in Chapter 2. Hyphae were incubated with 1 mM tyrphostin 63 prior to fixation.

3.2.2 *Protein extraction, partial purification and protein tyrosine kinase assay*

A. bisexualis

Cytosolic crude fraction: The growing edge of *A. bisexualis* mycelia were cut, quick frozen with liquid nitrogen, ground and extracted with buffer A (30 mM Tris-HCl, pH 7.1, 20 mM NaF, 5 mM EGTA, 7 mM EDTA, 2 mM DTT, 50 mM KCl, 2 mM $NaVO_3$, 2 mM PMSF, 20% glycerol). The extract was centrifuged at 10,000 g for 30 mins, the supernatant and pellets obtained were stored on ice prior to being assayed.

Triton-X crude fraction: The pellet was further re-suspended in buffer A, containing 2 % Triton X-100 and gently shaken on ice for 60 mins. The re-suspended pellet was then centrifuged at 900 g for 20 mins and the supernatant was collected, this was referred to as the Triton X-100 soluble fraction.

S. cerevisiae

Yeast cells (strain SY1129 (F131)) were streaked on YPD agar plates and incubated overnight at 30 °C. An isolated colony was selected and then cultured in 10 ml YPD media overnight at 30 °C. After this, 10 ml of the overnight culture was poured into 1 L

YPD media and further incubated at 30 °C overnight on an orbital shaker. Cells were then centrifuged at 5,000 g for 30 mins and the pellet obtained was washed twice with ice-cold 40 mM PBS pH 7.0. The pellet was then re-suspended with the extraction buffer as above and vortexed with pre-chilled ice cold glass beads for 20 mins and further sonicated for 30 mins. Lysed cells were then centrifuged at 10,000 g for 30 mins.

3.2.3 *Partially purified proteins*

The supernatants obtained as described above were then applied to a phosphocellulose (Sigma) column (1cm X 15 cm) that had been equilibrated with buffer A. The column was washed with buffer B (washing buffer containing 30 mM Tris-HCl, pH 7.1, 7 mM EDTA, 6 mM 2-mercapthoethanol, 10 % glycerol 1 mM Na_3VO_4) until the A_{280} of the elutent was below 0.1, and was then eluted with a gradient of zero to 1 M NaCl in buffer C (eluting buffer contained 40 mM Hepes pH 7.0, 7 mM EDTA, 2 mM Na_3VO_4, 20 % glycerol, 2 mM DTT). Fractions of 2 ml were collected and the kinase activity was determined by ELISA (see below). Fractions containing tyrosine kinase were then desalted using a Centriprep column, which was continuously centrifuged at 900 g for 1 hour and the column was refilled with buffer without salt and the process repeated 5 times. The desalted fraction was then applied to a poly(Glu:Tyr)4:1, which was pre-equilibrated with buffer C. The column was then washed with 150 ml of buffer C. The bound protein was then eluted with buffer C containing 0.5 mM NaCl. One ml of the fraction was collected and tested for tyrosine kinase activity by ELISA.

3.2.4 *The detection of tyrosine kinase activity by ELISA*

For the tyrosine kinase ELISA, 96-microtiter wells were coated with 150 µl of 1.25 µM poly(Glu:Tyr)$_{4:1}$ (Sigma) and incubated at 45 °C overnight. Wells were then blocked with blocking solution (5% skim milk, 10 mM PBS pH 7.2) for 45 mins at 37 °C and washed with a washing buffer (10 mM PBS pH 7.2, 0.05% Tween- 20) 5 times. The phosphorylation reaction (the final volume of which is 250 µl) contains 300 µM ATP, tyrosine kinase buffer (50 mM Hepes pH 7.0, 20 mM $MgCl_2$, 1 mM $MnCl_2$, 1 mM

Na_3VO_4) and 50 µl of the soluble crude fraction, the Triton X-100 soluble fraction or 10 µl (2 units) of growth epidermal factor receptor (EGFR) which was used as a positive control. Wells were incubated at 37 °C for 45 mins. Wells were then washed with a washing buffer 5 times. Phosphotyrosine was probed by the addition of a 1:2000 dilution of anti-phosphotyrosine antibody conjugated with horse radish peroxidase (HRP) for 45 mins at 37 °C. After this wells were washed 5 times with a washing buffer. HRP colour development solution (Sigma Fast OPD and Sigma fast Tablets) was added and incubated in the dark for 7 mins, then 2.5 N of H_2SO_4 was added. Colorimetric change was determined at a wavelength of 492 nm with the microtiter plate reader (Multiskan® MCC/340).

For assays in the presence of inhibitors, either soluble crude or Triton X100 soluble fractions were pre-incubated with different concentrations of tyrphostins for 10 mins on ice, then assayed on the poly(Glu:Tyr)$_{4:1}$- coated wells as described previously. The control contained DMSO at a concentration similar to those in the tyrphostin solutions.

3.2.5 *Detection of tyrosine kinase activity by a coupled assay*

For these reactions a phosphorylation mixture was prepared using non-coated microtiter plates. Each reaction mixture contained 1 mM ATP, 1.25 µM poly (Glu:Tyr)$_{4:1}$, 100 µl of the appropriate cell fractions and tyrosine kinase buffer to a final volume of 300 µl. For inhibition by tyrphostins, the appropriate concentration of tyrphostin was added. The reaction was incubated at 37 °C for 45 mins.

The coupled assay was carried out to a final volume of 1 ml in a plastic cuvette. The coupled assay mixture contained 0.3 mM NADH, 1 mM phosphoenolpyruvate (PEP), 20 units of pyruvate kinase (PK), 7-10 units of lactic dehydrogenase (LDH) and buffer (containing 100 mM Hepes, pH 7.5, 20 mM $MgCl_2$, 1 mM 2-mercaptoethanol (Biorad), 20 µg/ml BSA and 5 mM $MnCl_2$). The coupled assay was initiated by the addition of 300 µl of the phosphorylation mixture into 700 µl of the coupled assay mixture and then the reaction was monitored by following the reduction of NADH at 340 nm for 2-3 mins. From this the initial reaction rate was calculated.

3.2.6 *The effect of tyrphostin on tip growth*

The growing margin of a mycelial sheet of *A. bisexualis* growing on cellophane overlaying PYG agar was cut about 1 cm behind tips and mounted in a flow-through chamber with 2 % low melting point agar in PYG media. The mounted hyphae were left at room temperature for 2 hours in PYG media. The control hyphae were exposed to 1% dimethyl sulphoxide (DMSO) in PYG media. The stock solution of tyrphostins were made in DMSO and freshly diluted in PYG media to give the required concentration of tyrphostin. To monitor hyphal growth rate, hyphae were grown in PYG media for 30 mins and then incubated with the required concentration of tyrphostin for 1 hour. After 1 hour, the inhibitor solution was replaced with PYG media. Hyphae were then allowed to grow in PYG media for another 1 hour. The rate of extension of the hyphal tip was monitored at 5 mins intervals using a 10x objective lens microscope (Olympus BH2). Statistical analyses were carried out using Statistix 8.

3.2.7 *The effect of tyrphostin on mycelial growth*

An agar plug of growing mycelia of *A. bisexualis* was inoculated onto PYG agar plates on which the media agar was overlaid by cellophane. Control plates contained 1% DMSO. The experimental plates contained different concentrations of tyrphostin 63 and 25 in the agar. Mycelia were imaged after 36 hours incubation at 20 °C. Digital images were generated using a Microtek Scanmaker V6USL Scanner (Microtek Lab Incorporated). Stored digitised images were processed using a combination of Metamorph (Universal Imaging Corporation, West Chester, PA, USA) and Adobe PhotoShop (Adobe Systems Incorporated) software prior to calculation of mycelial area which was carried out using ImageJ software that is available in the public domain via the NIH. The website for software download is ftp://rsbweb.nih.gov/pub/image-J/. Mycelial area was calculated by counting the number of black pixels in each image and multiplying this by the area that each pixel represented. The area of the inoculation plug was subtracted from the obtained value.

3.3 Results

3.3.1 *The effect of tyrphostin 63 on phosphotyrosine containing proteins in A. bisexualis hyphae*

To investigate the possible role of a tyrosine kinase in the phosphorylation of tyrosine that was observed in Chapter 2, hyphae were firstly incubated with 1 mM tyrphostin 63 for 20 mins in the dark at room temperature prior to fixation. Hyphae were then double stained with two primary antibodies, an anti-β4 integrin antibody and an anti-phosphotyrosine antibody. In hyphae that were treated with tyrphostin 63, the phosphotyrosine staining was diminished but the β4-integrin staining remained (Error! Reference source not found.). Hyphal tips were rounded, a shape that is common in slowly growing or non-growing hyphae (Error! Reference source not found. A, B). The effect of tyrphostin on growth is described in more detail below. Hyphae that were grown in the absence of tyrphostin had the long tapered tip that is characteristic of *A. bisexualis*.

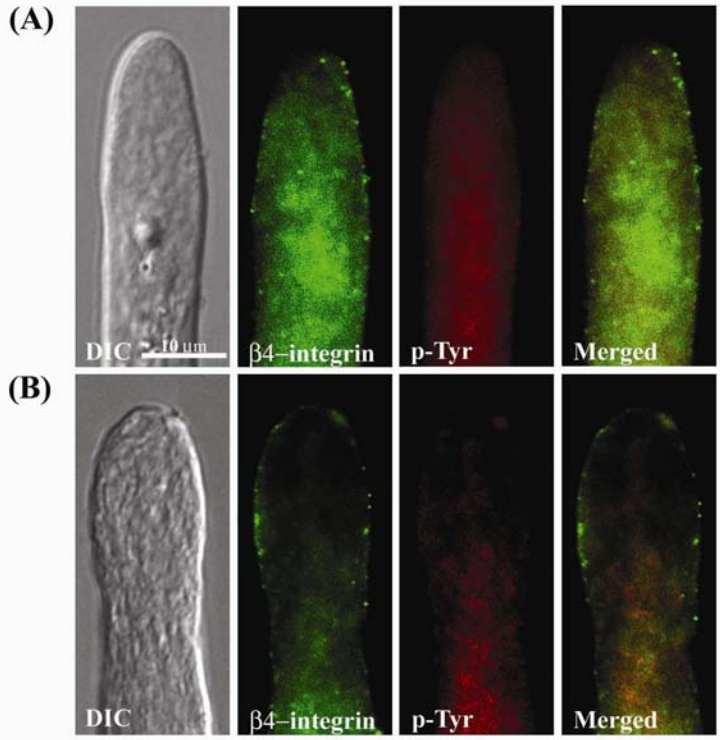

Figure 3.3. The effect of tyrphostin 63 on phosphotyrosine staining in two hyphae (A, B). Hyphae were treated with 1 mM tyrphostin 63 for 20 mins prior to fixation.

3.3.2 *The presence of protein tyrosine kinase activities in A. bisexualis and S. cerevisiae*

3.3.2.1 *Protein tyrosine kinase activity in A. bisexualis by ELISA.*

Protein extracts taken from the growing margin of five day old cultures were tested for tyrosine kinase activity using an ELISA method, the details of which are shown in Appendix 1. The study did not attempt to characterise tyrosine kinases but looked for the presence of tyrosine kinase activity in cell fractions. As a consequence, a time course of reaction as well as kinetic properties of enzymes was not fully addressed due to time constraints. This is clearly an area of some interest for future studies. The incubation time for the phosphorylation reaction was 45 mins (as described previously in (Cleaveland et al., 1990). Cytosolic crude and Triton-X soluble fractions showed significant levels of tyrosine kinase activity (**Figure 3.3.** and **Figure 3.7.**) respectively.

In the cytosolic crude fraction, tyrosine kinase activity decreased significantly in the presence of 2 mM tyrphostin 63 ($P<0.0001$, $n= 7$) and 1 mM tyrphostin 25 ($P<0.0001$, $n= 7$) (**Figure 3.3.**). However, 2 mM tyrphostin 51 did not have ($p>0.05$, $n= 7$) any inhibitory effect on kinase activity. The inhibitory effect was also tested on EGFR which was used as a control. In the absence of inhibitors, 2 units of EGFR gave an absorbance at 492 nm of 1.12 ± 0.38. In contrast, in the presence of 0.25 mM tyrphostin 25 and 51, it gave values of 0.1 ± 0.04, and 0.25 ± 0.09, respectively. Tyrosine kinase activity was also tested in the presence of 1% (v/v) DMSO which was the highest concentration required for solubility of the tyrphostins. DMSO did not inhibit tyrosine kinase activity at this concentration.

To further investigate the kinase activity genistein was used which is another tyrosine kinase inhibitor, inhibiting kinases by competing at ATP binding sites. At 0.5 mM of genistein, tyrosine kinase activity was significantly ($p<0.0001$, $n= 7$) reduced in the cytosolic crude fraction by 62%. Moreover, 1 mM of genistein significantly ($p<0.0001$, $n= 7$) inhibited about 75% of kinase activity (**Figure 3.4.**).

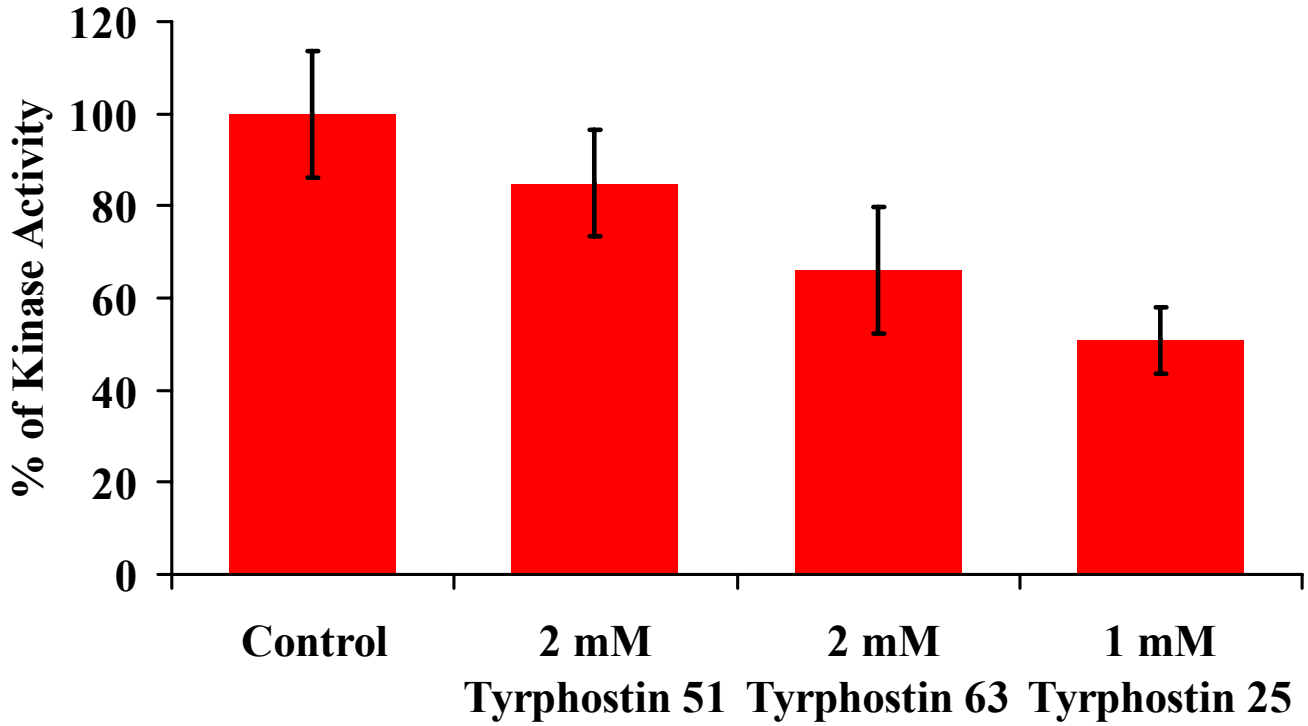

Figure 3.3. The tyrosine kinase activity of cytosolic crude fractions from *A. bisexualis* as determined by ELISA. Control contains 1% (v/v) DMSO. Data are presented as percentage relative to the control. The Absorbance at 492 nm value for the control was 0.257 ± 0.035. Averaged absorbance of kinase activities at 492 mm tyrphostin 51, tyrphostin 63 and tyrphostin 25 are, 0.218 ± 0.0298, 0.17 ± 0.035, and 0.131 ± 0.018, respectively. Data are shown as mean absorbance values ± SD.

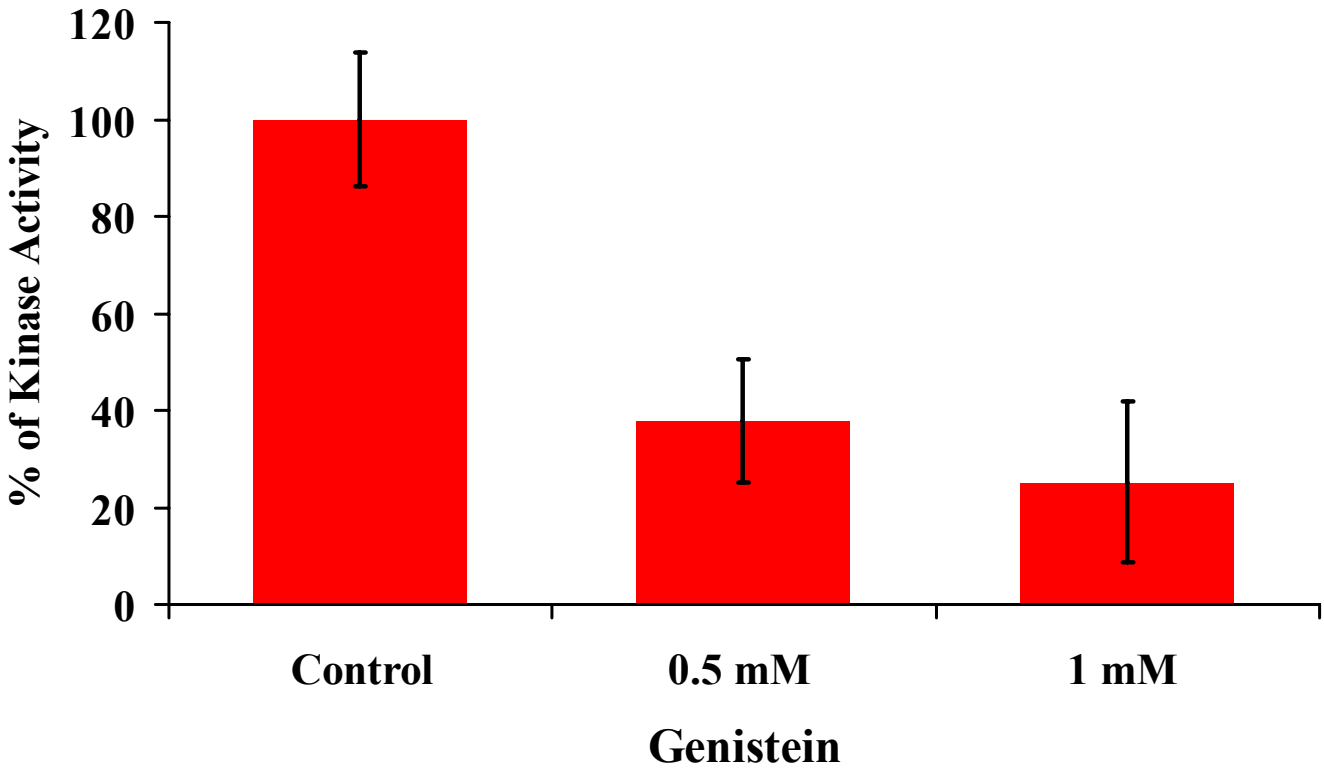

Figure 3.4. The inhibitory effect of genistein on tyrosine kinase activity in a cytosolic crude fraction of *A. bisexualis* as determined using an ELISA. Control contains 1% (v/v) DMSO. Tyrosine kinase activity was determined at the absorbance of 492 mm. Averaged absorbance of control, 0.5 mM, and 1 mM of genistein are 0.152 ± 0.021, 0.0573 ± 0.019, and 0.0384 ± 0.025, respectively. Data are shown as mean absorbance values ± SD.

A Triton X-100 soluble fraction was also tested for tyrosine kinase activity. The method for using Triton X-100 to extract proteins present in the cell debris was modified from that previously described in (Torruella et al., 1985) and (He et al., 1996). The cell debris of *A. bisexualis* mycelia that remained after the removal of the cytosolic crude fractions was extracted with 2% Triton X-100 buffer and centrifuged at 900 g for 20 mins at 4 °C. It was found that the centrifugation used affected kinase activity. A number of centrifugal forces were tested and it was found that kinase activity was absent when centrifugation was higher than 900 g.

The Triton X-100 soluble fraction showed a very high level of tyrosine kinase activity (**Figure 3.7.**), giving 1.4 ± 0.26 (n=7) absorbance at 492 nm. In the presence of 0.25 mM of tyrphostin 63, kinase activity was significantly ($p<0.001$, n= 7) reduced by 25%. Furthermore, at 0.25 mM two additional tyrphostins, tyrphostin 25 and tyrphostin 51 also strongly inhibited kinase activity. Tyrphostin 25 and tyrphostin 51 significantly reduced ($p<0.0001$, n= 7) tyrosine kinase activity by 85%.

Partial purification of both the cytosolic crude and Triton X-100 soluble fractions was attempted using a phosphocellulose column. An SDS-PAGE showed that the partially purified fraction contained proteins with molecular masses ranging from 26 to 85 kDa (Error! Reference source not found.**.** A, lane 2). However, none of these are likely to be kinases as the partially purified fractions of the soluble crude did not have any tyrosine kinase activity that was detectable by ELISA. Prior to applying the soluble crude fraction into a phosphocellulose column, the activity of the soluble crude was tested by ELISA and gave 0.2-0.3 absorbance at 492 nm. This absorbance was low in comparison with the absorbance obtained from the Triton X-100 soluble fraction, which as described above is about 0.9-1.4 at 492 nm. The partially purified fraction of Triton X-100 soluble still showed tyrosine kinase activity as determined by ELISA.

An SDS-PAGE revealed several protein bands in the partially purified Triton X-100 soluble fractions (Error! Reference source not found.**.** B, lane 2). A number of bands were observed with especially prominent ones at 28, 34, 41 and 88 kDa which may possibly contribute to the tyrosine kinase activity. The tyrosine kinase activity from the partially purified Triton X-100 fraction was reduced in the dose dependent manner by tyrphostin 25 and tyrphostin 51 (**Figure 3.6.**).

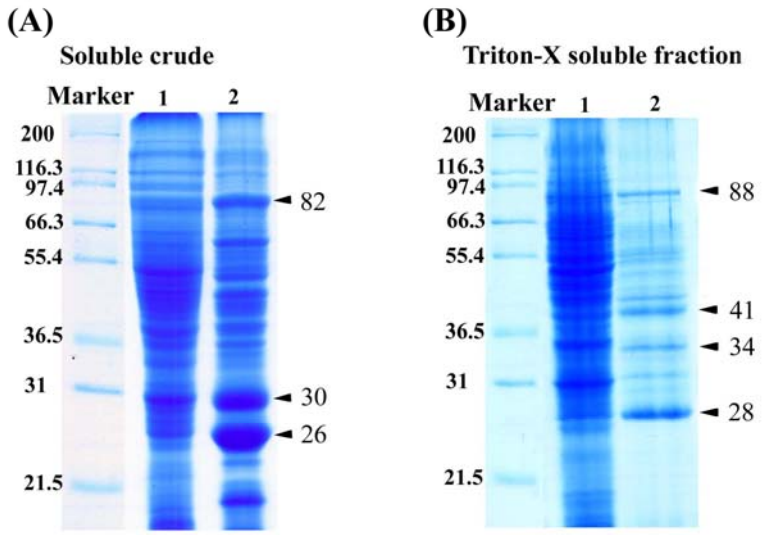

Figure 3.6. (A) is an SDS-PAGE of the soluble crude fraction (lane 1) and the partially purified fraction (lane 2) from *A. bisexualis*.
(B) is an SDS-PAGE of the TritonX-100 soluble fraction (lane 1) and partially purified fraction of the TritonX-100 fraction (lane 2) from *A. bisexualis*. Molecular weight makers are indicated. Prominent bands of 26, 30, and 82 kDa (A, lane 2) and 28, 34, 41, and 88 kDa (B, lane 2) are indicated.

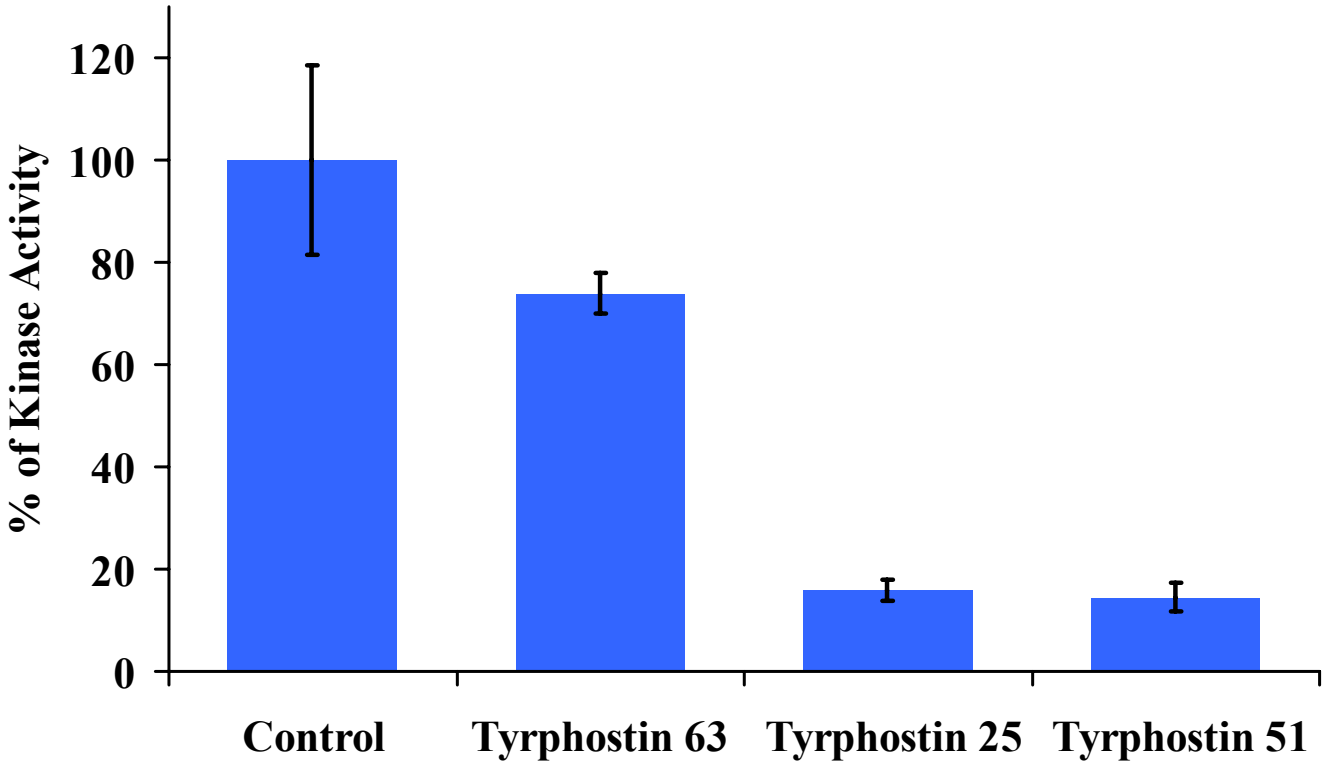

Figure 3.5. Inhibitory effect of tyrphostins on tyrosine kinase activity obtained from the Triton X-100 soluble fraction of *A. bisexualis* as determined using ELISA. All concentrations of tyrphostins contain 0.24% (v/v) of DMSO. The original absorbance at 492 nm of control, tyrphostin 63, tyrphostin 25, and tyrphostin 51 are 1.4 ± 0.26, 1.03 ± 0.056, 0.222 ± 0.031, and 0.20 ± 0.038, respectively. Data are shown as mean absorbance values ± SD

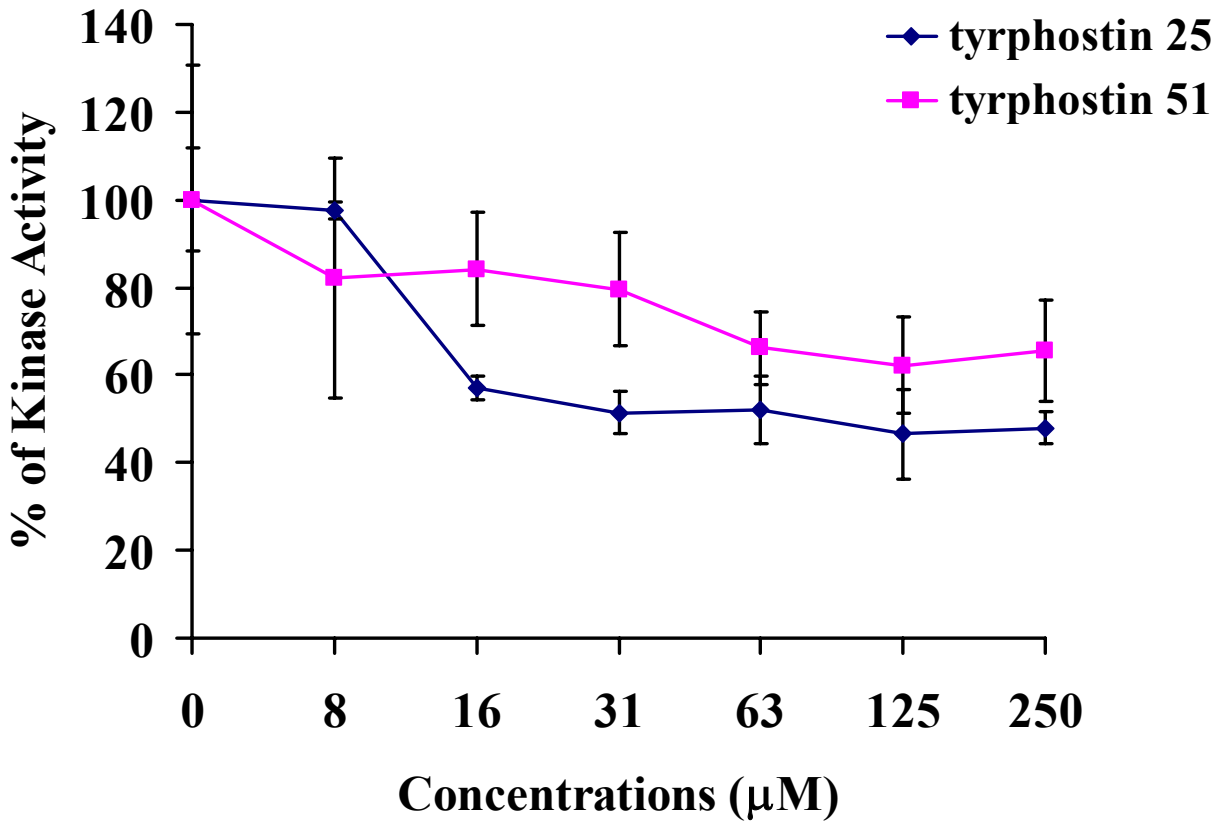

Figure 3.6. Dose dependent inhibition by tyrphostin 25 and tyrphostin 51 on kinase activity of the partially purified fractions of the Triton X-100 soluble fraction from *A. bisexualis*. The kinase activity was determined by ELISA. The absorbance at each concentration is the average of three experiments. Data are presented as percentages relative to the control.

3.3.2.2 *Protein tyrosine kinase activity in A. bisexualis by the coupled assay*

Kinase activities were also determined using a coupled assay method. The method used was modified from that of (Qiu and Miller, 2002). If tyrosine kinases are present in *A. bisexualis* extracts, in the presence of poly(Glu:Tyr)$_{4:1}$ and ATP, tyrosine kinase should phosphorylate poly(Glu:Tyr)$_{4:1}$ and release ADP. This reaction is coupled to the dephosphorylation of phosphoenolpyruvate (PEP) by pyruvate kinase (PK). The pyruvate produced is subsequently utilised by lactate dehydrogenase (LDH) with oxidation of NADH. The oxidation of NADH is then measured by spectrophotometer at 340 nm. The production of ADP from the kinase reaction is thus reflected by the amount of NAD^+ produced (see appendix 1).

The soluble crude fraction of *A. bisexualis*, in the presence of poly(Glu:Tyr)$_{4:1}$ and ATP, gave tyrosine kinase activity of 10.2 ± 2.4 x 10^{-2} units/ml (n=7) (**Figure 3.9.**). In the presence of ATP alone, the soluble crude fraction was able to utilise ATP through autophosphorylation. Autophosphorylation led to "activity" of 8.6 ± 1.3 x 10^{-2} units/ml (n=7). There is no significant ($p>0.05$, n= 7) difference between kinase activities with or without poly(Glu:Tyr)$_{4:1}$. Thus it is likely that most of phosphorylating activity in the soluble crude fraction is due to autophosphorylation. Since the soluble crude is therefore likely to have little kinase activity, inhibitory experiments were not carried out.

In contrast the Triton X-100 soluble fraction had tyrosine kinase activity. A value of 4 ± 0.89 x 10^{-2} (n=8) units/ml was obtained in the presence of poly(Glu:Tyr)$_{4:1}$ and ATP compared to 2 ± 0.74 x 10^{-2} (n=8) units/ml with ATP alone. These values are significant ($p<0.001$, n= 8) difference. In order to further evaluate the tyrosine kinase activity present in the Triton X-100 soluble fraction, 0.25 mM of tyrphostin was incubated with the Triton X-100 fraction on ice for 10 mins prior to the phosphorylation reaction. In the presence of tyrphostins 25 and 51, tyrosine kinase activity was significantly ($p<0.0001$ and $p<0.0001$, respectively, n= 8) reduced (**Figure 3.8.**). This suggests that the tyrosine kinase activity present in the Triton X-100 soluble fraction is sensitive to tyrphostins. Concentrations of tyrphostin and DMSO that the fractions were exposed to were not found to inhibit the activity of PK or LDH in the coupled assay.

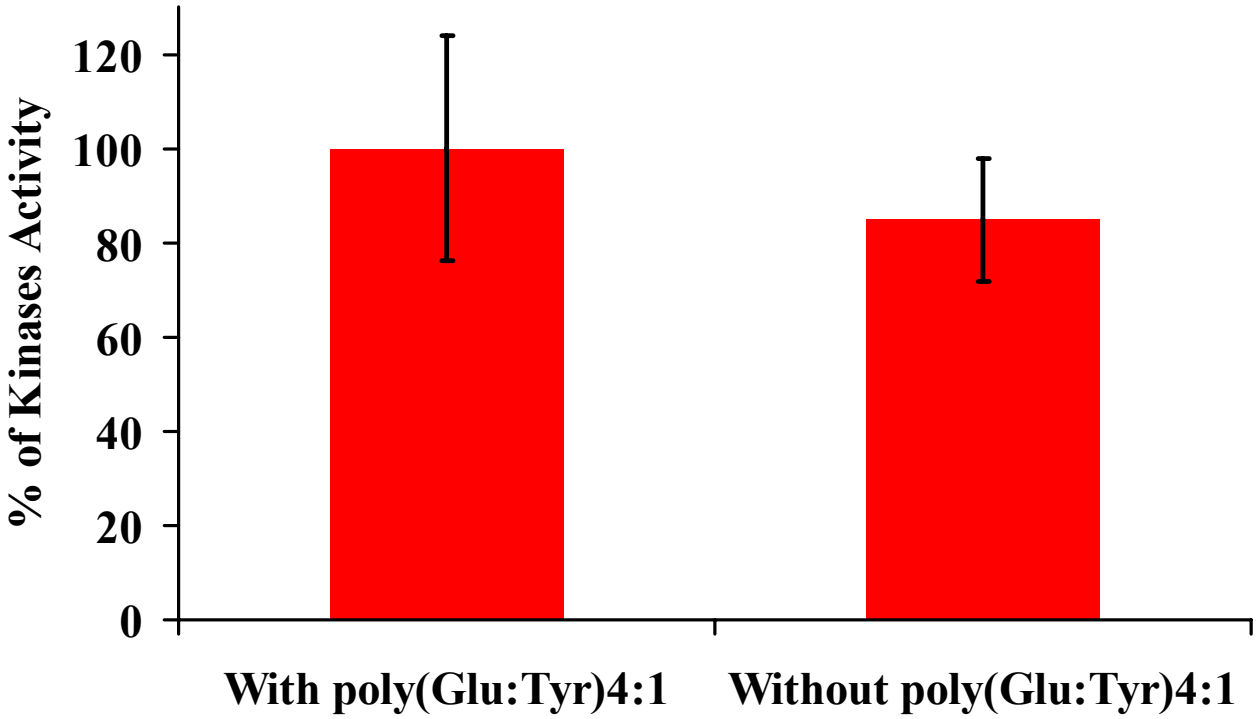

Figure 3.7. Tyrosine kinase activity of the soluble crude fraction of *A. bisexualis* with and without the exogenous substrate poly(Glu:Tyr)$_{4:1}$. The production of ADP due to phosphorylation reaction was determined using the coupled assay. The original kinase activities from the phosphorylation reaction is 10.2 ± 2.4x10^{-2} (n=8) units/ml with poly(Glu:Tyr)$_{4:1}$ and 8.6 ± 1.3x10^{-2} (n=8) units/ml without poly(Glu:Tyr)$_{4:1}$. Data are shown as mean absorbance values ± SD.

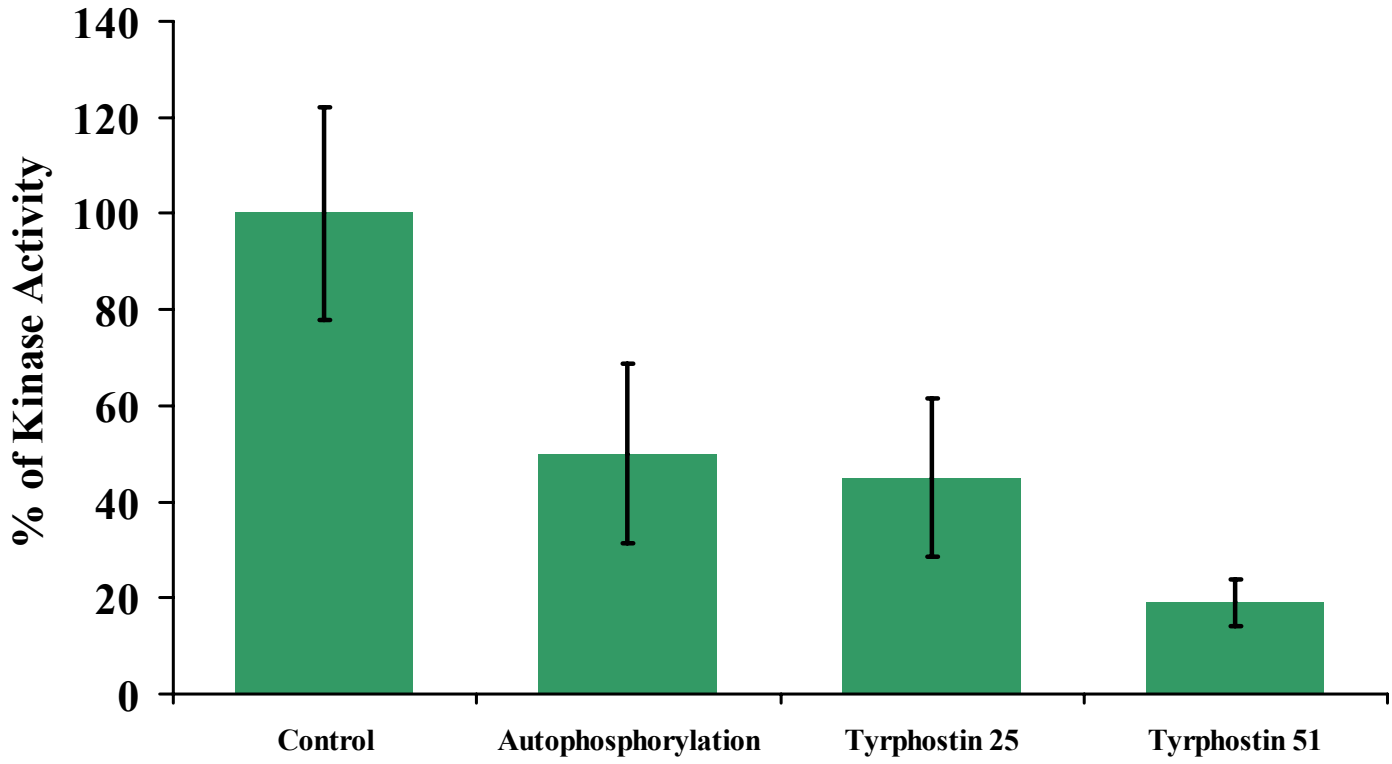

Figure 3.8. Inhibitory effect of tyrphostins on tyrosine kinase activity in the Triton X-100 soluble fractions of *A. bisexualis*. 0.25 mM of tyrphostin 25 and tyrphostin 51 was used. Original kinase activities are $3.88 \pm 0.89 \times 10^{-2}$ units/ml for the control, $1.79 \pm 0.66 \times 10^{-2}$ units/ml for tyrphostin 25, $0.758 \pm 0.21 \times 10^{-2}$ units/ml for tyrphostin 51 and $2.05 \pm 0.74 \times 10^{-2}$ units/ml for autophosphorylation. Data are shown as mean absorbance values ± SD.

3.3.2.3 *Protein tyrosine kinase activities in S. cerevisiae as determined by ELISA and the coupled assay*

The soluble crude fraction of yeast was partially purified using a combination of a phosphocellulose column, a Sephadex G-100 column and a poly(Glut:Tyr)$_{4:1}$ affinity column. Fractions containing tyrosine kinase activity from the phosphocellulose column were desalted using a Centriprep column. Then, the desalting fractions were applied to a poly(Glu:Tyr)$_{4:1}$ affinity column and eluted with 0.5 M NaCl. Tyrosine kinase activity was determined by ELISA (**Figure 3.9.**). Tyrosine kinase activity of fractions obtained from each step are also summarised in Error! Reference source not found.**.** The purification fold was increased from 130-fold by the phosphocellulose of phosphocellulose column to 230-fold by the affinity column.

The proteins present in the above fractions were examined by SDS-PAGE (Error! Reference source not found.**.**) There are five major bands that are possibly responsible for kinase activity. Proteins at 93, 50, 45, and 35 kDa bound to the poly(Glu:Tyr)$_{4:1}$-Sepharose column since these proteins showed weak or no bands in the unbound fraction washed out from the poly(Glu:Tyr)$_{4:1}$-Sepharose column (Error! Reference source not found.**.** lane 4). Especially, the 93 kDa was absent in unbound fractions. The 35 kDa protein showed a stronger band in the bound fraction but there was a trace of this in the unbound fraction.

Furthermore, 0.5 mM of tyrphostin 25 and genistein significantly ($p<0.001$, $n=8$) reduced kinase activity in partially purified fractions after passing through a poly(Glu:Tyr)$_{4:1}$- Sepharose affinity column by 54 % and 58 % respectively. However, at 1 mM tyrphostin 63 significantly reduced kinase activity only 38 % ($p<0.05$, $n=8$). In order to confirm, phosphorylation by tyrosine kinases present in partially purified fractions in the yeast, MAPKK inhibitor; PD098059 was incubated with cell fractions. At 0.5 mM PD098959 significantly ($p<0.001$) reduced kinase activity by 52 % (**Figure 3.10.**).

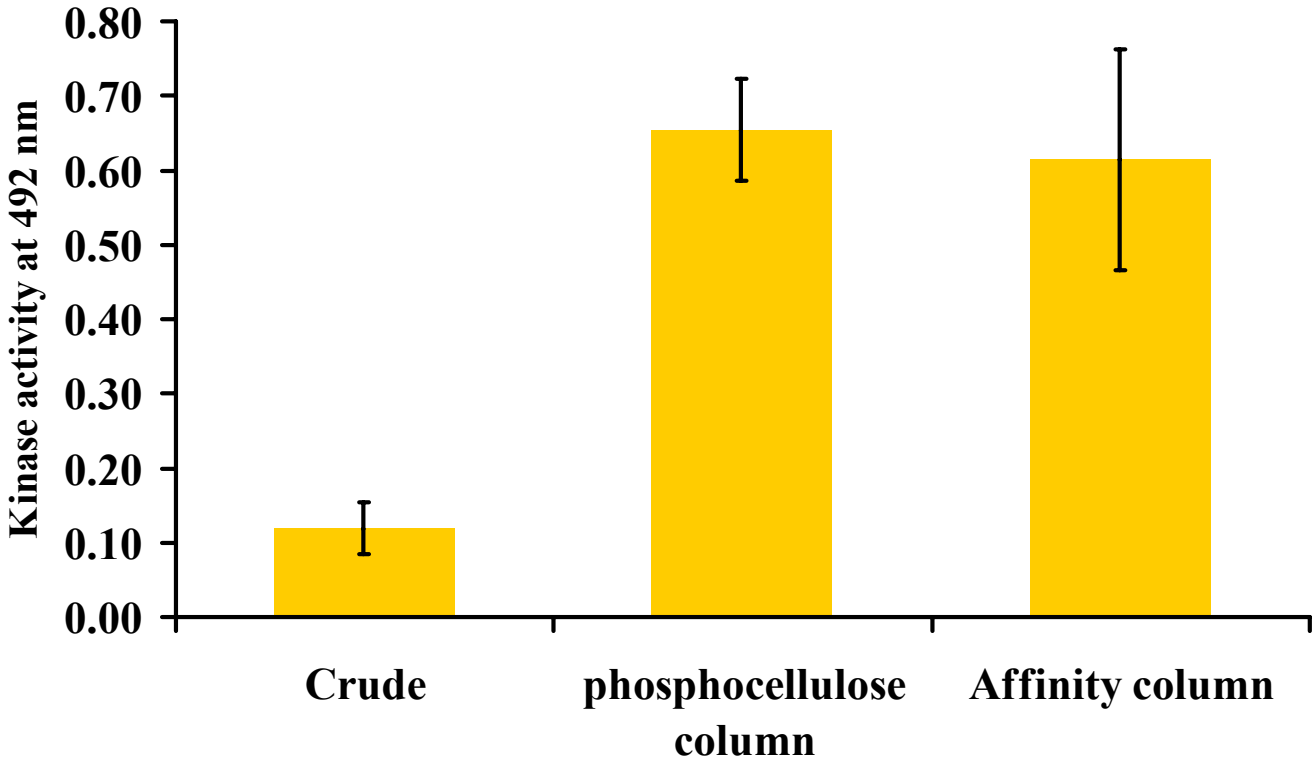

Figure 3.9. The tyrosine kinase activity obtained after various purification steps of *S. cerevisiae* as determined by ELISA. Averaged absorbance at 492 nm of tyrosine kinase activities crude, phosphocellulose column and affinity column are 0.119 ± 0.034 (n= 6), 0.654 ± 0.09 (n=9), and 0.613 ± 0.148 (n=9), respectively. Data are shown as mean absorbance values ± SD.

Table 3.2. Protein tyrosine kinase activity of *S. cerevisiae* at different stages of purification.

Purification steps	Total volume (ml)	Total protein (mg)	Specific activity (Abs 492/mg)	Purification folds
Crude	20	61.4	0.002	1
Phosphocellulose column	14	4.5	0.26	130
Sephadex G-100	9	2.7	0.28	156
Poly(Glu:Tyr)$_{4:1}$-Sepharose	7	1.8	0.46	230

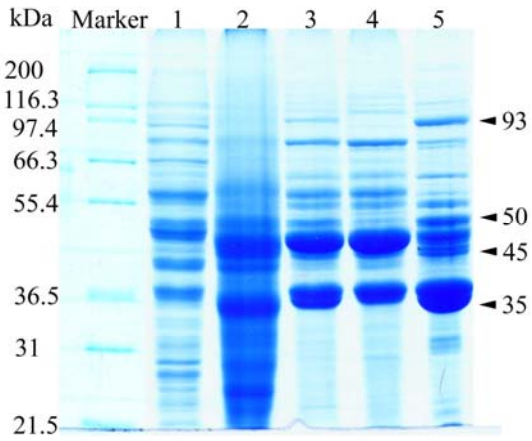

Figure 3.11. SDS-PAGE of proteins obtained from partial purified fractions of *S. cerevisiae*, lane 1= crude, lane 2= phosphocellulose column, lane 3= Sephadex G-100 lane 4= unbound proteins from poly(Glu:Tyr)4:1 column, lane 5= poly(Glu:Tyr)$_{4:1}$ Sepharose column. Marker is shown as kDa.

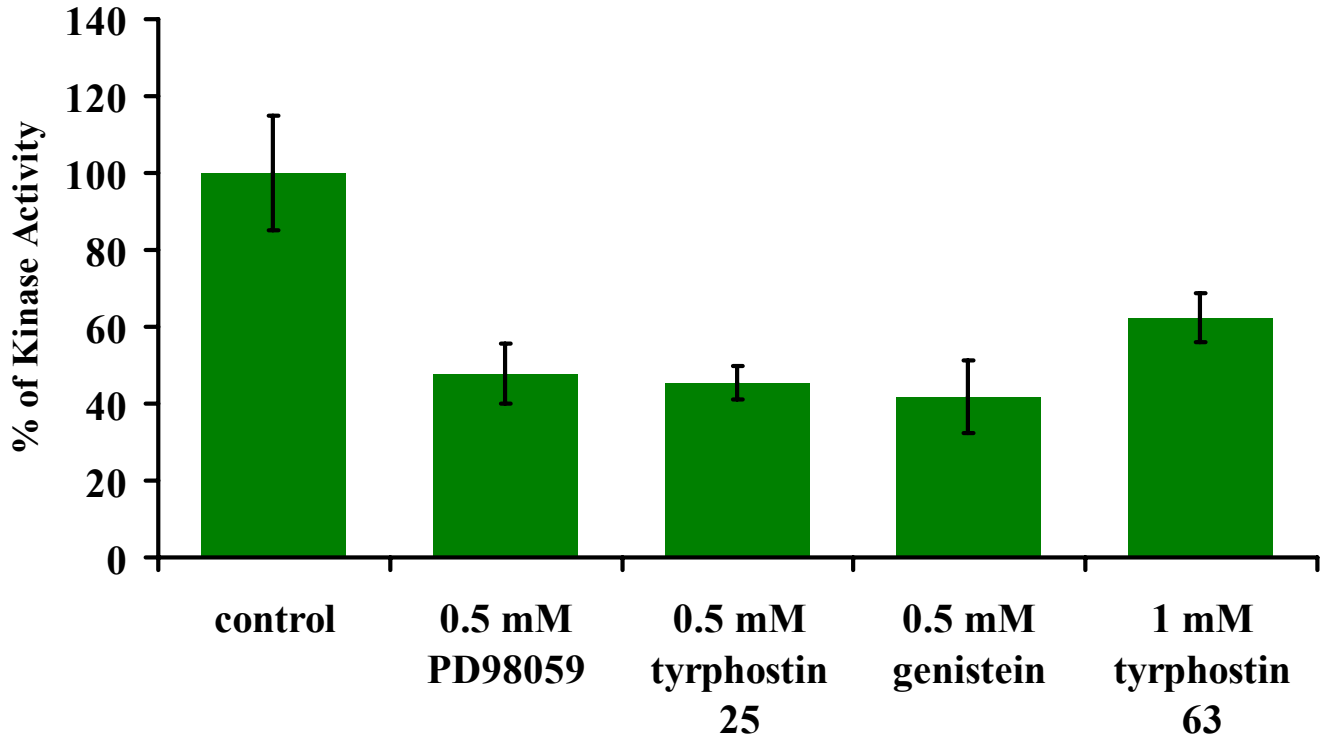

Figure 3.10. The effect of inhibitors on tyrosine kinase activity of *S. cerevisiae*. Tyrosine kinase activity was determined by ELISA. Original absorbances after treatment with PD98059, tyrphostin 25, genistein, and tyrphostin 63 are 0.21 ± 0.04, 0.2 ± 0.02, 0.19 ± 0.04 and 0.28 ± 0.03 respectively. The control was 0.44 ± 0.07. Both control and inhibitors contain 1.6 % (v/v) of DMSO.

3.3.3 *Extension rate of individual hyphae of A. bisexualis*

To evaluate the possible role of tyrosine phosphorylation in the regulation of tip growth tyrphostin 63 and tyrphostin 25 were added in growth media. The rate of tip extension of hyphae was measured in a perfusion chamber containing PYG low melting point agar. Hyphae were allowed a 60 mins recovery period. To begin the experiment, mycelia were allowed to grow for 30 mins; the tip extension was monitored at 5 mins intervals. After 30 mins, tyrphostins dissolved in PYG media were added (**Figure 3.14.** black arrow) and the rate of tip growth measured for 60 mins. After that tyrphostin was withdraw (**Figure 3.14.** red arrow) and the perfusion chamber was gently washed twice with 700 ul of PYG media and hyphae were allowed to grow in PYG media containing 1 % DMSO for another 60 mins. The growth rates showed in **Figure 3.14** were obtained from the mean values of 10 individual hyphae. Tyrphostin 63 significantly ($P<0.0001$, $n= 7$) reduced the rate of tip growth of (**Figure 3.14.**), in a dose dependent manner. After 5 mins administrating 0.5 mM tyrphostin 63 to hyphae, tip growth declined from 5.2 to 5.0 μm/min and then continually declined after 60 mins to 3.3 μm/min. After removal of the inhibitor, tip growth did not recovery after 60 mins and reduced further to about 2.9 μm/min.

At 1mM tyrphostin 63, tip growth reduced to a greater extent than 0.5 mM. Five minutes after administrating the inhibitor, tip growth was 4.6 μm/min and it continued to reduce to 2.5 μm/min after 60 mins. Tip growth reduced further to 1.8 μm/min 60 mins after removal of the inhibitor. At both 0.5 and 1 mM tyrphostin 63 affected the tip morphology. Tip morphology changed into a blunt shape after about 10-20 mins. Swelling of sub-apical regions was visible after 20-30 mins. Tyrphostin 25 also affected tip growth. Hyphae were treated with 1.5 mM tyrphostin 25, tip growth gradually declined from 4.4 μm/min to 3.6 μm/min after 60 mins treatment. However, after the inhibitor was removed, tip growth was stable and started to recovery back to 3.8 μm/min. At 0.75 mM tyrphostin 25 had little effect on tip growth. Blunt tips and swelling were observed in hyphae treated with 1.5 mM tyrphostin 25. Control hyphae were grown in

the presence of 1% (v/v) of DMSO. At this concentration, hyphae grow on averaged rate 5.2 µm/min. There was no change of tip morphogenesis in the control hyphae.

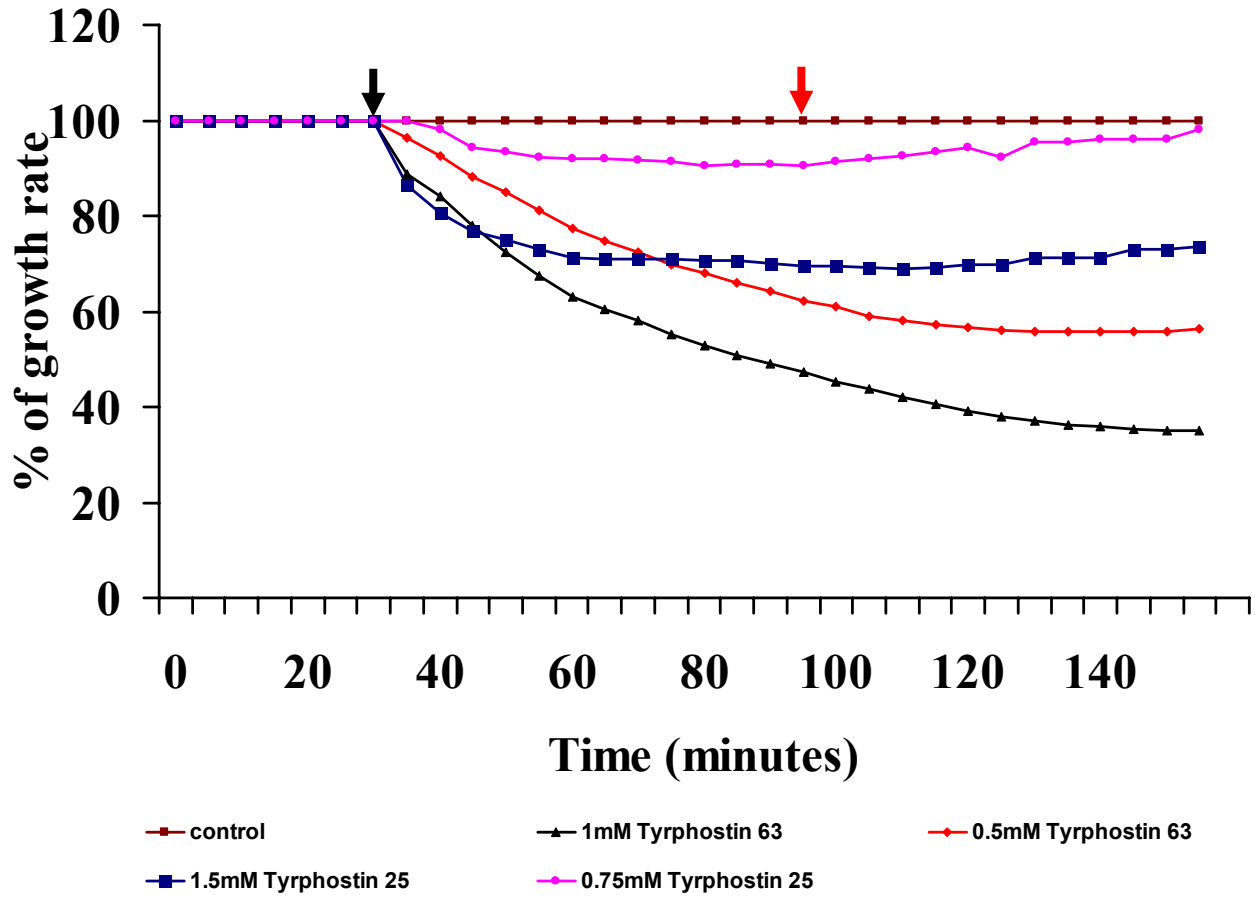

Figure 3.11. The effect of tyrphostin 63 and tyrphostin 25 on tip growth of hyphae of *A. bisexualis*. Inhibitors were added at the black arrow and removed at the red arrow. Data are shown as the average value of 7 hyphae. Growth rate of the control was 5.2 µm/min.

3.3.4 *The effect of tyrphostins on mycelial area*

Tyrphostin 63 and tyrphostin 25 were tested to investigate their effect on the growth of mycelium (Error! Reference source not found..). After 36 hrs post inoculation, the mycelia were imaged. The area of mycelia was calculated. At 0.5 and 1mM tyrphostin 63, the area of mycelia was significantly ($P< 0.0001$, $n= 7$) reduced by 73 % and 95% respectively. Mycelial area was also significantly ($P<0.0001$, $n= 7$) decreased by 67% with 1.5 mM tyrphostin 25. However, 0.75 mM of tyrphostin 25 ($P>0.05$, $n= 7$) showed no effect on mycelial area (**Figure 3.12.**).

The mycelial area of *A. bisexualis* was reduced in the presence of tyrphostin 63 and the reduction was dose-dependent. It is very interesting to note that tyrphostin 25, another potential tyrosine kinase inhibitor showed less of an inhibitory effect. This should not be expected since tyrphostin 25 has lower IC_{50} than tyrphostin 63 toward EGFR (Levitzki, 1990). One possible explanation for this is that the ability of the inhibitors to cross the cell wall and then the plasma membrane are different. Base on the structures, tyrphostin 63 has a less polar side chain (1-OH) in comparison with tyrphostin 25 (2-OH). Therefore, tyrphostin 63 is likely to cross the cell wall and plasma membrane easier than tyrphostin 25.

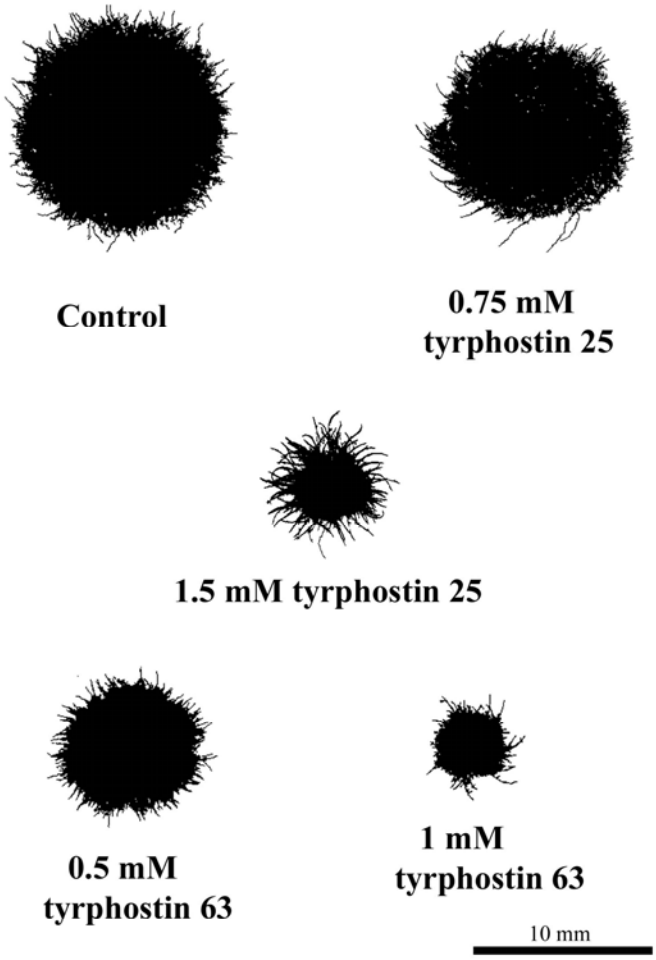

Figure 3.15. Binarised digital images of mycelial of *A. bisexualis* grown with or without tyrphostins. The control contained 1 % DMSO. The maxinum DMSO in treatment is 1%. Bar is 10 mm.

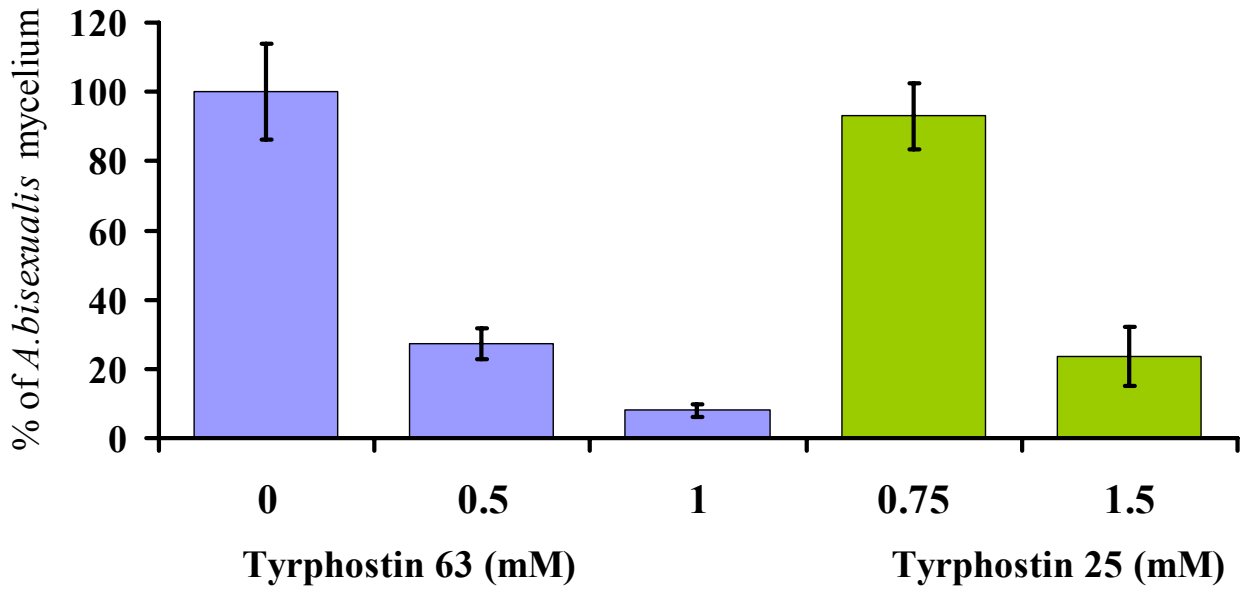

Figure 3.12. Mycelial area of *A. bisexualis* grown in the presence of tyrphostin 63 and tyrphostin 25. The control contained 1% (v/v) of DMSO. In the presence of tyrphostin 63, at 0.5 mM and 1 mM significantly reduced ($p<0.0001$, $n= 7$) the mycelial area of *A. bisexualis*. Also tyrphostin 25, at 1.5 mM significantly reduced ($p<0.0001$, $n=7$) the area of mycelia but 0.75 mM did not have any inhibitory affect ($p>0.05$, $n=7$).

3.4 Discussion

The previous chapter suggested the presence of proteins that contain phosphorylated tyrosine residues in *A. bisexualis*. This would suggest the presence of kinases that facilitate such phosphorylation. In the present chapter the possibility that tyrphostin inhibits the tyrosine kinase activity which was responsible for tyrosine phosphorylation was investigated. Hyphae that were treated with tyrphostin 63 for 20 mins before fixation showed a reduction of phosphotyrosine staining while staining of integrin-like proteins was not affected. This data suggest that tyrosine phosphorylation is sensitive to the presence of tyrphostins.

The tyrphostins are a group of synthetic compounds that were originally designed to bind the substrate subsite in the kinase domain of the epidermal growth factor receptor, against which tyrphostins 25, 51 and 63 have IC_{50} values of 3 μM, 0.8 μM and 6.5 mM respectively (Levitzki, 1990). They have since been used to inhibit a number of other tyrosine kinases, with the sensitivity to a particular tyrphostin dependant upon the identity of the kinase (Levitzki and Gazit, 1995). The results in this thesis show that the kinase activity is more sensitive to tyrphostins 25 and 51 than to tyrphostin 63, which is in keeping with a number of animal tyrosine kinases. In other walled cells tyrphostins have been found to block the cell cycle of *S. cerevisiae* (Fujimura, 1997) and to inhibit a STY dual specificity kinase in peanut (Rudrabhatla and Rajasekharan, 2004). In *Fucus*, tyrphostin 25 was found to have no effect on either germination of embryos or the elongation of rhizoids, although a number of other tyrosine kinase inhibitors affected germination and two of these had a moderate inhibitory effect on rhizoid elongation (Corellou et al., 2000). It is possible that the lack of effect of tyrphostin reflects the concentration that was used (10 μM) as inhibition of tip growth of *A. bisexualis* occurs at low millimolar concentrations.

This study also shows that tyrosine phosphorylating activity was present in cytosolic crude and Triton X-100 soluble fractions. The level of kinase activity in the cytosolic crude fraction was low in comparison with activity present in the Triton X-100 fraction.

This contrasts with results from *Fucus* embryos where attempts to characterise tyrosine kinase activity in cytosolic crude fraction were unsuccessful (Corellou et al., 2000). In the cytosolic crude fraction of *A. bisexualis*, inhibition of kinase by tyrphostins required high dose of inhibitors relative to dose of inhibitor used in the Triton X-100 fraction. This may suggest that the kinase activity present in the cytosolic crude fraction comes from a dual-specific kinase. Other possible reasons for less kinase activity in the cytosolic crude fraction are the presence of tyrosine phosphatases or a high background of autophosphorylation. Tyrosine phosphatases have been reported in fungi and plants (Dickman and Yarden, 1999; Luan et al., 2001). Even though, there are no report of tyrosine phosphatases in oomycetes, this can not be ruled out since they are highly conserved in eukaryotic cells (Luan et al., 2001).

Genistein was also found to reduce tyrosine kinase activity in the cytosolic crude fraction. Unlike tyrphostins, genistein is designed to bind at the ATP binding site of tyrosine kinases and it can specifically bind to both receptor and non-receptor tyrosine kinases (Levitzki, 1990). However, one question that needs to be considered is what is the relative specificity of genistein to kinases? Genistein can inhibit serine/threonine kinases such as a protein kinase C in animal cells at concentrations greater than 300 μM (Akiyama et al., 1987). In this study, 0.5 and 1 mM was used, both of which concentration significantly reduced kinase activity. It is thus possible that the kinase activity in the cytosolic crude is due to dual specific kinases.

The other possibility is the process of autophosphorylation may be responsible for activity in the cytosolic crude fraction. The coupled assay shows that the cytosolic crude fraction has a high back ground level of autophosphorylation. In the presence of both poly(Glu:Tyr)$_{4:1}$ and ATP, kinase activity is very high, as well as activity obtained in the presence of ATP alone. This data suggest that the phosphate groups of ATP are not transferred to poly(Glu:Tyr)$_{4:1}$ but instead they are possibly transferred to proteins, which are present in the cytosolic crude fraction. The autophosphorylation as shown by the coupled assay has also been shown on tyrosine kinases obtained from animal cells (Barker et al., 1995; Qiu and Miller, 2002). However, it is possible that several kinases, including tyrosine kinase in animal cells and MAP kinases in animals, plants and fungi

are able to autophosphorylate on serine, threonine and tyrosine residues (Dickman and Yarden, 1999).

The data from this study also shows that a phosphocellulose column partially purified cytosolic crude fraction of *A. bisexualis* does not contain tyrosine kinase activity. There are several protein bands present in a partially purified fraction one of which has a mass of 26 kDa. This peptide also contains phosphotyrosine residues as previously described in chapter 2. A 26 kDa peptide was also found in *Papaver rhoeas* but this is most likely to be phosphorylated at serine/threonine residues (Rudd et al., 1996).

Despite of the absence of tyrosine kinase activity in the cytosolic fraction, the cell wall that remained after removal of the cytosolic fraction was extracted using buffer containing Triton X-100. The purpose of employing Triton X-100 is to extract proteins that are associated between the cell wall and plasma membrane. The method of this extraction was modified from that described previously by (Torruella et al., 1985; He et al., 1996). The Triton X-100 soluble fraction contained very high tyrosine kinase activity relative to activity found in the cytosolic fraction as determined by ELISA. Furthermore, this activity was sensitive to tyrphostin 25 and tyrphostin 51 but less sensitive to tyrphostin 63.

A partially purified Triton X-100 fraction also showed tyrosine phosphorylating activity and this activity was reduced in a dose dependent manner by tyrphostin 25 and tyrphostin 51. An SDS-PAGE showed prominent protein bands at 28, 34, 41, and 88 kDa, it is possible that these peptide bands may be responsible for the kinase activity in the partially purified Triton X-100 soluble fraction. To date there is no strong evidence to support the presence of tyrosine kinases similar to those of animals in oomycete, fungi and plants. However, the oomycete *Phytophthora* has nucleotide sequences that resemble tyrosine kinases present in *Dictyostelium discoideum*, *Caenorhabditis elegans*, *Homo sapiens*, *Rattus norvegicus*, and *Mus musculus*. The identities of these *Phytophthora* sequences are Ps31050460, Ps9834403, and Ps30499946, which can be found at http://cogeme.ex.ac.uk.

A membrane-bound insulin binding protein of 67 kDa has been purified from the fungus *N. crassa* but the protein possessed no tyrosine kinase activity with poly(Glu:Tyr)$_{4:1}$

substrate (Kole et al., 1991). In plants a high level of apparent tyrosine kinase activity has been reported pea plantlets (Torruella et al., 1985). However, author did not address the question of what proteins might be responsible for the kinase activity as there was no SDS-PAGE presented and the kinase activity assay did not include tests for autophosphorylation.

Even though the structure of plant receptor kinases (PRKs), which consists of an extracellular domain, a single membrane-spanning domain and a cytosolic kinase domain resembles receptor tyrosine kinases in animal cells, PRKs belong to the serine/threonine kinase family (Cock et al., 2002). Furthermore, no receptor kinases have been found in fungi such as yeast and *N. crassa* (Shiu and Bleecker, 2001). One interesting group of plant receptors are the wall associated kinases (WAKs), which function as mediators between the cell wall and plasma membrane. As such these are integral membrane proteins. WAK1 is most abundant in plant tissue and has a protein mass of about 68 kDa and can only be extracted by boiling plant material in buffer containing 4% (w/v) SDS (He et al., 1996). The kinase activity shown in the Triton X-100 soluble fraction of *A. bisexualis* may not be a WAK like-kinase as SDS-PAGE did not show any proteins at 68 kDa. However, this possibility can not be ruled out since the cell wall of oomycetes is more similar to the plant cell wall than the fungal cell wall.

For comparison, the kinase activity from the budding yeast *S. cerevisiae* was determined. Although the *S. cerevisiae* genome does not contain an animal type tyrosine kinase gene sequence, it appears that some serine/threonine kinases are able to phosphorylate tyrosine residues of the poly(Glu:Tyr)$_{4:1}$ synthetic peptide substrate. The data from this study suggest that partially purified fractions of yeast have high levels of tyrosine kinase activity. An SDS-PAGE shows proteins of 35, 45, 50, and 93 kDa that may be responsible for this activity. The 93 kDa protein is close in size to Swe1, which has a mass of about 92.5 kDa. Swe1 is a serine/tyrosine dual-specificity kinase and plays a vital role in the mitotic process in *S. cerevisiae*. Swe1 is a negative regulator of the Cdc28 protein kinase by phosphorylation of Tyr-19 in the ATP binding site and consequently blocks the cells entry into mitosis (Sia et al., 1998; Shulewitz et al., 1999).

Several serine/threonine kinases have been found in yeast, which are able to phosphorylate poly(Glu:Tyr)$_{4:1}$. Chip technology has been used to identify 27 kinases able to phosphorylate poly(Glu:Tyr)$_{4:1}$ (Magherini et al., 2004). Tyrosine kinase activity in *S. cerevisiae* had previously been detected by using poly(Glu:Tyr)$_{4:1}$ as a substrate for in vitro phosphorylation assays (Schieven et al., 1986). The purified protein tyrosine kinase activity is associated with a 40 kDa yeast protein with features that resemble protein-serine kinases (Dailey et al., 1990). In addition the calmodulin-dependent protein kinase and cAMP-dependent protein kinase are able to phosphorylate poly(Glu:Tyr)$_{4:1}$ on tyrosine (Stern et al., 1991).

To further address kinase activity present in the partially purified fraction of yeast, the inhibitory effect of various kinase inhibitors was investigated. Both tyrphostin 25 and genistein strongly inhibited the kinase activity. In contrast, tyrphostin 63 significantly reduced kinase activity. In order to investigate whether that the activity present in yeast comes from tyrosine -like kinases or serine/threonine kinases, an inhibitor of the MAP kinase kinase PD098059 was included in the phosphorylation assay. The data shows that PD098059 significantly inhibits kinase activity when compared to tyrphostin 25 and genistein. This may suggest that the kinase activity present in yeast comes from a tyrosine-like kinase possibly comes from MAPKK. PD098059 is designed to specifically bind to MAP kinase kinase (MAPKK), and acts as a non-competitive inhibitor (Alessi et al., 1995). It does not affect the activities of some serine/threonine kinases, tyrosine kinases and phosphatidylinositol 3-kinase in animal cells (Alessi et al., 1995).

In addition to inhibition of tyrosine phosphorylation, tyrphostin 63 also showed inhibition of tip growth. At both 0.5 and 1 mM, it reduced the rate over 50%. At 1.5 mM tyrphostin 25 reduced tip growth rates by 30%. Hyphae treated with tyrphostin 63 took a longer time for hyphae to recover after removal of the inhibitor compared with hyphae treated with tyrphostin 25. This suggests that the binding of this inhibitor is reversible. The exact target of tyrphostins in hyphae is still unknown although it may well be proteins that have identified using immunocytochemistry and biochemical assays. Treatment of hyphae with tyrphostins also resulted in a change in hyphal morphology. Both tyrphostins induced sub-apical swelling and subsequently tips formed a blunt shape.

This swelling of sub-apical hyphae possibly indicates delocalised, sub-apical exocytosis, previously reported in hyphae of *S. ferax* (Bachewich and Heath, 1998),.

In Fucoid algae (Corellou et al., 2000) showed the tyrosine kinase inhibitor; herbimycin A inhibited the germination of zygotes. Furthermore, genistein prevented germination but had no effect on growth of germinated zygotes and embryos. However, (Corellou et al., 2000) found that tyrphostin 25 had no inhibitory effect on germination at ranges of 5-10 μM, which is a lower concentration than used in this study which may account for the difference in results.

Genistein was not used in the study of growth rates because the solubility of genistein required a final DMSO concentration of more than 1 %(v/v). At this concentration it shows toxicity to *A. bisexualis*. Furthermore, using genistein as an inhibitor in living organisms may be not useful since genistein itself is a phytoestrogen compound in plants (Dixon and Ferreira, 2002). Moreover, at low doses genistein promotes hyphal growth in the oomycete *Phytophthora sojae* (Connolly et al., 1999). Inhibition by tyrphostins has been reported for the cell cycle progression of *S. cerevisiae* (Fujimura, 1997). The mechanism by which tyrphostin blocks the yeast cell cycle remains unclear, but it is possible that tyrphostin inhibits a kinase which phosphorylates a protein kinase responsible for cell cycle pathways. At 10 and 50 μM, tyrphostin 25 completely blocks carrot somatic embryogenesis (Barizza et al., 1999).

Taken together, the data in this chapter illustrates that tip growth of *A. bisexualis* may utilise tyrosine phosphorylation in signalling mechanisms. The perturbation of this pathway may result in the reduction of hyphal polarity establishment. Tyrosine kinase inhibitors significantly reduce tyrosine kinase activity *in vitro*, suggesting that tyrosine like-kinases may be present in cell fractions derived from *A. bisexualis*. However, kinase activity by serine/threonine kinases can not be rule out as the latter kinases are found in diverse multicellular organisms.

Chapter 4 : The role of actin and actin-binding proteins in tip growth of *A. bisexualis*

4.1 Introduction

Eukaryotic cells have the ability to organise directed movement to migrate, feed, divide or drive the internal transport of material. The direction of movement is mediated in different ways in cells and is associated with dissipation of energy. Cytoskeletal proteins such as microtubules and actin filaments are vital for these functions by converting energy derived from ATP hydrolysis into directed movement. This chapter firstly addresses the essential background of actin. The various functions of actin will be extensively addressed in other organisms such as plants and fungi for comparison with oomycetes. Actin-binding proteins as well as signalling molecules, which are involved in the organisation of actin, will be included.

4.1.1 *Actin cytoskeleton*

Actin is an ubiquitous 43-kDa adenine nucleotide-binding protein involved in a wide range of fundamental processes in eukaryotic cells, including cell motility, cytokinesis, vesicle transport and the establishment and maintenance of cell morphology (Vorobiev et al., 2003). Actin has no enzyme activity, and thus its participation in such cellular processes resides in its ability to provide a dynamic filamentous scaffold upon which many regulatory and motor proteins interact. Actin exists in two different forms of protein structure; a globular or monomeric form (G-actin) and a filamentous form (F-actin).

4.1.2 *Actin structure*

The crystal structure of actin has been described in a number of organisms including the yeast *S. cerevisiae* (Vorobiev et al., 2003). Actin is highly conserved among organisms and thus it is likely that in the oomycetes it has a similar structure to that in other organisms. Actin in *A. bisexualis* contains 376 amino acid residues and has a molecular weight of approximately 43-kDa (Bhattacharya et al., 1992). The sequence identity of actin from *A. bisexualis* compared to other organisms is shown in **Table 4.1.** The full comparative protein sequence is shown in appendix 2.

Table 4.1. Sequence similarity (%) between different actins from different organisms.

Actin	*P. infestans*	*N. crassa*	*S. cerevisiae*	*Dictyostelium*	α-actin of human muscle
A. bisexualis	98 %	82%	81%	87%	84%

Each G-actin subunit is composed of four subdomains; subdomain 1 (residues 1-32, 70-144, and 338-375), subdomain 2 (residues 33-69), subdomain 3 (residues 145-180 and 270-337), and subdomain 4 (residues 181-269) (Vorobiev et al., 2003) (**Error! Reference source not found.**). Consistent with the high level of sequence conservation, the overall structural similarity of *A. bisexualis* and other organisms is due to small deviations between the less conserved structures. The most variable region of the actin molecule appears to be the DNase I loop (residues 35-53) in subdomain 2.

The DNase I loop is likely to reflect the plasticity of this segment altering conformation in response to nucleotide and polymerisation states (Vorobiev et al., 2003). The four subdomains are primarily held together and stabilised by salt bridges and hydrogen bonds between the phosphate groups of a bound nucleotide (i.e. ATP or ADP) and its associated divalent cation which are localised in the central position of actin molecule. The actin subunit is also distinctly polar, that is subdomain 2 has significantly less and subdomain 1 significantly has more mass than the other two subdomains (Steinmetz et al., 1997). The highest conservation is found in the interior of the protein and in extensive parts of the two lower subdomains 1 and 3. The core appears to be an ancient nucleotide-binding pocket and clearly is informative in elucidating common properties, such as the conformations of open and closed states coupled to interdomain motion around hinge regions or the mechanism of nucleotide hydrolysis (Troys et al., 1999).

The formation of F-actin occurs by actin-actin contact between G- actin molecules. The F-actin filament can be described as consisting of either two right- handed helices of a relative long pitch or a single left-handed helix of a shallow pitch. The region contributing to longitudinal F-actin contacts are located in subdomain 3 (residues 166-169, 286-289, 322-325), subdomain 4 (residues 202-204, 243-245), subdomain 1 (residues 375) and in subdomain 2 (residues 40-45) (Holmes et al., 1990). At the physiological ionic strength, in the presence of ATP, F-actin coexist with G-actin, this G-actin polymerises itself into polar, helical filaments in which subunits are connected by a 167° rotation and 2.7 nm axial rise (Pantaloni et al., 2001). Asymmetric subunits assemble into intrinsically polar F-actin filaments by always adding onto the filament ends in the same orientation with respect to the filament axis (Kim et al., 2000). This filament polarity can be visualised by stoichiometric binding of myosin S-1 to F-actin in vivo, thereby yielding decorated filament with an arrowhead-like appearance (Steinmetz et al., 1997).

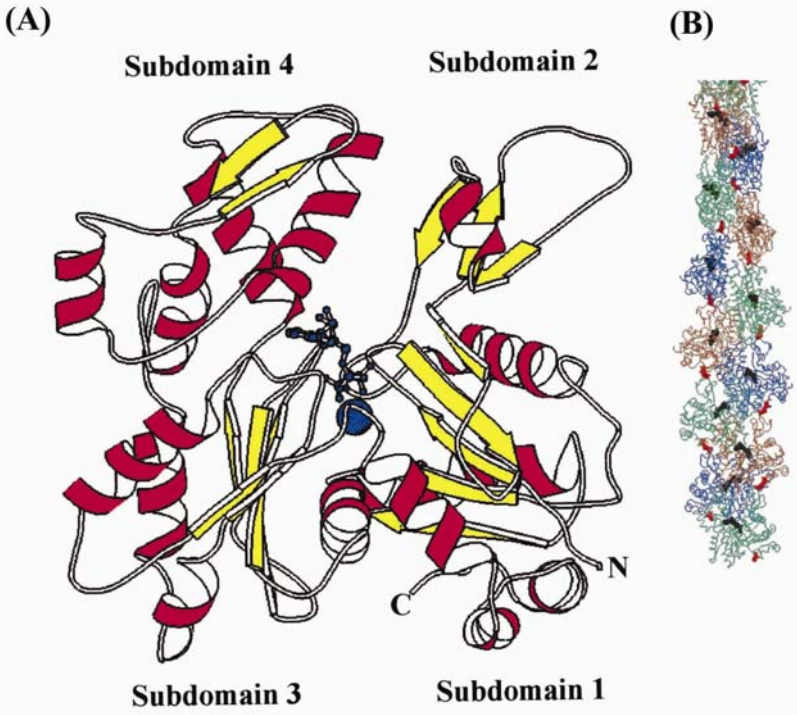

Figure 4.1. Representation of the three-dimentional structure of muscle actin with a nucleotide and divalent cation (shown in blue) bound in the central cleft; α-helices are shown in red and β-strands in yellow. The four subdomains and the NH_2- and COOH- terminus are indicated (A) (Troys et al. 1999). The model of F-actin, individual monomers are shown as colored backbone traces, Ca^{2+} -ADP as black spheres (Kim et al. 2000).

Using the fluorescence signal of actin pyrenated at Cys374, the time course for polymerising G-actin monomers into F-actin filaments is distinctly sigmoidal. It can be divided into at least three distinct phases. The lag phase, monomer activation and nucleus formation predominate and this process strongly depends on the type of divalent cation (Ca^{2+} or Mg^{2+}). After a significant number of nuclei have been formed, rapid subunit addition ensues, and the polymerisation reaction progresses into the elongation phase during which the relationship of total polymer versus time is approximate linear. The extent of filament elongation strongly depends on the exact polymerisation conditions. Finally at the steady state the monomer and polymer concentration remain invariant and the monomer concentration equals the critical concentration for polymerisation (Steinmetz et al., 1997). However, subunit exchange between the polymer and the monomer pools continues by a phenomenon called "treadmilling".

In the treadmilling cycle of F-actin at steady state (**Figure 4.1**.), all rates are equal to the rate-limiting step. The cycle comprises disassociation of ADP-actin from what is referred to as the pointed end, ATP exchange for bound ADP on G-actin, followed by association of ATP-G-actin to what is referred to as the barbed ends. The rates of nucleotide exchange, which depend on the concentration of ADP-G-actin and ATP-G-actin can not be the rate-limiting step in the treadmilling cycle. Therefore, the rate-limiting step in the treadmilling cycle is the rate of subunit dissociation from the pointed ends. Hence, factors affecting the rate of depolymerisation from the pointed ends are expected to affect the turnover of actin filaments (Carlier and Pantaloni, 1997).

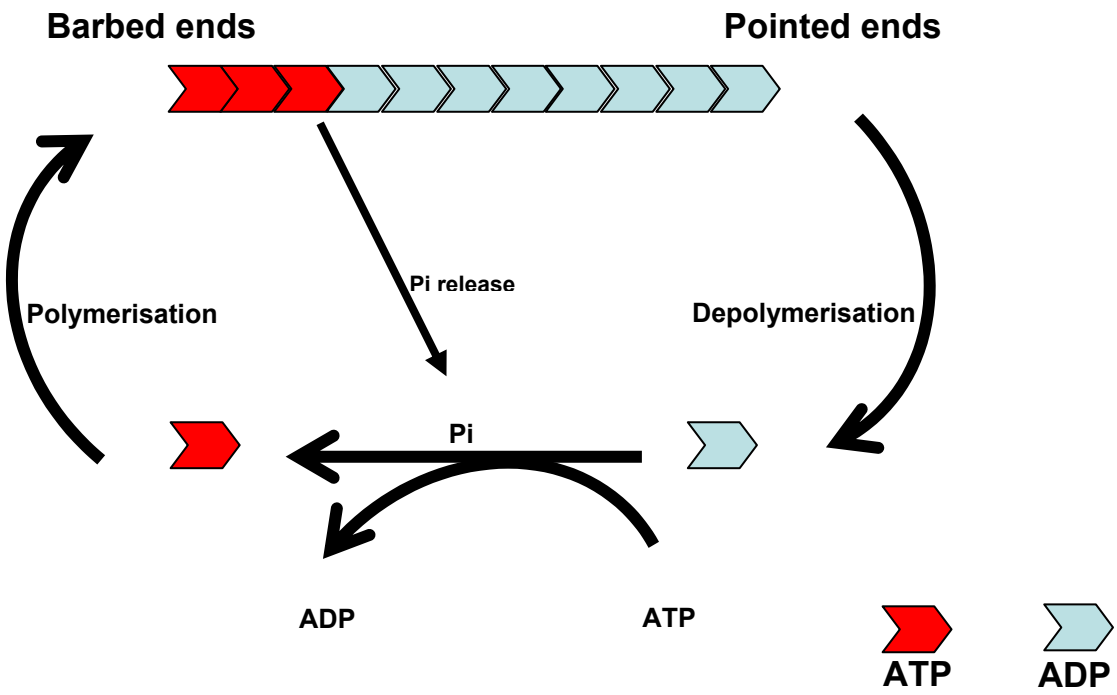

Figure 4.1. Treadmilling of actin filaments in the steady state in the presence of ATP (Carlier et al., 2003).

4.1.3 *Organisation of actin dynamic in living cells*

The mechanism underlying dynamic changes in actin organisation have been the subject of much interest. A major property of actin is its ability to self-assemble in helical, polar, dynamic filaments. The controlled assembly of actin filaments in response to appropriate stimuli generates cell protrusions called lamellipodia, filopodia and pseudopodia (Carlier et al., 2003). The extension of lamellipodia is considered as the paradigm of so-called 'actin-based motile processes'. Observations of the forward movement of the leading edge of motile cells and of the associated dynamics of actin filaments in the extending lamellipodia has revealed two points of interest (Carlier et al., 2003). Firstly, filaments with their barbed ends pointing toward the leading edge were constantly generated and growing at the plasma membrane during movement, while depolymerising occurs at the rear of the lamellipodium. Lamellipodium extension therefore results from the steady-state cycle of actin assembly, the flux of depolymerised actin subunits being used to feed the growth of barbed ends formed at specific sites at the leading edge, in a rapid treadmilling process (Chen et al., 2000).

The treadmilling process occurring *in vivo*, involves proteins referred to as actin binding proteins which regulate the treadmilling of actin filaments. Some of these actin binding proteins are considered in more depth below.

1. Actin depolymerising factor (ADF)/cofilin (AC)

AC proteins are an essential group of actin-binding proteins (18 kDa) that are ubiquitous among eukaryotes (Carlier et al., 2003). Their highly complex regulation allows them to modulate with spatial and temporal precision the turnover of filaments that is needed for many actin based process in non-muscle cells. AC accelerates pointed-end depolymerisation, which is the rate limiting step in the treadmilling cycle. A new steady state of actin assembly is established in the presence of AC, in which a high steady state concentration of monomeric ATP-G-actin supports fast barbed end growth to balance AC induced fast pointed depolymerisation (Pantaloni et al., 2001).

AC binds to ADP-actin with higher affinity than ADP-Pi-actin or ATP-actin, suggesting that the change in conformation of F-actin that follows Pi release enhances AC binding (Chen et al., 2000). The most important finding that came from electron microscopy studies was the discovery that AC changes the twists of actin filaments when it binds which indicates that the AC family has a unique property (Bamburg et al., 1999). Normally F-actin has a helical twist that results in a crossover every 35 nm (**Figure 4.2**. top). Actin filaments bound with AC have a shorter actin crossover every 27 nm, although the rise per subunit remains the same (**Figure 4.2**. bottom). The consequence of this AC induced helical twist of about -5 degree per subunit is weakening of the lateral actin-actin contact in the filament (Bamburg et al., 1999). The AC-induced twist also eliminates the phalloidin-binding site on F-actin so that AC-saturated F-actin does not stain with fluorescent phalloidin (Chen et al., 2000). Although AC binding results in dramatic changes in actin filament structure, at low resolution the conformation of the actin subunit itself appears largely unchanged. All AC proteins show *in vitro* pH dependence in their depolymerising activity due to an increase in critical concentration for the AC-actin complex as pH increases. This enhanced depolymerisation is most pronounced *in vitro* between pH 7 and 7.5 (Bamburg et al., 1999).

Figure 4.2. ADF/Cofillin on actin filament

ACs from most animals, plants and protists are regulated by phosphorylation on a highly conserved serine residue but this phosphorylation does not appear in yeast and *D. discoideum* AC (Bamburg et al., 1999). In vertebrates, serine 3 is phosphorylated by Lim kinase. In plants, however, Ca^{2+}-stimulated protein kinase activity has been identified that phosphorylates ADF on serine 6, suggesting that plants have evolved a different kinase for ADF regulation (Allwood et al., 2001).

2. Arp2/3 complex

The Arp2/3 complex is composed of two Arps (Actin-related proteins), Arp2 and Arp3 and five unique proteins (p40, p35, p21, p18 and p14), all with an apparent stoichiometry of 1:1 with each other (Millard et al., 2004). The Arp2/3 complex has been localised to the junctions of the Y-shaped actin filament branch seen in the cortical actin net work at the leading edge of motile cells (Wear et al., 2000). The Arp2/3 complex nucleates actin polymerisation in vitro resulting in the formation of Y-shaped branches on the sides of existing filaments (**Error! Reference source not found.**.). Immunocolocalisation of Arp2/3 in the lamellipodium, microscopic observation, and polymerisation studies show that when activated by WASP (Wiskott - Aldrich syndrome) proteins, Arp2/3 multiplies the filaments by branching them. Actin filaments form a dendritic Y-branched array in the lamellipodium; daughter branches grow at 70° angle from the mother branch. Arp2/3 is located at the branching points, and the barbed ends of the two branches face the leading edge of the lamellipodium (Pantaloni et al., 2001).

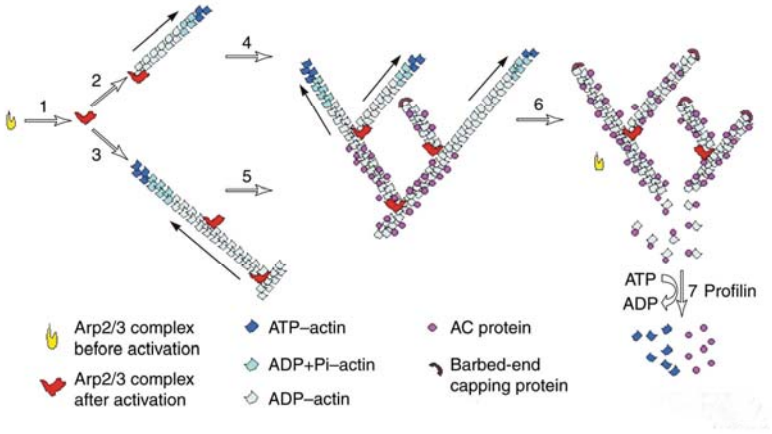

Figure 4.4. Schematic diagram showing actin dynamics at the leading edge of migrating cells. (1) The Arp2/3 complex is activated and can either (2) nucleate or capture the end pointed end of an actin filament and then (4) bind laterally to a pre-existing filament or (3) bind laterally along a pre-existing filament and then (5) nucleate or capture a filament pointed end. Barbed end growth in the presence of AC is rapid owing to the higher steady-state concentration of ATP-G-actin. Filament depolymerisation occurs further back from the membrane (6), where a free pointed end becomes exposed as a result of severing or inactivation of the Arp2/3 complex. Nucleotide exchange on the released AC-ADP-actin subunits (7) is very slow and can be rate limiting for the recycling of the actin and AC. Profilin greatly enhances the nucleotide exchange.

3. WASP family proteins

WASP is a 502 amino acid proline-rich protein expressed exclusively in haematopoietic cells. An isoform was later isolated from brain and called N-WASP, although it is in fact widely expressed (Millard et al., 2004). There are currently thought to be five proteins belonging to the WASP family: namely WASP, N-WASP, Scar/WAVE1, Scar/WAVE2, and Scar/WAVE3 (Weaver et al., 2003). Conserved features of WASP are the carboxy-terminal effecter domain-commonly referred to as the 'verprolin homology, cofilin homology and acidic' or VCA domain (Wear et al., 2000). The VCA domain binds monomeric actin and this binding, which has been localised to the V-region (verprolin homology), is essential for stimulation of Arp2/3 nucleation activity. The N-terminal of WASP-family proteins is more divergent among family members. Each possesses a proline-rich region adjacent to the WCA domain that acts as a binding site for various SH3 domain-containing proteins (Millard et al., 2004). In the full-length WASP protein, binding of actin and Arp2/3 complex to VCA is prevented due to an auto-inhibited fold of WASP. Binding of PIP2, Cdc42-GTP and Grb2 to their respective targets on WASP promotes a structural change of WASP, exposing the VCA domain for association with G-actin and Arp2/3 complex (Carlier et al., 2003).

4. Profilin

Profilin specifically interacts with ATP-G-actin. A thus formed profilin-actin complex productively associates with barbed ends exclusively (Carlier et al., 2003). Profilin has been shown to enhance the extent of Cdc42-induced Arp2/3 complex nucleation, both in neutrophil extracts and *in vitro* with purified proteins (Yang et al., 2000). To be most effective, profilin had to simultaneously bind poly-L-proline and monomeric actin. Profilin binding to Cdc42/PIP_2-activated WASP may result in complete activation by further relieving the inhibitory interaction between the VAC domain and the amino terminus (Wear et al., 2000). Furthermore, the close proximity of this profilin-bound actin subunit to the site of the Arp2/3-WASP interaction may contribute to the nucleation of actin polymerisation.

4.1.4 *Actin and components of focal adhesion proteins*

In animal cells, large number of proteins found in focal adhesions and cell junction sites and these proteins associate with F-actin, suggesting that these proteins may act at different stages of cell adhesion and junction assembly. For example talin and vinculin may be involved in focal adhesion formation, whereas α-actinin may be more important in maintaining or stabilising microfilament attachment in mature focal adhesions.

Talin is a 235-kDa protein of focal adhesions, which can be cleaved into a 47-kDa N-terminal globular head domain and a 190-kDa rod domain. Talin functions by interacting with particular structural and regulatory proteins of focal adhesions. The N-terminal domain has been shown to bind to focal adhesion kinases, polyphosphoinositides and integrins. Likewise, the C-terminal domain binds also to the integrin cytoplasmic domain and, in addition, to vinculin and to actin filaments. At pH 6.4 and low ionic strength talin could extensively crosslink actin filament into ordered bundles (Schmidt et al., 1999). The absence of talin and vinculin protein sequences in *Arabidopsis* may suggest that plants, possibly fungi and oomycete do not required these proteins for maintaining cell shape.

4.1.5 *Actin and cell polarity*

In *S. cerevisiae*, actin is absolutely required for polarised morphogenesis. During bud growth, actin cables extend from the mother cell into the bud and actin patches localise to growth sites on the bud surface. In yeast, two distinct multi-protein complexes, the polarisome and the Arp2/3 complex function down stream of the Cdc42 GTPase module to direct the localised assembly of actin filaments at polarisation sites.

The polarisome regulates the formation of linear, unbranched actin filaments. The key component of polarisome is the formin Bni1p, which binds to the barbed ends of actin filaments and nucleates microfilament assembly. In yeast, the regulation of actin patch formation is driven by the WASP homologue Las17p/Bee1p, Arp2/3 and the class I myosin Myo3p (Harris and Momany, 2004). The polarisome seems likely to direct the formation of actin cable at polar growth sites in filamentous fungi as well. Most

polarisome components as well as Arp2/3 proteins are conserved in filamentous fungi (Palmieri and Haarer, 1998). Taken together, these observations suggest that signals emanating from Cdc42 GTPase modules trigger local organisation of actin filaments via similar mechanism in filamentous fungi and yeast.

4.1.6 *Actin and tip growth*

Actin is thought to play a critical role in regulating tip growth. Tip morphogenesis involves the control of tip expansion and localisation of exocytosis of vesicles which contribute both the plasma membrane and cell wall precursors. Tip growth is thought to be driven by the coordination of turgor pressure and a gradient of regulated yielding the cell wall that generates the hyphal shape. However, tip expansion in oomycetes such as *A. bisexualis* and *S. ferax* may be more complicated. Oomycetes fail to regulate turgor pressure and can grow in the absence of measurable turgor. This suggests that a protrusive force other than turgor pressure may be present under certain conditions. This force has been suggested to be similar to that of amoeboid pseudopodia protrusion (as described above) and thus based on actin (Heath and Steinberg, 1999).

In oomycetes, the organisation of the apical F-actin correlates with apical extensibility, being most concentrated at the extreme tip where the wall is weakest, F- actin patches are prominent in the sub-apical zones. However, this arrangement may not apply to all hyphae as an actin depleted zone has recently been described in the apical region of *A. bisexualis* (Yu et al., 2004). A similar actin depleted region has also shown in pollen tubes (Vidali and Hepler, 2001)

A role for actin in tip growth is suggested as the actin distribution is growing and non-growing tips displays different pattern. Furthermore a new tip formation in branches and spore germination is characterised by the accumulation of apical actin (Bachewich and Heath, 1998). In yeast, cortical actin patches may be involved in several processes in the cell. Cortical patches are though to be cytoplasmic actin cable anchoring points to the cell membrane (Doyle and Botstein, 1996). In polarised, budding yeast, actin patches are localised to sites of polarised cell surface and actin cables are aligned along the mother-bud axis (Boldogh et al., 2001) Also supporting a role in tip growth is the observation

that disruption of actin with cytochalasins or latrunculins leads to ballooning of tips in pollen tube, oomycete, and fungi (Gupta and Heath, 1997; Gibbon et al., 1999).

In this chapter a possible role for the proteins studied in the previous two chapters in directing actin dynamics was investigated. Tyrphostin was found to affect F-actin organisation in a manner that could not be simply accounted for by a slower growth rate. A study was also made looking for the presence of the actin binding protein, talin which is a component of adhesions in animal cells.

4.2 Materials and Methods

A. bisexualis was cultured as described in previous chapters. Alexa 488 phalloidin was purchased from Molecular Probes. Monoclonal mouse IgG1 anti-chicken gizzard talin was purchased from Sigma. Latrunculin B was purchased from Biomol, Research Labs, Inc.

4.2.1 *The effect of tyrphostins and TPA on actin staining*

Hyphae from a growing culture of A. *bisexualis* were cut 1 cm behind their growing tips and allowed to recover for 60 mins in liquid PYG. To investigate the effect of tyrosine kinase inhibitors and tetrapentyl ammonium chloride (TPA) on F-actin, hyphae were incubated with tyrphostin 63 or TPA for 20 mins. Hyphae were then fixed for 30 mins in 50 mM PIPES buffer pH 6.8 containing 4% formaldehyde and 0.5 % methylglyoxal and then rinsed twice in 50 mM PIPES buffer pH 6.8. Fixed hyphae were stained for actin with Alexa 488 Phalloidin for 30 mins at room temperature and washed twice with buffer for 15 mins each time. Prior to microscopic examination, 0.1 % w/v p-phenylenediamine was added to all samples for preventing photo bleaching. Samples were examined immediately after staining using an MRC1024 confocal microscope (Bio-Rad, Mississauga, Ontario).

4.2.2 *Immunocytochemistry of talin-like protein in A. bisexualis*

A. bisexualis: Five day old mycelial sheets were excised and allowed to grow in PYG media for 60 mins. To investigate the effect of latrunculin B (Lat B) on talin-like protein, some mycelial sheets were incubated with Lat B for 20 mins. Mycelial sheets were fixed in 4% formaldehyde, 0.5 % methylglyoxal in saline buffer containing 60 mM PIPES pH 6.8, 2 mM EGTA, 2 mM $MgCl_2$, 137 mM NaCl, and 0.268 mM KCl for 45 mins at room temperature. Fixed mycelial sheets were rinsed for 5 times for 5 mins with the washing solution (0.05% v/v Tween-20 in saline) then the cell wall was digested for 15 mins in 10 mg/ml Driselase (Sigma) and membranes were permeabilised in 0.1% (v/v) Triton X-100 (Biorad) for 20 mins. The mycelial sheets were again rinsed in the washing solution 2x5

mins and blocked for 30-45 mins in blocking solution containing 2.5 % (w/v) skim milk powder and 5% (w/v) BSA (Sigma) in saline and washed 4x5 mins after blocking.

The mycelial sheets were incubated overnight with a 1:100 dilution of mouse monoclonal IgG_1 antibody raised against chicken gizzard talin, at 4 °C. The mycelial sheets were rinsed 5x5 mins and incubated with a 1:1000 dilution of the secondary antibody, Alexa™ 488 goat anti-mouse IgG (H+L) conjugate. The mycelial sheets were then washed extensively with the washing solution before addition of anti-fading solution and visualised by epifluorescence microscopy (Bio-Rad, Mississauga, Ontario).

4.2.3 *Immunoblotting of talin-like protein in A. bisexualis and S. cerevisiae*

A. bisexualis: Forty plates of *A. bisexualis* grown on PYG overlaid with cellophane were cut 1 cm from the margin of mycelia and frozen with liquid nitrogen, then ground. The powder was then re-suspended in buffer containing 50 mM Tris-HCl pH 6.2, 10 mM NaF, 7 mM EDTA, 2 mM DTT, 20 % glycerol, 7 mM β-mercapthoethanol, 2 mM PMSF, 250 mM sucrose and centrifuged at 10,000 g for 45 mins. The cytosolic fraction was then precipitated on ice by the addition of trichloroacetic acid (TCA) to a final concentration 10% for 30 mins. After centrifugation the precipitates were mixed with 5x Laemmli buffer, they were heated for 5 mins in a boiling water bath. Proteins were separated on a 5% stacking gel and 12% separating polyacrylamide gel. After SDS/PAGE, proteins were transferred to nitrocellulose membrane in a buffer containing 15.6 mM Tris-Base and 120 mM glycine and the transfer ran at 30 V at 4 °C overnight. Transferred proteins were stained with 0.1% w/v Ponceau red to check homogeneity of the transfer. The nitrocellulose blots were then blocked in 10 mM PBS containing 5 % BSA and 0.05 % Tween-20 for 2 hours at room temperature then washed with Tris-Buffer saline (TBS) 2 x 20 mins. The nitrocellulose membrane was incubated 4 °C overnight with a 1:250 dilution of mouse monoclonal IgG_1 antibody raised against chicken gizzard talin which was used as primary antibody. The membrane was visualised by Western Breeze.

S. cerevisiae: Yeast cells (strain SY1129(F131)) were streaked onto a YPD agar plate and incubated overnight at 30 °C, an isolated colony was selected and cultured in 10 ml YPD media overnight at 30 °C. Then, 10 ml of the overnight culture was poured into 1 L YPD media and further incubated at 30 °C overnight on an orbital shaker. Cells were centrifuged at 5,000 g for 30 mins and the pellet was washed twice with ice-cold 40 mM PBS pH 7.0. The pellet was then re-suspended with buffer as described for *A. bisexualis* and vortexed with pre-chilled ice cold glass beads for 20 mins (1 min vortex and 1 min on ice) and further sonicated for 30 mins on ice. Lysed cells were then centrifuged at 10,000 g for 30 mins. Electrophoresis and immunoblotting was carried out as similar for *A. bisexualis*.

4.2.4 *Co-localisation of actin and talin-like protein in A. bisexualis and S. cerevisiae*

A. bisexualis: Prior to experiments, Five day old mycelial sheets were excised and allowed to grow in PYG media for 60 mins. Mycelial sheets were fixed in 4% formaldehyde, 0.5 % methylglyoxal in saline buffer containing 60 mM PIPES pH 6.8, 2 mM EGTA, 2 mM $MgCl_2$, 137 mM NaCl, and 0.268 mM KCl for 45 mins at room temperature. Fixed mycelial sheets were rinsed for 5x 5 mins with the washing solution (0.05% v/v Tween-20 in saline) then the cell wall was digested for 15 mins in 10 mg/ml Driselase (Sigma) and membranes were permeabilised in 0.1% (v/v) Triton X-100 (Biorad) for 20 mins. The mycelial sheets were again rinsed in the washing solution 2 times for 5 mins and blocked for 30-45 mins in blocking solution containing 2.5 % (w/v) skim milk powder and 5% (w/v) BSA (Sigma) in saline and washed 4 times for 5 mins after blocking. The mycelial sheets were incubated overnight with a 1:100 dilution of primary antibodies mouse monoclonal IgG_1 antibody raised against chicken gizzard talin, at 4 °C. The mycelial sheets were rinsed 5 times for 5 mins and incubated with a 1:1000 dilution of the secondary antibody, Alexa™ 488 goat anti-mouse IgG (H+L) conjugate. After washing twice, they were then incubated with Texas Red-Phalloidin for 45 mins at room temperature in the dark. Hyphae were then washed extensively with washing solution.

Before examination, anti-fading solution (containing 0.1 % (w/v) of p-phenylenediamine dihydrochloride dissolved in nanopure water) was added to prevent photo bleaching.

S. cerevisiae: Yeast cells were cultured as previously described. Yeast cells were fixed in fixing solution as previously described for *A. bisexualis*. After washing with saline, fixed cells were incubated in KS solution (containing 100 mM KPO_4 buffer pH 7.0, 1.2 M sorbitol) at 4°C overnight. The cell wall was then digested with 10 mg/ml Driselase in KS solution containing 0.5 % β-mercapthoethanol for 30 mins at room temperature. Cells were centrifuged and re-suspended in 0.5 % v/v Triton-X in 100 mM KPO_4 buffer pH 7.0 and incubated at room temperature for 20 mins. Cells were washed and fixed to slides at 45°C for 30 mins. The slide was then washed 3 times and blocked with blocking solution (containing 1% w/v BSA, 0.05 % v/v Tween-20 and 40 mM PBS pH 7.0) for 45 mins at room temperature, then slides were washed 5 time for 5 mins and incubated with primary antibodies and secondary antibodies as previously described. Anti-fading solution was added prior to visualisation under the microscope.

4.3 Results

4.3.1 *The effect of tyrphostins on the F-actin in A. bisexualis*

To assess whether inhibition of tyrosine phosphorylation affects the F-actin cytoskeleton, hyphae were incubated with tyrphostin 63 for 20 mins, fixed in a formaldehyde/methylglyoxal combination fixative and stained with Alexa phalloidin. Growing hyphae that had not been exposed to tyrphostin showed an apical actin cap with or without an actin depleted zone (Yu et al., 2004) and a sub-apical array of peripheral plaques and diffuse filaments (Error! Reference source not found.. A). Hyphae that had been grown in the presence of 0.5 and 1 mM tyrphostin 63 showed a significant difference in actin organisation. In these hyphae, the apical cap was less predominant and the plaques moved to a position that was much closer to the tip. The transition in organisation from filamentous actin to plaques moving away from the tip was noticeably sharper. The transition effect appeared to be dose-dependent with a sharper transition with 1 mM tyrphostin 63 (Error! Reference source not found.. C) compared to 0.5 mM tyrphostin 63 (Error! Reference source not found.. B). Hyphae that had been exposed to tyrphostin and then returned to normal growth media prior to fixation showed the F-actin pattern typical of growing hyphae (Error! Reference source not found.. D).

To assess whether the observed effects of tyrphostin 63 on the cytoskeleton was not simply a consequence of slower growth rates, hyphae were treated with tetrapentyl ammonium chloride (TPA). TPA is a K^+ channel blocker that has previously been used to slow growth rates in the oomycete *S. ferax* (Kaminskyj et al., 1992). For this comparison TPA was added at a concentration of 2 mM that slowed tip growth the same amount as 1 mM tyrphostin 63 (growth at these concentrations was 25% of that control hyphae). Both TPA and tyrphostin 63 shortened the F-actin cap and decreased the intensity of staining at the tips of hyphae (Error! Reference source not found.. A-C). In a representative experiment the measured distance (mean ± SD) from the tips to the first actin plaques were 41 ± 5 μm (control, n= 5 hyphae), 15 ± 5 μm (tyrphostin 63, n= 6 hyphae), and 17 ± 5 μm (TPA, n= 8 hyphae). The differences between the tyrphostin 63

and TPA-treated hyphae and the control hyphae were statistically significant ($P<0.05$; t test).

There was no significant difference between tyrphostin 63 and TPA-treated hyphae ($P>0.05$; t test). With tyrphostin 63, however, the transition from the cap to plaques was much sharper than in TPA-treated hyphae. Hyphal morphology was also affected by the compounds, TPA gave tips with a bulbous shape (Error! Reference source not found.. B), while tyrphostin 63 eliminated the long taper (Error! Reference source not found.. C) that is characteristic of *A. bisexualis* (Error! Reference source not found.. A).

4.3.2 *Immunocytochemistry of talin-like protein in A. bisexualis hyphae*

To assess the presence of the ABP talin in *A. bisexualis* hyphae were treated with an anti-talin antibody. The latter protein is a component of focal adhesions and acts by stabilising ECM-integrin-actin links and promoting signalling downstream of active integrins. Staining of talin-like protein was mainly distributed in sub-apical regions (Error! Reference source not found.. D) with less staining in the apical region of hyphae (Error! Reference source not found.. B). By counting each patch of immunofluorescence signal of the putative talin-like proteins in hyphae, from 0-10 μm behind the tip there was approximately 4.75 ± 1.75 patches (n=20); or 19 % of total fluorescence signal and from 10-40 μm behind the tip approximately 20.8 ± 3.9 patches (n=20); or 81 % of total fluorescence signal. The distribution of immunofluorescence signals of talin-like proteins in apical and sub-apical region are significantly different ($P< 0.05$; *t* test). Moreover, staining does not appear specifically to be localised at the peripheral region of hyphae.

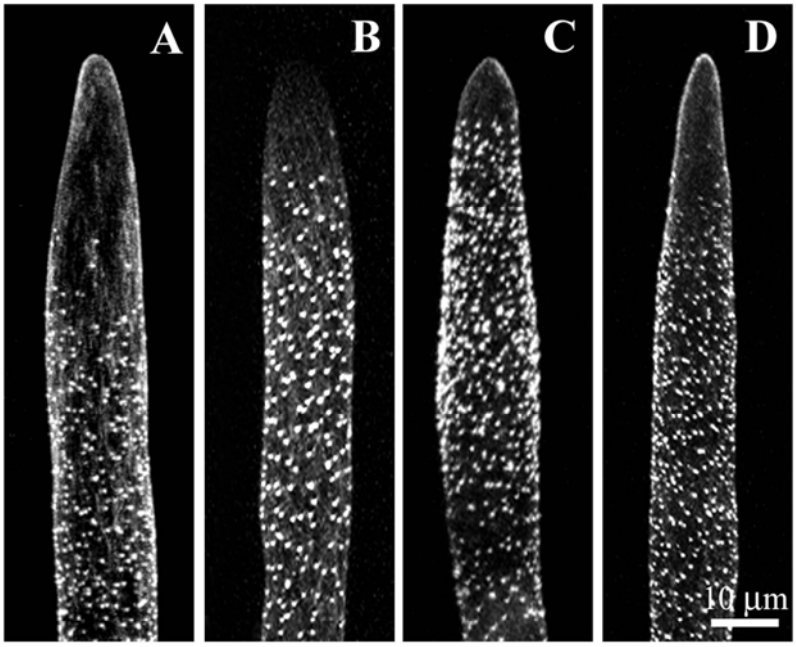

Figure 4.5. Hyphae exposed to tyrphostin 63 (0.5 mM in (B), 1 mM in (C)) grow at a slower rate and show different F-actin patterns relative to a control hyphae (A). The transition from the actin cap at the tip to sub-apical plaques is much sharper in hyphae exposed to tyrphostin. These changes are reversible, the hypha in (D) was exposed to tyrphostin and upon removal of the inhibitor, the hyphae was allowed to resume normal growth in PYG media for 45 mins.

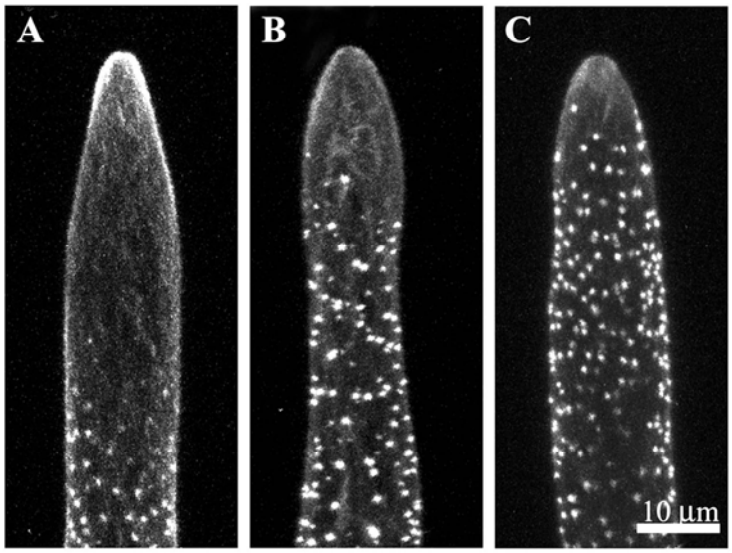

Figure 4.6. Hyphae exposed to 2 mM Tetrapentyl ammonium chloride (TPA) (B) or 1 mM tyrphostin 63 (C) show different F-actin patterns relative to each other and to a control hyphae (A). The concentrations of TPA and tyrphostin 63 were chosen as they slow tip growth by 75 %. Both compounds shortened the F-actin cap and decreased the intensity of staining. With tyrphostin 63 the transition from the cap to plaques was much sharper than in either the control or the TPA-treated hyphae. Hyphal shape was also affected by the compounds, TPA gave tips with a bulbous shape (B) while tyrphostin 63 eliminated the long taper (C) that is characteristic of *A. bisexualis* (A).

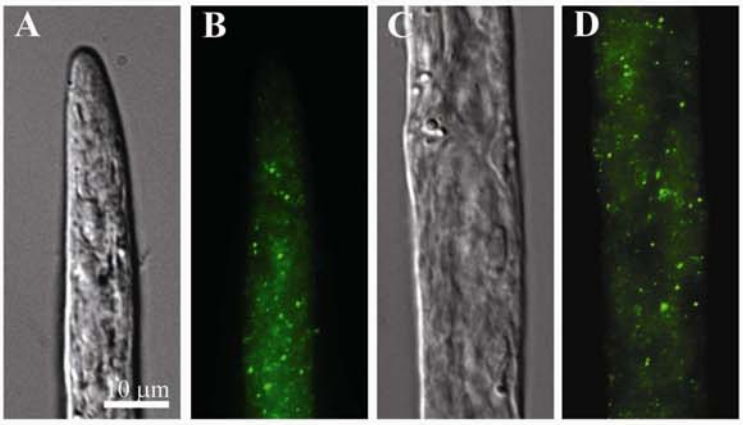

Figure 4.7. Immunocytochemistry of talin-like protein in hyphae of *Achlya*. Talin- like protein staining was located in apical region (B) and sub-apical region (D) of hyphae. Bar is 10 µm.

To further investigate whether the disruption of F-actin by Lat B affects the distribution of the talin-like protein staining in hyphae of *A. bisexualis*, hyphae were treated with 1μM of Lat B for 20 mins prior to fixation and then stained with the anti-talin antibody. Hyphae treated with Lat B showed swollen tips (Error! Reference source not found.**.** A), the distribution of talin-like protein staining was mainly located in the peripheral region of hyphae and the majority of immunofluorescence signal was located mainly (20.25 ± 6.8 (n=8); 64 %) in sub-apical regions (Error! Reference source not found.**.** B). The distribution of immunofluorescence signal patches of talin-like protein in hyphae treated with Lat B, 0-10 μm from the tip was approximately 11 ± 4.75 (n=8); or 36 % of fluorescence signal. The number of stained patches was significantly increased ($P<0.05$; *t* test) in the apical region in comparison with non-treated hyphae However, there was no significantly difference ($P>0.05$; *t* test) in the distribution of talin-like protein in the region 10-40 μm from the tip in non-treated versus treated hyphae. The presented confocal image shows staining of talin-like proteins are mainly located in the peripheral region (Error! Reference source not found.**.** D).

4.3.3 *Immunoblotting of talin-like protein in A. bisexualis hyphae*

In an attempt to identify the proteins responsible for the staining in hyphae, immunoblotting on mycelial extracts was carried out using the same antibody as above. There are three bands, with approximate molecular weights of 49, 42, and 35 kDa that were present in the supernatant at 10,000 g (**Error! Reference source not found.**. lane A). For comparative purposes, immunoblotting was also carried out on *S. cerevisiae* extracts. Only one very weak band with a molecular weight of about 37 kDa was present (**Error! Reference source not found.**. lane B).

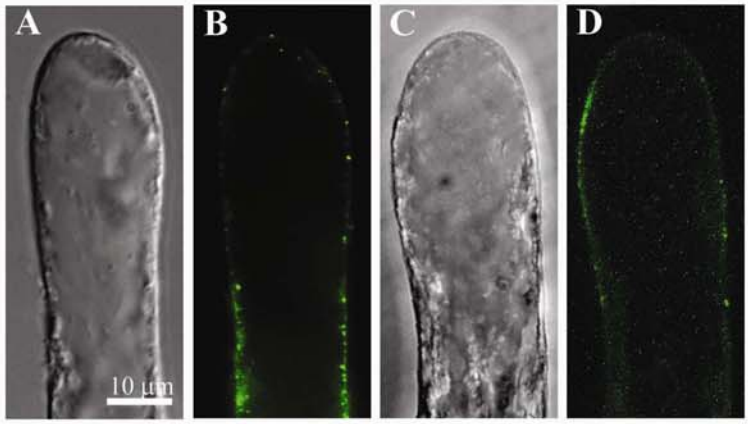

Figure 4.8. Immunocytochemistry of talin-like protein in the presence of 1 µM latrunculin B. The distribution of Talin-like protein staining is disrupted in apical and sub-apical regions. Immunostaining is mainly located in cortical region of hyphae (B). The confocal image confirms that the distribution of talin-like protein staining is mainly at the peripheral region of hyphae (D). Bar is 10 µm.

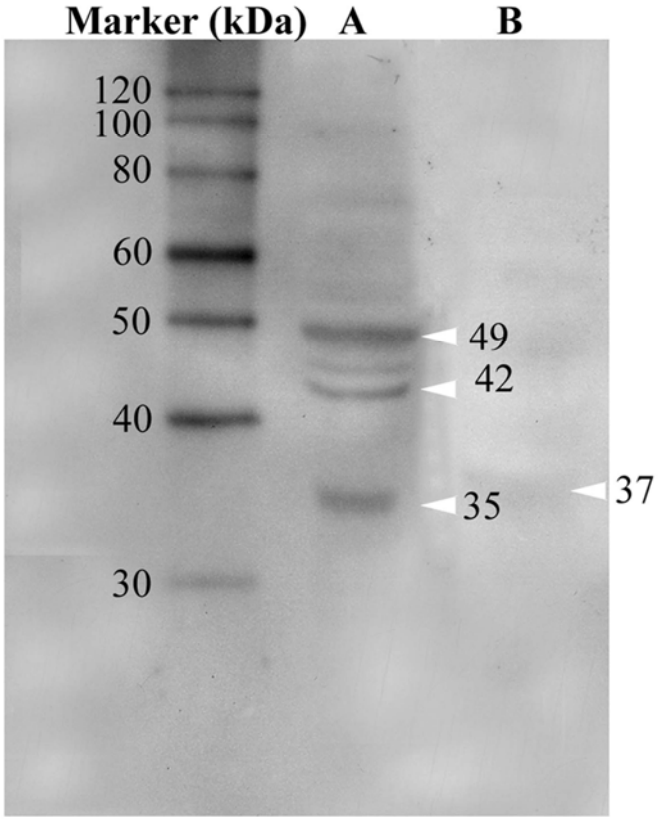

Figure 4.9. Immunoblotting of talin-like protein in *A. bisexualis* and *S. cerevisiae.* There are three polypeptides present in a cytosolic crude fraction of *A. bisexualis* that are recognised by the anti-talin antibody (A). Only one polypeptide in a cytosolic crude fraction of yeast weakly bound by the anti-talin antibody (B).

4.3.4 *Co-localisation of talin-like protein and F-actin in A. bisexualis hyphae and S. cerevisiae*

To determine whether this talin-like protein is associated with F-actin in hyphae of *A. bisexualis*, hyphae were co-stained with the anti-talin antibody and Texas Red phalloidin. Total numbers of Immunofluorescent patches of talin-like protein and the numbers of talin-like protein patches that co-localised with F-actin were counted from hyphal tips to a distance 40 µm back from the tips. Numbers of talin-like protein patches not associated with F-actin were calculated. The talin-like protein in hyphae of *A. bisexualis* does not appear to co-localise with F-actin. Numbers of total talin-like protein and unassociated talin-like protein were not significantly different ($P>0.05$; *t* test, **Table 4.2.**). As previously suggested, the talin-like protein was more predominant in the sub-apical region of *A. bisexualis* (Error! Reference source not found.**.**).

For comparative purposes, an investigation of the talin-like protein was carried out in S. *cerevisiae* (Error! Reference source not found.**.**). Immunofluorescence of talin-like protein was distributed throughout yeast cells. The total numbers of immunofluorescence patches of talin-like protein were counted from 20 yeast cells, which are given approximately 7.45 ± 3.3 or 100 % of distribution of fluorescence patches (**Table 4.3.**). The number of those that were not associated with F-actin was approximately 6.05 ± 2.8 or 81%. The total number of talin-like protein was not significantly ($P>0.05$; *t* test) different from those of unbound talin-like protein. This data suggests that as in *A. bisexualis* the talin-like protein in yeast also does not co-localise with F-actin.

Table 4.2. The distribution of co-localised talin-like proteins with F-actin in hyphae of *A. bisexualis*. Total number of fluorescence spots of talin-like protein and spots which were co-localised with actin were counted. The number of unbound talin-like proteins were obtained by subtracting the numbers of fluorescence spots of bound talin-like protein with F-actin from the total number of fluorescence spots of talin-like protein. The region from the tip to 40 μm behind tip was examined.

Total fluorescence patches of talin-like protein	19 ± 5.2 (n=15 hyphae)	100 %
Fluorescence patches of unbound of talin-like protein with F-actin	18.2 ± 5.3 (n=15 hyphae)	95%

Table 4.3. The distribution of immunofluorescence of talin-like proteins in *S. cerevisiae*. Numbers represent the immunofluorescence patches of talin-like proteins in yeast cells.

Total fluorescence patches of talin-like protein	7.45 ± 3.3 (n= 20 cells)	100%
Fluorescence patches of unbound of talin-like protein with F-actin	6.05 ± 2.8 (n= 20 cells)	81%

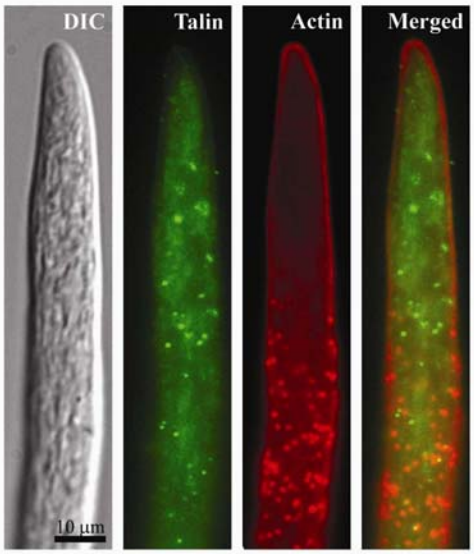

Figure 4.10. Immunofluorescence of talin-like proteins and actin in *A.bisexualis* hyphae.

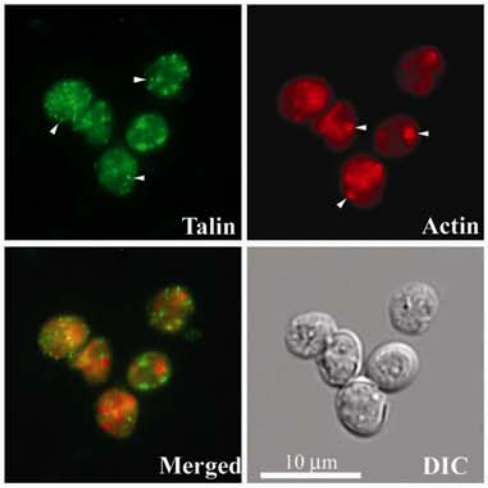

Figure 4.11. Immunofluorescence of talin-like proteins and actin in *S.cerevisiae* cells.

4.4 Discussion

The actin cytoskeleton has been implicated in the development and maintenance of polarised growth as disruption of actin and actin associated molecules result in loss of cell development. In yeast, three essential elements are required for polarised growth: cortical tag, a set of proteins that localises to the cell pole, believed to mark sites of polarised cell growth; GTPases, which are though to direct cytoskeletal regulatory components to growth sites; and the cytoskeleton, which appear to direct secretary vesicles to the growth site (Casamayor and Snyder, 2002). In oomycete hyphal tips however, such elements are still largely unknown but there are several lines of evidence that indicate that actin plays a central role in tip growth. Oomycete hyphal tips contain two populations of F-actin with different organisation. The cortical population consists of a fibrillar cap in the apex, and cables and plaques sub-apically, while the central population is diffuse and less organised (Jackson and Heath, 1993a)

The presented results show that the organisation of F-actin in hyphae of *A. bisexualis* was disturbed by tyrphostin 63 which also results in a reduction of tip growth. In hyphae treated with the inhibitor, the transition between the F-actin cap and sub-apical plaques was diminished with actin plaques locating close to the tips of hyphae. The tyrphostin 63 affect on F-actin was dose-dependent and reversible. Tyrphostin 63 does not appear to affect actin in the same way as latrunculin B, an actin polymerising agent (Error! Reference source not found.). Latrunculin disruption of actin causes tips to balloon with the ballooning extending sub-apically in the oomycete *S. ferax* (Gupta and Heath, 1997). While the exact inhibitory target of tyrphostin 63 *A. bisexualis* is unknown, previous chapters suggest a kinase capable of phosphorylating tyrosine residues. This may affect F-actin via actin binding proteins. Several actin binding proteins (ABPs) involved in actin polymerisation are regulated by phosphorylation.

There is as yet no report of actin binding proteins in *A. bisexualis*. However, both *P. infestans* and *P. sojae* have actin depolymerising factor and Arp2/3, which is analogous to those found in *Lilium longiflorum*, *Arabidopsis thaliana* and *Zea mays* (http://www.pfgd.org). This may suggest that tyrphostin may affect such processes via ABPs (Chen et al., 2000; Foissner et al., 2002). Alternatively, tyrphostin may block tyrosine phosphorylation of F-actin itself. Tyrosine phosphorylation of F-actin has been

found in leaflet movement in Mimosa (Kameyama et al., 2000). Interestingly, a single tyrosine residue at position 53 in *D. discoideum* (equivalent to position 54 of *A. bisexualis),* becomes tyrosine phosphorylated in amoeboid actin and phosphorylation of this site contributes to the binding of DNase to actin (Jungbluth et al., 1995). Furthermore, a change of the tyrosine phosphorylation state of actin results in the cell-shape changes in *D. discoideum* amoeboid (Gauthier et al., 1997). Also, tyrphostin may affect protein kinases and affect the phosphorylation state of myosin or of actin-cross linking proteins, which regulate tension within actin cytoskeleton (Grabski et al., 1998). Other tyrosine kinase inhibitors such as genistein have been shown to disrupt actin organisation and axis formation in *Pelvetia* zygotes (Corellou et al., 2000).

Disruption of F-actin in *A. bisexualis* by tyrphostin 63 and TPA gave different tip morphologies and this may suggest that the inhibitors are likely to affect different targets. Hyphae treated with TPA showed a bulbous shape while those treated with tyrphostin 63 give a blunt shape. TPA was used as an inhibitor to block K^+ channels and reduce the growth rate of oomycete *S. ferax* (Garrill et al., 1993). The K^+ channels are inhibited by TPA, which inhibits tip extension transiently. Because the K^+ movement is into the cell, the K^+ permeable channels may function in maintaining intracellular osmolarity during the volume increase due to tip extension (Lew, 1998). These data suggest that the cytoskeletal rearrangements that occur upon exposure to tyrphostin are unlikely to arise simply because of a slower growth rate.

In animal cells, tyrphostins have a strong affect on actin organisation. Specific tyrphostins selectively disrupt either cell-cell junctions or cell-substrate attachment and many disrupt both. Disruption of elements by tyrphostins suggests that a certain steady-state level of tyrosine phosphorylation is required for the maintenance of these structures within the cell (Farooki et al., 1998). In animal cells, structural components of focal adhesion and cell junctions are composed of several anchoring proteins that include vinculin, α-actinin, β-catenin, α-catenin, and talin (Brunton et al., 2004). The latter protein is a component of focal adhesions and acts by stabilising ECM-integrin-actin links and promoting signalling downstream of active integrins. Nevertheless, there is currently no evidence for the existence of talin-like proteins in plants, fungi and oomycetes. In fact protein sequences for talin is absent in the *Arabidopsis* genome

database (Hussey et al., 2002). In spite of this, this study also looked for the presence of talin or talin-like protein(s) in hyphae of *A. bisexualis* and any association with F-actin.

The immunocytochemistry and immunoblotting results suggest that *A. bisexualis* has proteins that are antigenically related to talin. The distribution of this talin-like protein is predominantly in the sub-apical region (10-40 μm from the tip). However, these proteins do not co-localise with F-actin. The monoclonal anti-talin antibody is raised against an epitope located on the 190 kDa fragment talin of chicken gizzard, which corresponds to an antigen with a molecular weight of approximately 38 kDa (Otey et al., 1990). Nonetheless, this antibody does not bind to 47 kDa fragment of talin. Immunoblotting strongly shows three polypeptide bands at molecular weight 35, 42, and 49 kDa are antigenically bound to the anti-talin antibody. Interestingly, these polypeptides present in *A. bisexualis* are much close to the 38 kDa antigen used to raise the antibody.

S. cerevisiae also contains talin-like protein staining throughout the cells. However, immunoblotting showed only a weak peptide band, in contrast with those from *A. bisexualis*, with a molecular weight of approximately 37 kDa. The polypeptides found in *A. bisexualis* and *S. cerevisiae* have molecular weights somewhat smaller than that of intact talin and this may be proteins with epitopic similarity to talin rather than being talin itself.

Although, there is no evidence to support the presence of actual talin in oomycetes, at least one protein found in *S. cerevisiae* shares a conserved sequence with talin in animal cells. The best characterised actin-binding site in animal talin ABS3 (residues 2345-2541) is located close to the C-terminal region and is highly conserved across species. It contains a so- called I/LWEQ module that is found in actin-binding proteins such as Sla2p in *S. cerevisiae* (Lee et al., 2004). This C-terminal conserved sequence tagged with GFP has recently been useful as a molecular tool for studying F-actin in plants (Ketelaar et al., 2004). However, there is no protein sequence having similarity to Sla2p existence in the *P. infestans* and *P. sojae* protein databases.

The above raises the question of whether tip growing cells require anchoring proteins to maintain cell morphology and cell development. In the plant cell membrane, an enrichment of heterotrimeric G-protein, along with several unidentified anchored proteins

as well as arabinogalactan proteins (AGPs) have been found (Wasteneys and Galway, 2003). In oomycetes, the cortical F-actin is believed to be anchored to the plasma membrane and cell wall (Kaminskyj and Heath, 1995; Bachewich and Heath, 1997). However, the relative ease with which the apical cortical F-actin contracted back to form aligned bundles in the first 7 μm of the hyphae upon plasmolysis suggest that this plasma membrane associated F-actin may not be tightly anchored through to the wall. On the other hand, the central F-actin may be more strongly anchored, via the plasma membrane, to the wall in the apex. The tightly anchored actin in the very apex could also assist in restricting growth-related components to the extreme tip (Bachewich and Heath, 1997).

The presence of talin-like protein in *A. bisexualis* is mainly in the sub-apical region, where cables and plaques of F-actin predominate. Actin plaques present in the sub-apical region associated with the plasma membrane may be required for maintaining hyphal shape of the sub-apical region while tip growth take place at the apex of hyphae. It seems likely that talin-like proteins in *A. bisexualis* may be mediating linking between actin plaques and the plasma membrane, however, this is contradictory with results that talin-like proteins do not co-localise with F-actin in the sub-apical region. The disruption of F-actin by latrunculin B also disrupts the localisation of talin-like protein in hyphae. There is more staining of talin-like protein present at the apex of hyphae, this would suggest that talin-like proteins are presence in the cytoplasm and this also may suggest that the distribution of talin-like protein may require actin.

Taken together, this chapter suggests that the tyrosine kinase inhibitor tyrphostin affects F-actin organisation that subsequently leads to slow tip growth of *A. bisexualis*. Also there are proteins epitopic similarities to animal talin present in *A. bisexualis*. These proteins however do not associate with F-actin.

Chapter 5 : Conclusions

Tip growth in fungal and oomycete hyphae and pollen tubes and root hairs of plants requires the localised synthesis and expansion of the apical plasma membrane (PM) and cell wall. The complexity of tip growth suggests a high degree of regulation that is likely to arise via bidirectional interplay between the cell wall and cytoplasm, although the exact mechanism by which such communication might occur is unknown. However, there have been suggestions that proteins with functional similarity to the integrins of the metazoa might be involved in this process.

The data presented suggests that proteins with epitopic similarity to the human β4 integrin subunit are present at the tips of hyphae of the oomycete *Achlya bisexualis*. In view of their presence at wall-membrane attachment sites, these are referred to these as integrin-like proteins rather than integrin-cross-reactive proteins. Immunoblotting identified two proteins that may be responsible for this staining, a membrane associated protein of 85 kDa and a cytosolic protein of 65 kDa. These proteins co- localised with F-actin and with anti-phosphotyrosine antibodies, a finding that would be consistent with the integrin-like proteins functioning in a signaling pathway, between the cell wall and cytoplasm, which involves tyrosine phosphorylation. Inhibition of phosphorylation with tyrphostins slows tip growth suggesting that such a pathway may be important for tip growth.

In the animal literature the β4 subunit has aroused interest because of its roles in cell adhesion in hemidesmosomes, in the stabilisation of protrusions that are rich in actin, in the mediation of force necessary for cell movement and in signaling mechanisms that stimulate cell migration and invasion (Mercurio and Rabinovitz, 2001).

These processes and their underlying molecules and mechanisms may be relevant to tip growth as one model of this process describes the apical cytoplasm as being protruded like a pseudopodium (Heath and Steinberg, 1999). The description of a molecule that is antigenically related to the β4 subunit is consistent with such a model and is especially pertinent in a growing walled cell, in that such a molecule may be capable of providing structural support and providing a means for cell migration. The presence of β4 integrin-like molecules is not unprecedented in non-metazoan cells as there have been suggestions of such proteins in prokaryotes (May and Ponting, 1999).

In animals, the β4 subunit differs from other integrins in that, in its adhesive capacity in hemidesmosomes, it binds to laminin and intermediate filaments. These connections can change however, as cell migration is possible irrespective of any specific matrix environment (O'Connor et al., 1998) and there have been reports of linkages with the actin cytoskeleton (Rabinovitz and Mercurio, 1997). Thus, the demonstration of a β4-integrin like protein that is associated with F-actin is not without precedent. The β4 integrin is also structurally distinct from other integrins with a much larger cytoplasmic domain of about 1000 amino acid residues compared to the 40-50 residues of other subunits (Hynes, 2002). The antibody used in the present study was a monoclonal that was raised against the human β4 subunit. In the absence of sequence data for *A. bisexualis,* by comparing the nucleotide sequence of the human β4 integrin with the published genome of the related oomycete *Phytophthora sojae* (http://www.pfgd.org), a short sequence of 30 nucleotides was found over which there is 97% identity. While it is unsure if this sequence represents the epitopic site of the β4 integrin-like protein, it is interesting to note that similarly sized sequences of ten amino acids, that have high identity to the human β1 integrin, have been found in a number of cells reported to be devoid of true integrins (Nagpal and Quatrano, 1999).

In other tip growing cells, integrin-like proteins have been located predominantly at the cell apex (Kaminskyj and Heath, 1995; Sun et al., 2000; Degousee et al., 2002). It should be noted that these are referred to as integrins in some studies but due to the genome data discussed elsewhere in this thesis this term is regarded as somewhat presumptuous. Immunoblots indicate a range of sizes for the proteins responsible for this staining.

Kaminskyj and Heath, (1995) using an anti-β1 serum identified a 178 kDa protein from the oomycete *Saprolegnia ferax*, that under reducing conditions gave a band of 120 kDa. β1 integrin-like proteins have also been identified in immunoblots of cell extracts from fungi such as *Neurospora crassa* (Degousee et al., 2002), *Uromyces appendiculatus* (Correa et al., 1996) and *Candida albicans* (Marcantonio and Hynes, 1988) and from a range of plant cells including *Arabidopsis thaliana* (Faik et al., 1998), onion (Gens et al., 1996) and tobacco (Lynch et al., 1998). These proteins range in size from 60- kDa to 110- kDa. Integrin-like proteins do not appear to be restricted to those with epitopic similarity to the β1subunit, however, as an 84-kDa integrin β5-like protein has been reported in *Candida albicans* (Santoni et al., 1998) and in plants, a 150- kDa protein has been detected in lily and *Hemerocallis citrina* pollen tube extracts using anti-β3 and anti-α5 serum (Sun et al., 2000).

The observation that β4 integrin-like proteins are located at the tip in some hyphae, but are more common sub-apically in others, presents an apparent paradox if, as it is proposed, these proteins are required for growth. While all attempts were made to ensure that hyphae were growing prior to fixation, the individual hyphae within a hyphal mat will typically grow at different rates. One possible explanation for the different staining patterns could therefore be that the distribution is dependant upon growth rate. The lack of any obvious morphological differences between the two populations of hyphae, however, would argue against this, as faster growing hyphae typically have a longer taper. An alternate explanation could be that certain hyphae take slightly longer to fix and thus are prone to changes in the distribution of their proteins, although again this would likely be accompanied by a morphological change. A third possibility is that these represent areas and hyphae where branching is about to occur. Clearly, this area warrants further investigation with a definitive description of the location of these proteins unlikely until they are able to be examined in the living cell.

In animal cells, integrins are capable of bidirectional signaling (Hynes, 2002). Thus, the cell is able to control ligand-integrin interactions at the extra-cellular matrix, and conversely, the ligation of integrins can affect a variety of transduction pathways. When the α6β4 integrin dimer binds to the matrix the cytoplasmic domain of the β4 subunit

becomes phosphorylated at both serine and tyrosine residues (Dans et al., 2001). Tyrosine phosphorylation occurs via a Src family kinase. This induces the recruitment of an adaptor protein Shc that upon phosphorylation activates mitogen- activated protein kinase cascades and hence cell migration. The demonstration of the co-localisation of a β4-integrin like protein and phosphotyrosine residues is consistent with a similar mechanism operating in an oomycete. However, there are no reports of autophosphorylation of the β4 integrin, so the demonstration of autophosphorylation may be unique to the oomycete β4 integrin-like protein. It is also possible, however, that an associated kinase of similar molecular weight to the β4 integrin-like protein was present in the immunoblots and was responsible for the additional phosphorylation in the presence of ATP. Many cell signaling responses occur via integrin-induced autophosphorylation of integrin associated proteins (Westhoff et al., 2004).

The prevalence of tyrosine phosphorylation in oomycetes, plants and fungi is still an area of some controversy due to the absence of typical tyrosine kinase genes, or indeed any homologues of these in the genomes that have been sequenced. Despite this, there are an increasing number of reports of phosphorylated tyrosine residues and indeed tyrosine kinase activities in these organisms. These include pea (Torruella et al., 1985), *Saccharomyces cerevisiae* (Dailey et al., 1990), alfalfa (Duerr et al., 1993), tobacco (Zhang et al., 1996), maize (Trojanek et al., 1996), coconut (Islas-Flores et al., 1998), *Mimosa* (Kameyama et al., 2000), *Fucus* (Corellou et al., 2000) and *Candida albicans* (Santoni et al., 2002). This latter study is of interest in that the phosphorylated protein, CaFAK, was antigenically related to the focal adhesion kinases of vertebrates that functions in integrin-mediated signalling. In *C. albicans* αvβ3 and αvβ5 integrin-like proteins, upon binding to vitronectin, stimulate tyrosine phosphorylation of CaFAK (Santoni et al., 2002).

Immunoblots of *A. bisexualis* extracts identified a number of proteins that contained phosphotyrosine residues. One of these had an approximate molecular weight of 85 kDa which is the same as the β4 integrin-like protein that was isolated in the microsomal fraction. While it cannot be certain that these are the same protein, this is consistent with the co-localisation that we observed being due to phosphorylated tyrosine residues in the

β4 integrin-like protein itself. The possibility can not be discounted, however, that co-localisation is due to the interaction of other phosphotyrosine containing proteins that interact with the β4 integrin-like protein.

Additional prominent bands of 26- kDa and 60- kDa were visible. This is thought to be the first report of phosphotyrosine containing proteins in an oomycete. Reported sizes of phosphotyrosine containing proteins in plant and fungal species include 97 and 57 kDa in pea (Torruella et al., 1985), 40-65 kDa in maize (Trojanek et al., 1996), 10-63 kDa in *Catharanthus roseus* (Rodriguez-Zapata and Hernández-Sotomayor, 1998) and 26 kDa in *Papaver rhoeas* (Rudd et al., 1996). The fact that no phosphotyrosine staining was observed in cells that had been exposed to tyrphostins suggests that, in addition to possible autophosphorylation there may be some phosphorylation that is due to the activity of a tyrosine kinase. This is further supported by the observation that the Triton-X100 extracted fraction and, to a lesser extent the crude fraction, showed tyrosine phosphorylation activity that could be inhibited by tyrphostins, in both ELISA and in coupled enzyme assays. Whether this activity is due to a tyrosine kinase or a dual-specificity kinase, however, is at present unclear as (Rudrabhatla and Rajasekharan, 2004) have shown a dual specificity kinase in peanut to be sensitive to tyrphostin. Regardless of this, the observation that the kinase activity was sensitive to tyrphostins, as was tip growth, suggests that the phosphorylation may be necessary for tip growth.

The tyrphostins are a group of synthetic compounds that were originally designed to bind the substrate subsite in the kinase domain of the epidermal growth factor receptor, against which tyrphostins 25, 51 and 63 have IC_{50} values of 3 μM, 0.8 μM and 6.5 mM respectively (Levitzki, 1990). They have since been used to inhibit a number of other tyrosine kinases, with the sensitivity to a particular tyrphostin dependant upon the identity of the kinase (Levitzki and Gazit, 1995). The results in this thesis show that the kinase activity is more sensitive to tyrphostins 25 and 51 than to tyrphostin 63, which is in keeping with a number of animal tyrosine kinases. In other walled cells tyrphostins have been found to block the cell cycle of *S. cerevisiae* (Fujimura, 1997) and to inhibit a STY dual specificity kinase in peanut (Rudrabhatla and Rajasekharan, 2004). In *Fucus*, tyrphostin 25 was found to have no effect on either germination of embryos or the

elongation of rhizoids, although a number of other tyrosine kinase inhibitors affected germination and two of these had a moderate inhibitory effect on rhizoid elongation (Corellou et al., 2000). It is possible that the lack of effect of tyrphostin reflects the concentration that was used (10 μM) as inhibition of tip growth of *A. bisexualis* occurs at low millimolar concentrations.

The demonstration of F-actin co-localising with the β4 integrin-like protein at wall membrane attachment sites has implications with regard to the role that these proteins may play in tip growth. Kaminskyj and Heath (1995) have suggested that a β1 integrin-F-actin association in *S. ferax* might anchor the cytoplasm, thus enabling apically directed contractions, facilitate the motility of organelles and provide a means for cell signalling. The first two of these functions would depend largely on a tip high gradient of integrin-like proteins, which is only observed in approximately one-half of *A. bisexualis* hyphae. The demonstration of co-localised phosphorylated tyrosine residues is, however, consistent with the latter function. One consequence of such signalling could be dynamic remodelling of the F-actin cytoskeleton. Such remodelling has been invoked in models of polarised growth in higher plants and is likely to involve the activation of actin-binding proteins by a variety kinases, phosphatases and phosphoinositides (Wasteneys and Galway, 2003; Wasteneys and Yang, 2004). With this in mind, it is interesting to note the effect of tyrphostin on the F-actin cytoskeleton and the recent description of an F-actin depleted zone in the actin caps at the tips of *A. bisexualis* hyphae (Yu et al., 2004). This zone may represent areas of growth where vesicles accumulate prior to exocytosis at the tip and it is possible to speculate that its activity and location could be controlled by the integrin-like proteins and any associated kinase.

The data presented also suggests that *S. cerevisiae* contains proteins with epitopic similarity to the human β4 integrin subunit. Immunoblotting identified only one candidate polypeptide in a microsomal pellet fraction. This polypeptide has a molecular weight at approximately 45 kDa. Immunofluorescence shows that staining of this integrin-like protein is mainly at cortical sites. However, the staining of integrin-like protein does not co-localise with phosphotyrosine containing proteins, which are located throughout cells.

Furthermore, immunoblotting shows that several proteins from *S. cerevisiae* contain phosphotyrosine residues especially prominent ones have molecular weights of approximately 35, 60, and 90 kDa.

In addition, using the amino acid sequence between residues 28-128 residues of the human β4 integrin subunit and comparing proteins from *S. cerevisiae* database, the search showed that there eight candidate proteins containing amino acid residues which show identity to amino acid of β4 integrin subunit. However, only one polypeptide has a molecular weight close to 45 kDa, which is shown by immunoblotting. Hem12p is 41.3 kDa and contains a transmembrane domain; this domain contains amino acid residues with 39 % identities to amino acid residues between 75-110 of the human β4 integrin subunit. Using ELISA and a coupled enzyme assay, the crude and partial purified fractions of *S. cerevisiae* have tyrosine kinase activity. This kinase activity is sensitive to tyrphostin 25 and tyrphostin 51. The SDS-PAGE shows protein bands which may be responsible for the kinase activity in partial purified fraction. These protein bands have sizes of 35, 45, 50 and 93 kDa.

In summary, the data of this thesis presents antigenic evidence suggesting the existence of a β4 integrin-like protein in hyphae of the oomycete *Achlya bisexualis* that co-localises with phosphotyrosine residues. The disruption of tyrosine phosphorylation by tyrosine kinase inhibitors causes abnormal F-actin organisation and that results in the reduction of hyphal growth in *A. bisexualis*. Similar proteins are present in *S. cerevisiae* but they do not show similar pattern of co-localisation.

References

Akiyama T, Ishida J, Ogawara H, Watanabe S, Itoh N, Shibuya M, Fukami Y (1987) Genistein, a specific inhibitor of tyrosine-specific protein kinase. Journal of Biological chemistry **262:** 5592-5595

Alessi DR, Cuenda A, Cohen P, Dudley DT, Saltie AR (1995) PD 098059 is a specific inhibitor of the activation of mitogen-activated protein kinase kinase *in vivo* and *in vitro*. The Journal of Biological Chemistry **270:** 27489-27494

Allwood EG, Smertenko AP, Hussey PJ (2001) Phosphorylation of plant actin depolymerising factor by calmodulin-like domain protein kinase. FEBS Letters **499:** 97-100

Arnaout MA, Goodman SL, Xiong J (2002) Coming to grips with integrin binding to ligands opinion. Current Opinion in cell biology **14:** 641-651

Bachewich CL, Heath IB (1997) Differential cytoplam-plasma membrane-cell wall adhesion patterns and their relationships to hyphal tip growth and organelle motility. Protoplasma **200:** 71-86

Bachewich CL, Heath IB (1998) Radial F-actin arrays precede new hypha formation in Saprolegnia: implications for establishing polar growth and regulating tip morphogenesis. Journal of cell science **111:** 2005-2016

Bamburg JR, McGough A, Ono S (1999) Putting a new twist on actin:ADF/cofilins module actin dynamics. Trends in Cell Biology **9:** 364-370

Barizza E, Schiavo F, Terzi M, Filippini F (1999) Evidence suggesting protein tyrosine phosphorylation in plants depends on the develpmental conditions. FEBS Letters **447:** 191-194

Barker SC, Kassel DB, Huang XH, Luther MA, Knight WB (1995) Characterization of pp60c-src tyrosine kinase activity a continuous assay: autoactivation of the enzyme is an intermolecular autophosphorylation process. Biochemistry **34:** 14843-14851

Bassilana M, Blyth J, Arkowitz RA (2003) Cdc24, the GDP-GTP exchange factor for Cdc42, is required for invasive hyphal growth of *Candida albicans*. Eukaryot. Cell. **2:** 9-18

Beglova N, Blacklow SC, Takagi J, Springer TA (2002) Cyteine-rich module structure reveals a fulcrum for integrin rearrangement upon activation. Nat. Struct. Biol. **9:** 282-287

Bhattacharya D, Stickel SK, Sogin ML (1992) Molecular phylogenetic analysis of actin genic regions from *Achlya bisexualis* (Oomycota) and *Costaria costata* (Chromophyta). Molecular Evolution **1991:** 525-536

Boldogh IR, Yang H, Nowakowski WD, Karmon SL, Hays LG, Yates JR, Pon LA (2001) Arp2/3 complex and actin dynamics are required for actin-based mitochondrial motility in yeast. PNAS **98:** 3162-3167

Brunton VG, MacPherson IRJ, Frame MC (2004) Cell adhesion receptors, tyrosine kinases and actin modulators: a complex three-way circuitry. Biochimica Biophysica Acta **121:** 121-144

Calderwood DA, Shattil SJ, Ginsberg MH (2000) Integrins and actin filaments: Reciprocal regulation of cell adhesion and signaling. The journal of biological chemistry **275:** 22607-22610

Calderwood DA, Yan B, de Pereda JM, Alvarez BG, Fujioka Y, Liddington RC, Ginsberg MH (2002) The phosphotyrosine binding-like domain of talin activates integrins. The journal of Biological Chemistry **277:** 21749-21758

Calderwood DA, Zent R, Grant R, Ree DJG, Hynes RO, Ginsberg MH (1999) The talin head domain binds to integrin beta subunit cytoplasmic tails and regulates integrin activation. Journal of Biological Chemistry **274:** 28071-28074

Canut H, Carrasco A, Galaud J, Cassan C, Bouyssou H, Vita N, Ferrara P, Pont-Lezica R (1998) High affinity RGD-binding sites at the plasma membrane of Arabidosisi thaliana links the cell wall. The Plant Journal **16:** 63-71

Carlier M, Pantaloni D (1997) Control of actin dynamics in Cell motility. Journal of Molecular Biology **269:** 459-467

Carlier M, Wiesner S, Clainche CL, Pantaloni D (2003) Actin-based motility as a self-organized system: mechanism and reconstitution in vitro. C.R. Biologies **326:** 161-170

Casamayor A, Snyder M (2002) Bud-site selection and cell polarity in budding yeast. Current Opinion in Microbiology **5:** 179-186

Cattelino A, Albertinazzi C, Bossi M, Critchley DR, de Curtis I (1999) A cell-free system to study regulation of focal adhesion and of the connected actin cytoskeleton. Molecular Biology of the cell **10:** 391

Chen CY, Wong EI, Vidali L, Estavillo A, Hepler PK, Wu H (2002) The regulation of actin organization by actin-depolymerizing factor in elongating pollen tubes. The Plant Cell **14:** 2175-2190

Chen H, Burnstein BW, Bamburg JR (2000) Regulating actin-filament dynamics *in vivo*. TIBS **25:** 19-23

Chuen Wong RW, Guillaud L (2004) The role of epidermal growth factor and its receptors in mammalian CNS. Cytokine and Growth Factor Reviews **15:** 147-156

Clark EA, Brugge JS (1995) Integrins and signal transduction pathways: the road taken. Science **268:** 233-239

Cleaveland JS, Kiener PA, Hammond DJ, Schacter BZ (1990) A microtiter-Based assay for detection of protein tyrosine kinase activity. Analytical Biochemistry **190:** 249-253

Cobb MH, Goldsmith EJ (1995) How MAP kinases are regulated. Journal of Biological Chemistry **270:** 14843-14846

Cock JM, Vanoosthuyse V, Gaude T (2002) Receptor kinase signalling in plants and animal: distinct molecular systems with mechanistic similarities. Curr Opin Cell Biol **14:** 230-236

Connolly MS, Williams N, Heckman CA, Morris PF (1999) Soybean isoflavones triggers a calcium influx in Phytophthora sojae. Fungal Genetics and Biology **28:** 6-11

Corellou F, Potin P, Brownlee C, Kloareg B, Bouget F (2000) Inhibition of the establishment of Zygotic polarity by protein tyrosine kinase inhibitors leads to an alteration of embryo pattern in fucus. Development Biology **219:** 165-182

Correa A, Staples RC, Hoch HC (1996) Inhibition of thigmostimulated cell differentiation with RGD-peptides in Uromyces germlings. Protoplasma **194:** 91-102

Critchley DR (2000) Focal adhesion: the cytoskeleton connection. Curr Opin Cell Biol **12:** 133-139

Dailey D, Schieven GL, Lim MY, Marquardt H, Gilmore T, Thorner J, Martin GS (1990) Novel yeast protein kinase (YPK1 gene product) is a 40-kilodalton phosphotyrosyl protein associated with protein-tyrosine kinase activity. Molecular and Cellular Biology **10:** 6244-6256

Dans M, Gagnoux-Palacios L, Blakie P, Klein S, Mariotti A, Giancotti FG (2001) Tyrosine phosphorylation of the β4 integrin cytoplasmic domain mediates Sch signaling to extracellular signal-regulated kinase and antagonisez formation of hemidesmosomes. Journal of Biological chemistry **276:** 1494-1502

Danyluk J, Carpentier E, Sarhan F (1996) Identification and Characterisation of a low temperature regulated gene encoding an actin-binding protein from wheat. FEBS Letters **389:** 324-327

Degousee N, Gupta GD, Lew RR, Heath IB (2000) A putative spectrin-containing membrane skeleton in hyphal tipes of *Neurospora crassa*. Fungal Genetics and Biology **30:** 33-44

DeMali KA, Wennerberg K, Burridge K (2003) Integrin signalling to the actin cytoskeleton. Current Opinion in cell biology **15:** 572-582

Deutscher MP (1990) Guide to Protein Purification, Vol 182. Academic Press, Inc.

Dickman MB, Yarden O (1999) Serine/Threonine protein kinases and phosphatases in filamentous fungi. Fungal Genetics and Biology **26:** 99-117

Dixon RA, Ferreira D (2002) Genistein. Phytochemistry **60:** 205-211

Doyle T, Botstein D (1996) Movement of yeast cortical actin cytoskeleton visualized in vivo. Proc. Natl. Acad. Sci. USA **93:** 3886-3891

Du J, Frieden C (1998) Kinetic studies on the effect of yeast cofilin on yeast actin polymerisation. Biochemistry **37:** 13276-13284

Duerr B, Gawienowski M, Ropp T, Jacobs T (1993) MserK1: A mitogen-activated protein kinase from a flowering plant. Plant Cell **5:** 87-96

Emerson S (1963) Slime, a plasmodiod variant of *Neurospora crassa*. Genetica **34:** 162-182

Emsley J, Knight CG, Farndale RW, Barnes MJ, Liddington RC (2000) Structure basis of collagen recognition by integrin alpha2beta1. Cell **101:** 47-56

Estruch JJ, Kadwell S, Merlin E, Crossland L (1994) Cloning and characterization of a maize pollen-specific calcium-depedent calmodulin-independent protein kinase. Proc. Natl. Acad. Sci. USA **91:** 8837-8841

Faik A, Laboure AM, Gulino D, Mandaron P, Falconet D (1998) A plant surface protein sharing structure properties with animal integrins. Eur. J. Biochem **253:** 552-559

Farooki AZ, Epstein DL, O'Brien ET (1998) Tyrphostins disrupt stress fibers and cellular attchments in endothelial monolayers. Experimental Cell Research **243:** 185-198

Foissner I, Grolig F, Obermeyer G (2002) Reversible protein phosphorylation regulates the dynamic organization of the pollen tube cytoskeleton: effect of calyculin A and okadaic acid. Protoplasma **220:** 1-15

Fowler JE, Quatrano RS (1997) Plant cell morphogenesis: Plasma membrane interaction with the cytoskeleton and cell wall. Annu. rev. Cell Dev. Biol. **13:** 697-734

Fujimura H (1997) Block of the cell cycle of the yeast Saccharomyces cerevisiae by tyrphostin, an inhibitor of protein tyrosine kinase. FEMS Microbiology Letters **153:** 233-236

Gale C, Finkel D, Tao N, Meinke M, McClellan M, Olson J, Kendrick K, Hostetter M (1996) Cloning and expression of a gene encoding an integrin-like protein in Candida albicans. Proc. Natl. Acad. Sci. USA **93:** 357-361

García-Gómez BI, Campos F, Hernandez M, Covarrubias AA (2000) Two bean cell wall proteins more abundant during waterdeficit are high in proline and interact with a plasma membrane protein. Plant Journal **22:** 277-288

Garey JR, Labbebois R, Chelstowska A, Rytka J, Harrison L, Kushner J, Labbe P (1992) Uroporphyrinogen Decarboxylase in Saccharomyces cerevisiae: HEM12 gene sequence and evidence for 2 conserved glycines essential for enzymatic activity. Eur. J. Biochem **205:** 1011-1016

Garrill A, Jackson SL, Lew RR, Heath IB (1993) Ion channel activity and tip growth: tip-localised, stretch-activated channels generate a Ca^{2+} gradient that is required for tip growth in the oomycete Saprolegnia ferax. J. Eur. Cell Biol. **60:** 358-365

Gauthier ML, Lydan MA, O'Day DH, Cotter DA (1997) Endogenous autoinhibitors regulate change in actin tyrosine phosphorylation during Dictyostelium spore germination. Cell. Signal **9:** 79-83

Gay JL, Greenwood AD (1966) Structural aspects of zoospore production in Saprolegnia ferax with particular reference to the cell and vacuolar membrane. In The Fungus Spore, Colston Papers **18:** 95-110

Geitmann A, Cresti M, Heath IB (2001) Cell Biology of Plant and Fungal Tip Growth.**:** 239

Gens JS, Reuzeau C, Doolittle KW, McNally JG, Pickard BG (1996) Covisualization by computational optical-sectioning microscopy of integrin and associated proteins at the cell membrane of living onion protoplasts. Protoplasma **194:** 215-230

Gibbon BC, Kovar DR, Staiger CJ (1999) Latrunculin B has different effects on pollen germination and tube growth. The Plant Cell **11:** 2349-2363

Gil ML, Penalver MC, Lopez-Ribot JL, Martinez JP (1996) Binding of extracellular Matrix proteins to *Aspergillus fumigatus* Conidia. Infection and immunity **64:** 5239-5247

Goehring AS, Mitchell DA, Tong AH, Keniry ME, Boone C, Sprague Jr GF (2003) Synthetic lethal analysis implicates Ste20p, a p21-activated protein kinase, in polarisome activation. Molecular Biology of the cell **14:** 1501-1516

Goldmann WH (2000) Kinetic determination of focal adhesion protein formation. Biochem. Biophys. Res. Commun **271:** 553-557

Grabski S, Arnoys E, Busch B, Schindler M (1998) Regulation of actin tension in plant cells by kinases and phosphatases. Plant Physiology **116:** 279-290

Grandis JR, Sok JC (2004) Signaling through the epidermal growth factor receptor during the development of malignancy. Pharmacology and Therapeutics **102:** 37-46

Green KJ, Jones JCR (1996) Desmosomes and hemidesmosomes-structure and function of molecular components. FASEB J. **10:** 871-881

Gupta G, Heath IB (1997) Actin distribution by latrunculin B causes turgor-related changes in tip growth of Saprolegnia hyphae. Fungal Genetics and Biology **21:** 64-75

Håkansson G, Allen JF (1995) Histidine and tyrosine phosphorylation in pea mitochondria: evidence for protein phosphorylation in respiratory redox signalling. FEBS Letters **372:** 238-242

Hang H, Lin Y, Huang D, Takahashi T, Sugiyama M (2003) Protein tyrosine phosphorylation during phytohormone-stimulated cell proliferation in *Arabidopsis* hypocotyls. Plant Cell Physiology **44:** 770-775

Harold RL, Money NP, Harold FM (1996) Growth and morphogenesis in *Saprolegnia ferax*: Is turgor reguired? Protoplasma **191:** 105-114

Harris SD, Momany M (2004) Polarity in filamentous fungi: movng beyond the yeast paradigm. Fungal Genetics and Biology **41:** 391-400

Harvey SL, Kellogg DR (2003) Conservation of Mechanisms controlling entry into Mitosis: Budding yeast Wee1 delays entry into mitosis and is required for cell size control. Current Biology **13:** 264-275

He Z, Fujiki M, Kohorn BD (1996) A cell wall-associated, Receptor-like protein kinase. The journal of biological chemistry **271:** 19789-19793

Heath IB (1987) Preservation of a labile cortical array of actin filaments in filaments in growing hyphal tips of the fungus Seprolegnia ferax. Eur. J. Cell Biol. **44:** 10-16

Heath IB (1990) The roles of actin in tip growth of fungi. Intl. Rev. Cytol **123:** 95-127

Heath IB (2000) Organisation and Functions of Actin in hyphal tip Growth. Kluwer Academic Publishers, Printed in the Netherlands **Staiger, C.J. et al (eds):** 275-300

Heath IB, Skalamera D (2001) Regulation of tip morphogenesis by the cytoskeleton and calcium ions. Cell Biology of plant and fungal tip growth **328:** 37-53

Heath IB, Steinberg G (1999) Mechanism of hyphal tip growth: Tube dwelling amebae revisited. Fungal Genetics and Biology **28:** 79-93

Henry CA, Jordan JR, Kropf DL (1996) Localised membrane-wall adhesion in Pelvetia zygotes. Protoplasma **190:** 39-52

Holloway SA, Heath IB (1977a) Morphogenesis and the role of microtubules in synchronous populations of Saprolegnia zoospores. *Exp. Mycol* **1:** 9-19

Holmes KC, Pope D, Gebhard W, Kabsch W (1990) Atomic model of the actin filament. Nature **347:** 44-49

Horwitz A, Duggan K, Buck CA, Beckerle MC, Burridge K (1986) Interaction of plasma membrane fibronectin receptor with talin-a transmembrane linkage. Nature **320:** 531-533

Hostetter MK (1999) Review: Integrin-like proteins in Candida spp. and other microorganism. Fungal Genetics and Biology **28:** 135-145

Hostetter MK (2000) RGD-mediated adhesion in fungal pathogens of human, plants and insects. Current Opinion in Microbiology **3:** 344-348

Hostetter MK, Tao NJ, Gale C, Herman DJ, McClellan M, Sharp RL, Kendrick KE (1995) Antigenic and functional conservation of an integrin I-domain in Saccharomyces cerevisiae. Biochem Mol Med. **55:** 122-130

Humphries MJ, Symonds EJH, Mould AP (2003) Mapping functional residues onto integrin crystal structures. Curr Opin in Structural Biology **13:** 236-243

Hussey PJ, Allwood EG, Smertenko AP (2002) Actin-binding proteins in the *Arabidopsis* genome database: properties of functionally distinct plant actin-depolymerizing factors/cofilins. Phil. Trans. R. Soc. Lond. B **357:** 791-798

Hynes RO (1992) Integrins: Versatility, modulation, and signaling in cell adhesion. Cell **69:** 11-25

Hynes RO (2002) Integrins: Bidirectional, Allosteric signaling machines. Cell **110:** 673-687

Ichimura K, Shinozaki K (2002) Mitogen-activatated protein kinase cascades in plants: a new nomenclature. TRENDS in Plant Science **7:** 301-308

Islas-Flores I, Oropeza C, Teresa Hernández-Sotomayor SM (1998) Protein Phosphorylation during Coconut Zygotic Embryo Development. Plant Physiology **118:** 257-263

Jackson SL, Hardham AR (1998) Dynamic rearrangement of the filamentous actin network occurs during zoosporogenesis and encystment in the oomycete *Phytophthora cinnamomi*. Fungal Genetics and Biology **24:** 24-33

Jackson SL, Heath IB (1990a) Visualisation of actin arrays in growing hyphae of the fungus *Saprolegnia ferax*. Protoplasma **154:** 66-70

Jackson SL, Heath IB (1993a) The dynamic behavior of cytoplasmic F-actin n growing hyphae. Protoplasma **173:** 23-34

Jonak C, Ökrész L, BÖgre L, Hirt H (2002) Complexity, cross talk and integration of plant MAP kinase signalling. Current Opinion in Plant biology **5:** 415-424

Jungbluth A, Eckerskorn C, Gerisch G, Lottspeich F, Stocker S, Schweiger A (1995) Stress-induced tyrosine phosphorylation of actin in *Dictyostelium* cells and localisation of the

phosphorylation site to tyrosine-53 adjacent to the DNase I binding loop. FEBS Letters **375:** 87-90

Kameyama K, Kishi Y, Yoshimura M, Kanzawa N, Sameshima M, Tsuchiya T (2000) Tyrosine phosphorylation in plant bending. Nature **407:** 37

Kaminskyj SGW, Garrill A, Heath IB (1992) The relationship between turgor and tip growth in Saprolegnia ferax: turgor is necessary but not sufficient to explain apical extension rates. Exp. Mycol **16:** 64-75

Kaminskyj SGW, Heath IB (1995) Integrin and spectrin homologues and cytoplasm-cell wall adhesion in tip growth. Journal of cell science **108:** 849-865

Katembe WJ, Swatzell LJ, CAM, Kiss JZ (1997) Immunolocalization of integrin-like proteins in *Arabidopsis* and *Chara*. Physiologicia Plantarum **99:** 7-14

Ketelaar T, Anthony RG, Hussey PJ (2004) Green Fluorescent Protein-mTalin Causes Defect in Actin Organisation and Cell Expression in Arabidopsis and Inhibites Actin Depolymerising Factor's Actin Depolymerising Activity in Vitro. Plant Physiology **136:** 3990-3998

Kiba A, Sugimoto M, Toyoda K, Ichinose Y, Yamada T, Shiraishi T (1998) Interaction between cell wall and plasma membrane via RGD motif is implicated in plant defense responses. Plant Cell Physiology **39:** 1245-1249

Kim E, Wriggers W, Phillips M, Kokabi K, Rubenstein PA, Reisler E (2000) Cross-linking Constraints on F-actin structure. Journal of Molecular Biology **299:** 421-429

Kohorn BD (2000) Plasma membrane-cell wall contacts. Plant Physiology **124:** 31-38

Kole HK, Muthukumar G, Lenard J (1991) Purification and properties of a membrane-bound insulin binding proteins, a putative receptor, from *Neurospora crassa*. Biochemistry **30:** 682-688

Kusari AB, Molina DM, Jr WS, Lau CS, Bardwell L (2004) A conserved protein interaction network involving the yeast MAP kinases Fus3 and Kss1. The Journal of Cell Biology **164:** 267-277

Labouré A, Faik A, Mandaron P, Falconet D (1999) RGD-dependent growth of maize calluses and immunodetection of an integrin-like protein. FEBS Letters **442:** 123-128

Laurent P, Voiblet C, Tagu D, de Carvalho D, Nehls U, De Bellis R, Balestrini R, Bauw G, Bonfante P, Martin F (1999) A novel class of ectomycorrhiza-regulated cell wall polypeptides in *Pisolithus tincotorius*. Molecular Plant Microbe Interact **12:** 862-871

Laval V, Chabannes M, Carriere M, Canut H, Barre A, Rouge P, Pont-Lezica R, Galaud J (1999) A family of Arabidosis plasma membrane receptors presenting animal β-integrin domains. Biochimica Biophysica Acta **1435:** 61-70

Lee G (2005) Tau and Src family tyrosine kinases. Biochimica Biophysica Acta **1739:** 323-330

Lee H, Bellin RM, Walker DL, Patel B, Powers P, Liu H, Garcia-Alvarez B, de Pereda JM, Liddington RC, Volkmann Nh, Hanein D, Critchley DR, Robson RW (2004) Characterisation of an Actin-binding Site within the Talin FERM Domain. Journal of Molecular Biology **343:** 771-784

Levitzki A (1990) Tyrphostins-Potential antiproliferative agents and novel molecular tools. Biochemical Pharmacology **40:** 913-918

Levitzki A, Gazit A (1995) Tyrosine kinase Inhibition: An Approach to Drug Development. Science **267:** 1782-1787

Lew RR (1998) Mapping fungal ion channel locations. Fungal Genetics and Biology **24:** 69-76

Lew RR (1999) Comparative analysis of Ca^{2+} and H^{+} flux magnitude and location along growing hyphae of *Saprolegnia ferax* and *Neurospora crassa*. Eur.J. Cell Biology **78:** 892-902

Lew RR, Levina NN, Walker SK, Garrill A (2004) Turgor regulation in hyphal organisms. Fungal Genetics and Biology **41:** 1007-1015

Liddington RC (2002) Will the real integrin please stand up? Structure **10:** 605-607

Liddington RC, Ginsberg MH (2002) Integrin activation takes shape. The journal of cell biology **158:** 833-839

Lopez-Franco R, Bracker CE (1996) Diversity and dynamics of the SpitzenkÖrper in growing hyphal tips of higher fungi. Protoplasma **195:** 90-111

Lu C, Takagi J, Springer TA (2001b) Association of the membrane proximal regions of the alpha and beta subunit cytoplasmic domains constrains an integrin in the inactivative state. Journal of Biological Chemistry **276:** 14642-14648

Luan S (2002) Tyrosine phosphorylation in plant cell signaling. PNAS **99:** 11567-11569

Luan S, Ting J, Gupta R (2001) Protein tyrosine phosphatases in higher plants. New Phytologist **151:** 155-164

Lynch TM, Lintilhac PM, Domozych D (1998) Mechanotransduction molecules in the plant gravisensory response: amyloplast/statolith membrane contain a β1 integrin-like protein. Protoplasma **201:** 92-100

Magherini F, Gamberi T, Paoli P, Marchetta M, Biagini M, Raugei G, Camici G, Ramponi G, Modesti A (2004) The in vivo tyrosine phosphorylation level of yeast immunophilin Fpr3 is influenced by the LMW-PTP Ltp1. Biochemical and Biophysical Reserach Communications **321:** 424-431

Maleri S, Ge Q, Hackett EA, Wang Y, Dohlman HG, Errede B (2004) Persistent activation by constitutive Ste7 promotes Kss1-medisted invasive growth but fail to support Fus3-dependent mating in Yeast. Molecular and Cellular Biology **24:** 9221-9238

Marcantonio EE, Hynes RO (1988) Antibodies to the conserved cytoplasmic domain of the integrin β1 subunit react with proteins in vertebrates, invertebrates and fungi. The journal of cell biology **106:** 1765-1772

Martel V, Racaud-Sultan C, Dupe S, Marie C, Paulhe F, Galmiche A, Block MR, Albiges-Rizo C (2001) Conformation, locolization, and integrin binding of talin depend on its interaction with phosphoinositides. The journal of biological chemistry **276:** 21217-21227

May AP, Ponting CP (1999) Intergrin α- and β4-subunit-domain homologues in cyanobacterial proteins. Trends in Biochemical Sciences **24:** 12-13

McMillan JN, Longtine MS, Sia RAL, Theesfeld CL, Bardes ESG, Pringle JR, Jew DJ (1999) The morphogenesis checkpoint in Saccharomyces cerevisiae: Cell cycle control of Swe1p degradation by Hsl1p and Hsl7p. Molecular and Cellular Biology **19:** 6929-6939

Mellersh DG, Heath MC (2001) Plasma membrane-cell wall adhesion is required for expression of plant defense responses during fungal penetration. The Plant Cell **13:** 413-424

Mercurio AM, Bachelder RE, Bates RC, Chung J (2004) Autocrine signaling in carcinoma: VEGF and the α6β4 integrin. Seminars in CANCER BIOLOGY **14:** 115-122

Mercurio AM, Rabinovitz I (2001) Toward a mechanistic understanding of tumor invasion-lessons from the α6β4 integrin. Seminars in CANCER BIOLOGY **11:** 129-141

Millard TH, Sharp SJ, Machesky LM (2004) Signalling to actin assembly via the WASP (Wiskott-Aldrich syndrome protein)-family proteins and the Arp2/3 complex. Biochemical Journal **380:** 1-17

Mizunuma M, Hirata D, Miyaoka R, Miyakawa T (2001) GSK-3 kinase Mck1 and calcineurin coordinately mediate Hsl1 down-regulation by Ca^{2+} in budding yeast. The EMBO Journal **20:** 1074-1085

Money NP (1997) Wishful thinking of turgor revisited: The mechanism of fungal growth. Fungal Genetics and Biology **21:** 173-187

Money NP, Davis CM, Ravishankar JP (2004) Biomechanical evidence for convergent evolution of the invasive growth process among fungi and oomycete water molds. Fungal Genetics and Biology **41:** 872-876

Money NP, Harold FM (1992) Extension growth of the water mold Achlya:interplay of turgor and wall strength. Proc. Natl. Acad. Sci. USA **89:** 4245-4249

Munnik T, Meijer HJG (2001) Osmotic stress activates distinct lipid and MAPK signalling pathways in plants. FEBS Letters **498:** 172-178

Nagpal P, Quatrano RS (1999) Isolation and characterization of a cDNA clone from *Arabidopsis thaliana* with partial sequence similarity to integrins. Gene **230:** 33-40

Nakashima I, Takeda K, Kawamoto Y, Okuno Y, Kato M, Suzuki H (2005) Redox control of catalytic activities of membrane-associated protein tyrosine kinases. Archives of Biochemistry and Biophysics **434:** 3-10

O'Connor KL, Shaw LM, Mercurio AM (1998) Release of cAMPgating by the α6β4 integrin stimulates lamellae formation and the chemotactic migration of invasive carsinoma cells. Journal of Cell biology **143:** 1749-1760

Otey C, Griffiths W, Keith B (1990) Characterisation of monoclonal antibodies to Chicken Gizzard Talin. Hybridoma **9:** 57-62

O'Toole TE, Katagiri Y, Faull RJ, Peter K, Temura R, Quaranta V, Loftus JC, Shattil SJ, Ginsberg MH (1994) Integrin cytoplasmic domain mediate inside-out signal transduction. Journal of Cell Biology **124:** 1047-1059

O'Toole TE, Mandelman D, Forsyth J, Shattil SJ, Plow EF, Ginsberg MH (1991) Modulation of the affinity of integrin alpha IIb beta3(GPIIb-IIIa) by the cytoplasmic domain of alpha IIb. Science **254:** 845-847

Palmieri SJ, Haarer BK (1998) Polarity and division site specification in yeast. Current Opinion in Microbiology **1:** 678-686

Pan X, Harashima T, Heitman J (2000) Signal transduction cascades regulating pseudohyphal differentiation of Saccharomyces cerevisiae. Current Opinion in Microbiology **3:** 567-572

Pantaloni D, Clainche CL, Carlier M (2001) Mechanism of actin-based motility. Science **292:** 1502-1506

Parker LL, Walter SA, Young PG, Piwnica-Worms H (1993) Phosphorylation and inactivation of the mitotic inhibitor Wee1 by the *nim/cdr1* kinase. Nature **363:** 736-738

Parsons JT (2003) Focal adhesion kinase: the first ten years. Journal of Cell science **116:** 1409-1416

Pawson T, Gish GD (1992) SH2 and SH3 domains: from structure to function. Cell **71:** 359-362

Pereyra E, Argimón S, Jackson SL, Moreno S (2003) RGD-containing peptides and cyclic AMP have antagonistic roles in the morphology of *Mucor rouxii*. Protoplasma **222:** 23-30

Plow EF, Haas TA, Zhang L, Loftus J, Smith JW (2000) Ligand Binding to Integrins. The journal of biological chemistry **275:** 21785-21788

Putnam-Evans C, Harman AC, Palevitz BA, Fechheimer M, Cormier MJ (1989) Calcium-dependent protein kinase is locolized with F-actin in plant cells. Cell Motil Cytoskeleton **12:** 12-22

Qiu H, Miller WT (2002) Regulation of the nonreceptor tyrosine kinase Brk by autophosphorylation and by autoinhibition. The journal of biological chemistry **277:** 34634-34641

Rabinovitz I, Mercurio AM (1997) The integrin $\alpha 6\beta 4$ functions in carcinoma cell migration on laminin-1 by mediating the formation and stabilisation of actin-containing motility structures. Journal of Cell biology **139:** 1873-1884

Rakwal R, Arawal GK (2003) Wound signaling-coordination of the octadecanoid and MAPK pathways. Plant Physiology and Biochemistry **41:** 855-861

Raudaskoski M, Pardo AG, Tarkka MT, Gorfer M, Hanif M, Laitiainen E (2001) Small GTPasee, Cytoskeleton and Signal Transduction in Filamentous Homobasidiomycetes. Cell Biology of Plant and Fungal Tip Growth **328:** 123-136

Ray PM, Green PB, Cleland R (1972) Role of turgor in plant cell growth. Nature **239:** 163-164

Ree DJG, Ades SE, Singer SJ, Hynes RO (1990) Sequence and domain structure of talin. Nature **347:** 685-689

Roberts K (1990) Structures at the plant cell surface. Curr Opin Cell Biol **2:** 920-928

Rodriguez-Zapata LC, Hernández-Sotomayor T (1998) Evidence of protein-tyrosine kinase activity in *Catharanthus roseus* roots transformed by *Agrobecterium rhizogenes*. Planta **204:** 70-77

Romeis T (2001) Protein kinases in the plant defence response. Current Opinion in Plant biology **4:** 407-414

Roskoski R (2004) Src protein-tyrosine kinase structure and regulation. Biochemical and Biophysical Reserach Communications **324:** 1155-1164

Rudd JJ, Franklin FCH, Lord JM, Franklin-Tong VE (1996) Increased phosphorylation of a 26-kD pollen protein is induced by the self-incompatibility response in *Papaver rhoeas*. The Plant Cell **8:** 713-724

Rudrabhatla P, Rajasekharan R (2004) Functional characterisation of peanut serine/threonine/tyrosine kinase: molecular docking and inhibition kinetics with tyrosine kinase inhibitors. Biochemistry **43:** 12123-12132

Santoni G, Birarelli P, Jin Hang L, Gamero A, Djeu JY, Piccoli M (1995) An α5β1-like integrin receptor mediates the binding of less pathogenic *Candida* species to fibronectin. Journal of Medical Microbiology **43:** 360-367

Santoni G, Gismondi A, Liu JH, Punturieri A, Santoni A, Frati L, Piccoli M, Djeu JY (1994) Candida albicans expresses a fibronectin receptor antigenically related to α5β1 integrin. Microbiology **140:** 2971-2979

Santoni G, Lucciarini R, Amantini C, Jacobelli J, Spreghini E, Ballarini P, Piccoli M, Gismondi A (2002) Candida albicans express a focal adhesion kinase-like protein that undergoes increased Tyrosine phosphorylation upon yeast cell adhesion to vitronectin and the EA.hy 926 human endothelial cell line. Infection and immunity **70:** 3804-3815

Santoni G, Spreghini E, Amantini C, Piccoli M (1998) Biochemical and antigenic characterization of a function alphaVbeta5 integrin vitronectin receptor in C. albicans yeast cells. Abstr. Am. Soc. Cell Biol. **December**

Sapperstein SK, Lupashin VV, Schmitt HD, Waters MG (1996) Assembly of the ER to Golgi SNARE complex required Uso1p. The journal of cell biology **132:** 755-767

Sawin KE (1999) Some Thought about Microtubules and Cell Polarity. Fungal Genetics and Biology **27:** 224-230

Schaller MD (2001) Biochemical signal and biological responses elicited by the focal adhesion kinase. Biochemical Biophys Acta **1540:** 1-21

Schieven G, Thorner J, Martin GS (1986) Protein- tyrosine kinase activity in Saccharomyces cerevisiae. Science **231:** 390-393

Schindler M, Meiners S, Cheresh DA (1989) RGD-dependent linkage between plant cell wall and plasma membrane: consequence for growth. Journal of Cell biology **108:** 1955-1965

Schmidt JM, Zhang J, Lee H, Stromer MH, Robson RM (1999) Interaction of Talin with Actin: Sensitive Modulation of Filament Crosslinking Activity. Archives of Biochemistry and Biophysics **366:** 139-150

Shimaoka M, Shifman JM, Jing H, Takagi J, Mayo SL, Springer TA (2000) Computation design of an integrin I-domain stabilised in the open high affinity conformation. Nat. Struct. Biol. **7:** 674-678

Shiu S, Bleecker AB (2001) Receptor-like kinases from *Arabidopsis* form a monophyletic gene family related to animal receptor kinases. PNAS **98:** 10763-10768

Shulewitz MJ, Inouye CJ, Thorner J (1999) Hs17 localizes to a septin ring and serves as an adater in a regulator pathway that relieves tyrosine phosphorylation of Cdc28 protein kinase in *Saccharomyces cerevisiae*. Molecular and Cellular Biology **19:** 7123-7137

Sia RAL, Bardes ESG, Lew DJ (1998) Control of Swe1p deradation by the morphogenesis checkpoint. The EMBO Journal **17:** 6678-6688

Silverman-Gavrila LB, Lew RR (2002) An IP3-activated Ca^{2+} channel regulates fungal tip growth. Journal of cell science **115:** 5013-5025

Srinivasan S, Vargas MM, Roberson RW (1996) Functional, organisational, and biochemical analysis of actin in hyphae tip cells of *Allomyces macrogynus*. Mycologia **88:** 57-70

Steinmetz M, Stoffler D, Hoenger A, Bremer A, Aebi U (1997) Actin: From cell biology to atomic detail. Journal of Structural Biology **119:** 295-320

Stern DF, Zheng P, Beidler DR, Zerillo C (1991) Spk1, a new kinase from *Saccharomyces cerevisiae*, phosphorylates protein on serine, threonine and tyrosine. Molecular and Cellular Biology **11:** 987-1001

Stone JM, Walker JC (1995) Plant protein kinase families and signal transduction. Plant Physiology **108:** 451-457

Sun Y, Qian H, Xu X, Han Y, Yen L, Sun D (2000) Integrin-like proteins in the pollen tube: Detection, localization and function. Plant Cell Physiology **41:** 1136-1142

Sun Y, Xu XD, Sun DY (1998) Immunoblots of integrin-like proteins in pollen tube member of *Hemerocallis citrina*. Acta Bot. Sin. **32:** 680-682

Suzuki K, Saito J, Yanai R, Yamada N, Chikama T, Seki K, Nishida T (2003) Cell-matrix and cell-cell interactions during corneal epithelial wound healing. Progress in Retinal and Eye Research **22:** 113-133

Takagi J, Erickson HP, Springer TA (2001) C-terminal opening mimics 'inside-out' activation of integrin $\alpha 5\beta 1$. Nat. Struct. Biol. **8:** 412-416

Takagi J, Petre BM, Walz T, Springer TA (2002) Global conformational rearrangement in integrin extracellular domains in outside-in and inside-out signaling. Cell **110:** 599-611

Torralba S, Raudaskoski M, Pedregosa A (1998) Effects of methyl benzimidazole-2-yl carbamate on microtubule and actin cytoskeleton in Aspergillus nidulans. Protoplasma **202:** 54-64

Torruella M, Casano LM, Vallejos RH (1985) Evidence of the activity of tyrosine kinase(s) and of the presence of phosphotyrosine proteins in pea plantlets. The journal of biological chemistry **261:** 6651-6653

Travis MA, Humphries MJ, Humphries JD (2003) An unraveling tale of how integrins are activated from within. Trends in Pharmacological Sciences **24:** 192-197

Trevithick JR, Galsworthy PR (1977) Morphology of slime variants of *Neurospora crassa* growing on a glass surface in liquid medium. 1. Under normal conditions and 2. In the presence of inhibitors. Arch. Microbiology. **115:** 109-118

Trojanek J, EK P, Scoble J, Muszynska G, Engstrom L (1996) Phosphorylation of plant proteins and the identification of protein-tyrosine kinase activity in maize seedlings. Eur. J. Biochem **235:** 338-344

Troys MV, Vandekerckhove J, Ampe C (1999) Structure modules in actin-binding proteins: towards a new classification. Biochimica Biophysica Acta **1448:** 323-348

Verde F (2001) Cell polarity: A tale of two Ts. Current Biology **11:** R600-R602

Vidali L, Hepler PK (2001) Actin and pollen tube growth. Protoplasma **215:** 64-76

Vinogradova O, Velyvis A, Velyviene A, Hu B, Haas TA, Plow EF, Qin J (2002) A structure mechanism of integrin αIIbβ3 "inside- out" activation as regulated by its cytoplasmic face. Cell **110:** 587-597

Vorobiev S, Strokopytov B, Drubin DG, Frieden C, Ono S, Condeelis J, Rubenstein PA, Almo SC (2003) The structure of nonvertebrate actin: Implications for the ATP hydrolytic mechanism. PNAS **100:** 5760-5765

Vuori K (1998) Integrin Signaling: Tyrosine phosphorylation events in focal adhesions. Journal of Membrane Biology **165:** 191-199

Wasteneys GO, Galway ME (2003) Remodeling the cytoskeleton for growth and form: An overview with some new views. Annu. Rev. Plant Biol **54:** 691-722

Wasteneys GO, Yang Z (2004) New views on the plant cytoskeleton. Plant Physiology **136:** 3884-3891

Watt FM (2002) Role of integrins in regulating epidermal adhesion, growth and differentiation. The EMBO Journal **21:** 3919-3926

Wayne R, Staves MP, Leopold AC (1992) The contribution of the extracellular matrix to gravisensing in characean cells. Journal of Cell Science **101:** 611-623

Wear MA, Schafer DA, Cooper JA (2000) Actin dynamics: Assembly and disassembly of actin networks. Current Biology **10:** R891-R895

Weaver AM, Young ME, Lee W, Cooper JA (2003) Integration of signals to the Arp2/3 complex. Current Opinion in cell biology **15:** 23-30

Westhoff MA, Serrels B, Fincham VJ, Frame MC, Carragher NO (2004) Src-mediated phosphorylation of focal adhesion kinase couple actin and adhesion dynamics to survival signaling. Molecular and Cellular Biology **24:** 8113-8133

Winter D, Podtelejnikov AV, Mann M, Li R (1997) The complex containing actin-related proteins Arp2 and Arp3 is required for the motility and integrity of yeast actin patches. Curr. Biol **7:** 519-529

Xiang X, Plamann M (2003) Cytoskeleton and motor proteins in filamentous fungi. Current Opinion in Microbiology **6:** 628-633

Xiong JP, Stehle T, Diefenbach B, Zhang R, Dunker R, Scott DL, Joachimiak A, Goodman SL, Arnaout MA (2001) Crystal structure of the extracellular segment of integrin αvβ3. Science **294:** 339-345

Xiong JP, Stehle T, Zhang R, Joachimiak A, Frech M, Goodman SL, Arnaout MA (2002) Crystal structure of the extracellular segment of integrin αVβ3 in complex with an Arg-Gly-Asp ligand. Science **296:** 151-155

Xu J (2000) MAP Kinases in Fungal pathogens. Fungal Genetics and Biology **31:** 137-152

Yan B, Calderwood DA, Yaspan B, Ginsberg MH (2001) Calpain cleavage promotes talin binding to the beta 3 integrin cytoplasmic domain. Journal of biological chemistry **276:** 28164-28170

Yang C, Huang M, DeBiasio J, Pring M, Joyce M, Miki H, Takenawa T, Zigmond SH (2000) Profilin enhances Cdc42-induced nucleation of actin polymerisation. Journal of Cell biology **150:** 1001-1012

Yu YP, Jackson SL, Garrill A (2004) Two distinct distribution of F-actin are present in the hyphal apex of the Oomycete *Achlya bisexualis*. Plant Cell Physiology **45:** 275-280

Zhang K, Letham DS, John PC (1996) Cytokinin control the cell cycle at mitosis by stimulating the tyrosine dephosphorylation and activation of p34cdc2-like H1 histone kinase. Planta **200:** 2-12

Appendix 1: Schematic of detection of tyrosine kinase activity

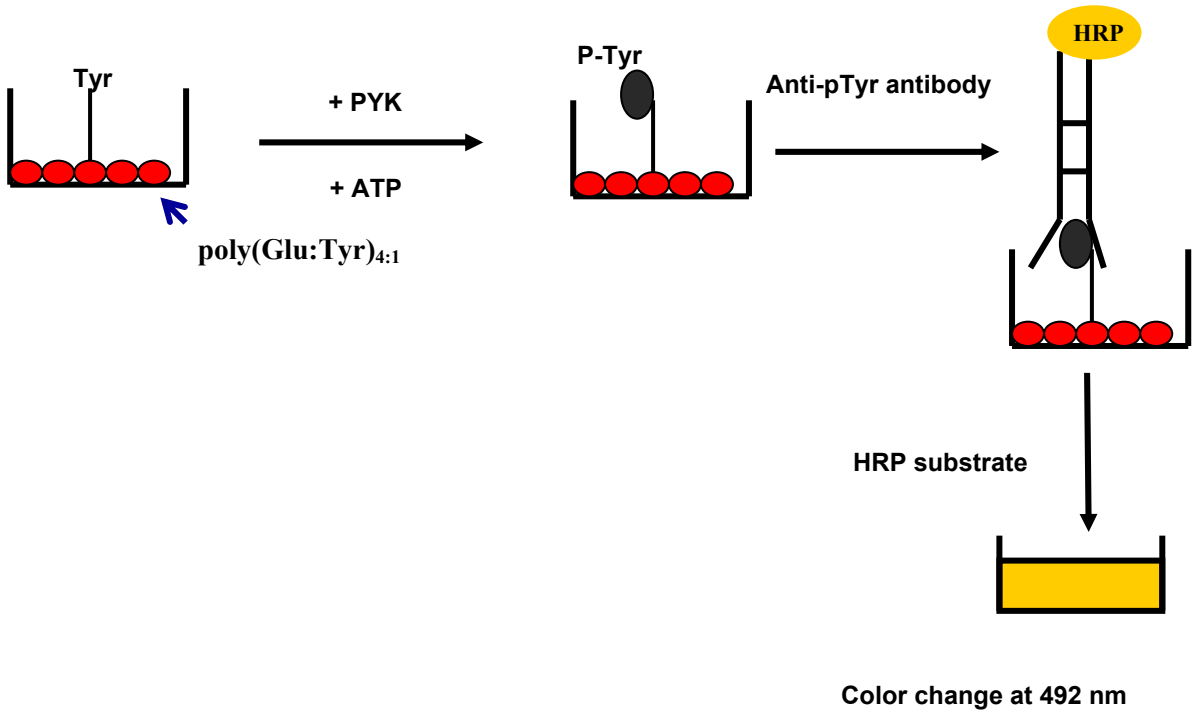

Scheme 1. Tyrosine kinase activity is determined using ELISA.

Each reaction contains

- 300 µM ATP
- Tyrosine kinase buffer
- 150 µl of 1.25 µM poly(Glu:Tyr)4:1 was coated to wells microtiter at 45 °C overnight.
- 50 µl of crude fractions or 2 units of EGFR for the positive control.
- Final volume is 250 µl

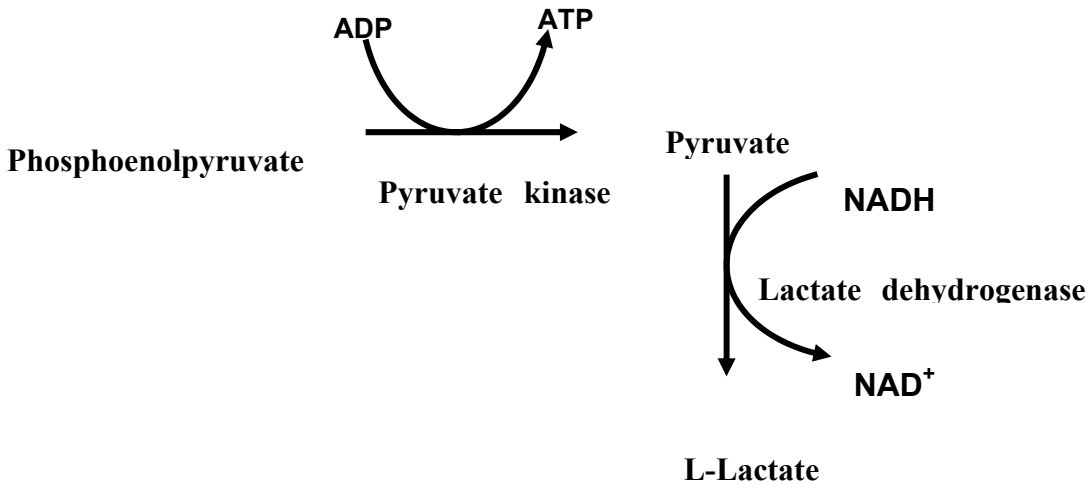

Scheme 2. Tyrosine kinase activity is determined using the coupled assay.

Each reaction contains:

- 0.3 mM NADH
- 1 mM phosphoenolpyruvate (PEP)
- 20 units of pyruvate kinase (PK)
- 7-10 units of lactic dehydrogenase (LDH)
- Buffer
- 300 µl of phosphorylation mixture
- The coupled assay was initiated by the addition of 300 µl of the phosphorylation mixture into 700 µl of the coupled assay mixture and then the reaction was monitored by following the reduction of NADH at 340 nm for 2-3 minutes.

Appendix 2: Sequence homology of actin among organisms

Note that Query is actin from *A. bisexualis*

1. *A. bisexualis* vs. *P. infestans*

```
Score = 751 bits (1940), Expect = 0.0
Identities = 370/376 (98%), Positives = 373/376 (98%)


Query: 1   MADDDVQALVVDNGSGMCKAGFAGDDAPRAVFPSIVGRPKHPGIMVGMDQKDAYVGDEAQ 60
           MADDDVQALVVDNGSGMCKAGFAGDDAPRAVFPSIVGRPKH GIMVGMDQKDAYVGDEAQ
Sbjct: 1   MADDDVQALVVDNGSGMCKAGFAGDDAPRAVFPSIVGRPKHLGIMVGMDQKDAYVGDEAQ 60

Query: 61  SKRGVLTLKYPIEHGIVTNWDDMEKIWHHTFYNELRVAPEEHPVLLTEAPLNPKANRERM
120
           SKRGVLTLKYPIEHGIVTNWDDMEKIWHHTFYNELRVAPEEHPVLLTEAPLNPKANRERM
Sbjct: 61  SKRGVLTLKYPIEHGIVTNWDDMEKIWHHTFYNELRVAPEEHPVLLTEAPLNPKANRERM
120

Query: 121 TQIMFETFNVPAMYVNIQAVLSLYASGRTTGCVLDSGDGVSHTVPIYEGYALPHAIVRLD
180
           TQIMFETFNVPAMYVNIQAVLSLYASGRTTGCVLDSGDGVSHTVPIYEGYALPHAIVRLD
Sbjct: 121 TQIMFETFNVPAMYVNIQAVLSLYASGRTTGCVLDSGDGVSHTVPIYEGYALPHAIVRLD
180

Query: 181 LAGRDLTDYMMKILTERGYSFTTTAEREIVRDIKEKLTYIALDFDQEMKTAAESSGLEKS
240
           LAGRDLTDYMMKILTERGYSFTTTAEREIVRDIKEKLTYIALDFDQEMKTAAESSGLEKS
Sbjct: 181 LAGRDLTDYMMKILTERGYSFTTTAEREIVRDIKEKLTYIALDFDQEMKTAAESSGLEKS
240

Query: 241 YELPDGNVLVIGNERFRTPEVLFQPALIGKEASGIHDCTFQTIMKCDVDIRKDLYCNIVL
300
           YELPDGNV+VIGNERFRTPEVLFQP+LIGKEASGIH+CTFQTIMKCDVDIRKDLYCNIVL
Sbjct: 241 YELPDGNVIVIGNERFRTPEVLFQPSLIGKEASGIHECTFQTIMKCDVDIRKDLYCNIVL
300

Query: 301 SGGTTMYPGISERMTKELTALAPSTMKIKVVAPPERKYSVWIGGSILSSLSTFQQMWISK
360
           SGGTTMYPGI ERMTKELTALAPSTMKIKVVAPPERKYSVWIGGSI SSLSTFQQMWISK
Sbjct: 301 SGGTTMYPGIGERMTKELTALAPSTMKIKVVAPPERKYSVWIGGSIQSSLSTFQQMWISK
360
```

```
Query: 361 AEYDESGPSIVHRKCF 376
           AEYDESGPSIVHRKCF
Sbjct: 361 AEYDESGPSIVHRKCF 376
```

2. *A. bisexualis* vs. *N. crassa*

```
Score =  659 bits (1699), Expect = 0.0
Identities = 308/374 (82%), Positives = 351/374 (93%)


Query: 3   DDDVQALVVDNGSGMCKAGFAGDDAPRAVFPSIVGRPKHPGIMVGMDQKDAYVGDEAQSK 62
           +++V ALV+DNGSGMCKAGFAGDDAPRAVFPSIVGRP+H GIM+GM QKD+YVGDEAQSK
Sbjct: 2   EEEVAALVIDNGSGMCKAGFAGDDAPRAVFPSIVGRPRHHGIMIGMGQKDSYVGDEAQSK 61

Query: 63  RGVLTLKYPIEHGIVTNWDDMEKIWHHTFYNELRVAPEEHPVLLTEAPLNPKANRERMTQ
122
           RG+LTL+YPIEHG+VTNWDDMEKIWHHTFYNELRVAPEEHPVLLTEAP+NPK+NRE+MTQ
Sbjct: 62  RGILTLRYPIEHGVVTNWDDMEKIWHHTFYNELRVAPEEHPVLLTEAPINPKSNREKMTQ
121

Query: 123 IMFETFNVPAMYVNIQAVLSLYASGRTTGCVLDSGDGVSHTVPIYEGYALPHAIVRLDLA
182
           I+FETFN PA YV+IQAVLSLYASGRTTG VLDSGDGV+H VPIYEG+ALPHAI R+D+A
Sbjct: 122 IVFETFNAPAFYVSIQAVLSLYASGRTTGIVLDSGDGVTHVVPIYEGFALPHAIARVDMA
181

Query: 183 GRDLTDYMMKILTERGYSFTTTAEREIVRDIKEKLTYIALDFDQEMKTAAESSGLEKSYE
242
           GRDLTDY+MKIL ERGY+F+TTAEREIVRDIKEKL Y+ALDF+QE++TAA+SS LEKSYE
Sbjct: 182 GRDLTDYLMKILAERGYTFSTTAEREIVRDIKEKLCYVALDFEQEIQTAAQSSSLEKSYE
241

Query: 243 LPDGNVLVIGNERFRTPEVLFQPALIGKEASGIHDCTFQTIMKCDVDIRKDLYCNIVLSG
302
           LPDG V+ IGNERFR PE LFQP+++G E+ GIH  TF +IMKCDVD+RKDLY NIV+SG
Sbjct: 242 LPDGQVITIGNERFRAPEALFQPSVLGLESGGIHVTTFNSIMKCDVDVRKDLYGNIVMSG
301

Query: 303 GTTMYPGISERMTKELTALAPSTMKIKVVAPPERKYSVWIGGSILSSLSTFQQMWISKAE
362
           GTTMYPG+S+RM KE+TALAPS+MK+K++APPERKYSVWIGGSIL+SLSTFQQMWISK E
Sbjct: 302 GTTMYPGLSDRMQKEITALAPSSMKVKIIAPPERKYSVWIGGSILASLSTFQQMWISKQE
361

Query: 363 YDESGPSIVHRKCF 376
           YDESGPSIVHRKCF
Sbjct: 362 YDESGPSIVHRKCF 375
```

3. *A. bisexualis* vs. *D. discoideum* (Slime mold)

```
Score =  683 bits (1762), Expect = 0.0
Identities = 327/373 (87%), Positives = 353/373 (93%)


Query: 4   DDVQALVVDNGSGMCKAGFAGDDAPRAVFPSIVGRPKHPGIMVGMDQKDAYVGDEAQSKR 63
           +DVQALV+DNGSGMCKAGFAGDDAPRAVFPSIVGRP+H G+MVGM QKD+YVGDEAQSKR
Sbjct: 3   EDVQALVIDNGSGMCKAGFAGDDAPRAVFPSIVGRPRHTGVMVGMGQKDSYVGDEAQSKR 62

Query: 64  GVLTLKYPIEHGIVTNWDDMEKIWHHTFYNELRVAPEEHPVLLTEAPLNPKANRERMTQI
123
           G+LTLKYPIEHGIVTNWDDMEKIWHHTFYNELRVAPEEHPVLLTEAPLNPKANRE+MTQI
Sbjct: 63  GILTLKYPIEHGIVTNWDDMEKIWHHTFYNELRVAPEEHPVLLTEAPLNPKANREKMTQI
122

Query: 124 MFETFNVPAMYVNIQAVLSLYASGRTTGCVLDSGDGVSHTVPIYEGYALPHAIVRLDLAG
183
           MFETFN PAMYV IQAVLSLYASGRTTG V+DSGDGVSHTVPIYEGYALPHAI+RLDLAG
Sbjct: 123 MFETFNTPAMYVAIQAVLSLYASGRTTGIVMDSGDGVSHTVPIYEGYALPHAILRLDLAG
182

Query: 184 RDLTDYMMKILTERGYSFTTTAEREIVRDIKEKLTYIALDFDQEMKTAAESSGLEKSYEL
243
           RDLTDYMMKILTERGYSFTTTAEREIVRDIKEKL Y+ALDF+QEM TAA SS LEKSYEL
Sbjct: 183 RDLTDYMMKILTERGYSFTTTAEREIVRDIKEKLAYVALDFEQEMATAASSSALEKSYEL
242

Query: 244 PDGNVLVIGNERFRTPEVLFQPALIGKEASGIHDCTFQTIMKCDVDIRKDLYCNIVLSGG
303
           PDG V+ IGNERFR PE LFQP+ +G E++GIH+ T+ +IMKCDVDIRKDLY N+VLSGG
Sbjct: 243 PDGQVITIGNERFRCPEALFQPSFLGMESAGIHETTYNSIMKCDVDIRKDLYGNVVLSGG
302

Query: 304 TTMYPGISERMTKELTALAPSTMKIKVVAPPERKYSVWIGGSILSSLSTFQQMWISKAEY
363
           TTM+PGI++RM KELTALAPSTMKIK++APPERKYSVWIGGSIL+SLSTFQQMWISK EY
Sbjct: 303 TTMFPGIADRMNKELTALAPSTMKIKIIAPPERKYSVWIGGSILASLSTFQQMWISKEEY
362

Query: 364 DESGPSIVHRKCF 376
           DESGPSIVHRKCF
Sbjct: 363 DESGPSIVHRKCF 375
```

4. *A. bisexualis* vs α-actin of human muscle

```
Score =  662 bits (1707), Expect = 0.0
Identities = 315/374 (84%), Positives = 346/374 (92%)


Query: 3   DDDVQALVVDNGSGMCKAGFAGDDAPRAVFPSIVGRPKHPGIMVGMDQKDAYVGDEAQSK 62
           +D+  ALV DNGSG+ KAGFAGDDAPRAVFPSIVGRP+H G+MVGM QKD+YVGDEAQSK
Sbjct: 4   EDETTALVCDNGSGLVKAGFAGDDAPRAVFPSIVGRPRHQGVMVGMGQKDSYVGDEAQSK 63


Query: 63  RGVLTLKYPIEHGIVTNWDDMEKIWHHTFYNELRVAPEEHPVLLTEAPLNPKANRERMTQ
122
           RG+LTLKYPIEHGI+TNWDDMEKIWHHTFYNELRVAPEEHP LLTEAPLNPKANRE+MTQ
Sbjct: 64  RGILTLKYPIEHGIITNWDDMEKIWHHTFYNELRVAPEEHPTLLTEAPLNPKANREKMTQ
123

Query: 123 IMFETFNVPAMYVNIQAVLSLYASGRTTGCVLDSGDGVSHTVPIYEGYALPHAIVRLDLA
182
           IMFETFNVPAMYV IQAVLSLYASGRTTG VLDSGDGV+H VPIYEGYALPHAI+RLDLA
Sbjct: 124 IMFETFNVPAMYVAIQAVLSLYASGRTTGIVLDSGDGVTHNVPIYEGYALPHAIMRLDLA
183

Query: 183 GRDLTDYMMKILTERGYSFTTTAEREIVRDIKEKLTYIALDFDQEMKTAAESSGLEKSYE
242
           GRDLTDY+MKILTERGYSF TTAEREIVRDIKEKL Y+ALDF+ EM TAA SS LEKSYE
Sbjct: 184 GRDLTDYLMKILTERGYSFVTTAEREIVRDIKEKLCYVALDFENEMATAASSSSLEKSYE
243

Query: 243 LPDGNVLVIGNERFRTPEVLFQPALIGKEASGIHDCTFQTIMKCDVDIRKDLYCNIVLSG
302
           LPDG V+ IGNERFR PE LFQP+ IG E++GIH+ T+ +IMKCD+DIRKDLY N V+SG
Sbjct: 244 LPDGQVITIGNERFRCPETLFQPSFIGMESAGIHETTYNSIMKCDIDIRKDLYANNVMSG
303

Query: 303 GTTMYPGISERMTKELTALAPSTMKIKVVAPPERKYSVWIGGSILSSLSTFQQMWISKAE
362
           GTTMYPGI++RM KE+TALAPSTMKIK++APPERKYSVWIGGSIL+SLSTFQQMWI+K E
Sbjct: 304 GTTMYPGIADRMQKEITALAPSTMKIKIIAPPERKYSVWIGGSILASLSTFQQMWITKQE
363

Query: 363 YDESGPSIVHRKCF 376
           YDE+GPSIVHRKCF
Sbjct: 364 YDEAGPSIVHRKCF 377
```

Appendix 3: Amino acid sequences of β4 integrin subunit of *Homo sapiens*

```
   1 magprpspwa rlllaalisv slsgtlanrc kkapvkscte cvrvdkdcay ctdemfrdrr
  61 cntqaellaa gcqresivvm essfqiteet qidttlrrsq mspqglrvrl rpgeerhfel
 121 evfeplespv dlyilmdfsn smsddldnlk kmgqnlarvl sqltsdytig fgkfvdkvsv
 181 pqtdmrpekl kepwpnsdpp fsfknvislt edvdefrnkl qgerisgnld apeggfdail
 241 qtavctrdig wrpdsthllv fstesafhye adganvlagi msrnderchl dttgtytqyr
 301 tqdypsvptl vrllakhnii pifavtnysy syyeklhtyf pvsslgvlqe dssnivelle
 361 eafnrirsnl diraldsprg lrtevtskmf qktrtgsfhi rrgevgiyqv qlralehvdg
 421 thvcqlpedq kgnihlkpsf sdglkmdagi icdvctcelq kevrsarcsf ngdfvcgqcv
 481 csegwsgqtc ncstgslsdi qpclregedk pcsgrgecqc ghcvcygegr yegqfceydn
 541 fqcprtsgfl cndrgrcsmg qcvcepgwtg pscdcplsna tcidsnggic ngrghcecgr
 601 chchqqslyt dticeinysa ihpglcedlr scvqcqawgt gekkgrtcee cnfkvkmvde
 661 lkraeevvvr csfrdedddc tysytmegdg apgpnstvlv hkkkdcppgs fwwlipllll
 721 llpllallll lcwkycacck aclallpccn rghmvgfked hymlrenlma sdhldtpmlr
 781 sgnlkgrdvv rwkvtnnmqr pgfathaasi nptelvpygl slrlarlcte nllkpdtrec
 841 aqlrqeveen lnevyrqisg vhklqqtkfr qqpnagkkqd htivdtvlma prsakpallk
 901 ltekqveqra fhdlkvapgy ytltadqdar gmvefqegve lvdvrvplfi rpedddekql
 961 lveaidvpag tatlgrrlvn itiikeqard vvsfeqpefs vsrgdqvari pvirrvldgg
1021 ksqvsyrtqd gtaqgnrdyi pvegellfqp geawkelqvk llelqevdsl lrgrqvrrfh
1081 vqlsnpkfga hlgqphstti iirdpdeldr sftsqmlssq ppphgdlgap qnpnakaags
1141 rkihfnwlpp sgkpmgyrvk ywiqgdsese ahlldskvps veltnlypyc dyemkvcayg
1201 aqgegpyssl vscrthqevp sepgrlafnv vsstvtqlsw aepaetngei tayevcyglv
1261 nddnrpigpm kkvlvdnpkn rmllienlre sqpyrytvka rngagwgper eaiinlatqp
1321 krpmsipiip dipivdaqsg edydsflmys ddvlrspsgs qrpsvsddtg cgwkfepllg
1381 eeldlrrvtw rlppeliprl sassgrssda eaphgppddg gaggkggslp rsatpgppge
1441 hlvngrmdfa fpgstnslhr mtttsaaayg thlsphvphr vlstsstltr dynsltrseh
1501 shsttlprdy stltsvsshd srltagvpdt ptrlvfsalg ptslrvswqe prcerplqgy
1561 sveyqllngg elhrlnipnp aqtsvvvedl lpnhsyvfrv raqsqegwgr eregvities
1621 qvhpqsplcp lpgsaftlst psapgplvft alspdslqls werprrpngd ivgylvtcem
1681 aqgggpataf rvdgdspesr ltvpglsenv pykfkvqart tegfgpereg iitiesqdgg
1741 pfpqlgsrag lfqhplqsey ssittthtsa tepflvdgpt lgaqhleagg sltrhvtqef
1801 vsrtlttsgt lsthmdqqff qt
```

Appendix 4: Comparing sequences of amino acid at 28-128 of β4 integrin subunit with protein sequences from *S. cerevisiae* database

YMR178W YMR178W SGDID:S0004790, Chr XIII from 618478-619302,

Length = 275

Score = 58 (25.5 bits), Expect = 1.3, P = 0.73

Identities = 17/57 (29%), Positives = 26/57 (45%)

```
Query:    14 VRVDKDCAYCTDEMFRDRRCNTQAELLAAGCQRESIVVMESSFQITEETQIDTTLRR 70
             V+V   C    DE+   +  +T +   A  C    I + E +    +ETQI  T+RR
Sbjct:     2 VKVTAACIIIGDEVLNGKVVDTNSTFFAKYCFDHGIQLKEIATIGDDETQIVDTVRR 58
```

YBR150C TBS1 SGDID:S0000354, Chr II from 544487-541203, reverse complement,

Score = 57 (25.1 bits), Expect = 1.4, Sum P(2) = 0.74

Identities = 11/34 (32%), Positives = 18/34 (52%)

```
Query:     1 RCKKA-PVKS-CTECVRVDKDCAYCTDEMFRDRR 32
             RC +  P+   C  C++ +KDC +   E  + RR
Sbjct:   116 RCTEIEPISGKCRNCIKYNKDCTFHFHEELKRRR 149
```

Score = 42 (19.8 bits), Expect = 1.4, Sum P(2) = 0.74

Identities = 15/40 (37%), Positives = 17/40 (42%)

```
Query:    52 MESSFQITEETQIDTT--LRRSQMSPQGLRVRLRPGEERH 89
             ME SF I  E  I     L+ S +        L PGEE H
Sbjct:   893 MEVSFNIFNEITIQDLNFLQFSSIPKLWENKTLEPGEEYH 932
```

YNL267W PIK1 SGDID:S0005211, Chr XIV from 140877-144077,

```
 Score = 59 (25.8 bits), Expect = 4.9, P = 0.992
 Identities = 18/58 (31%), Positives = 28/58 (48%)

Query:    44 CQR-ESIVVMESSFQITEETQIDTTLRRSQMSPQGLRVRLRPGEERHFELEVFEPLES
100
             CQ+  +    E  F I +  Q+  T+    M+ + L +RLR  E  HF L  F  L++
Sbjct:    55 CQKLATFPHSELQFYIPQLVQVLVTMETESMALEDLLLRLR-AENPHFALLTFWQLQA
111
```

YLR098C CHA4 SGDID:S0004088, Chr XII from 339474-337528, reverse complement,

```
 Score = 57 (25.1 bits), Expect = 5.0, P = 0.993
 Identities = 11/50 (22%), Positives = 24/50 (48%)

Query:     8 KSCTECVRVDKDCAYCTDEMFRDRRCNTQAELLAAGCQ--RESIVVMESS 55
             K C+ C++   +C +   ++   R   T  E L +  +  +E + ++ SS
Sbjct:    58 KPCSNCIKFRTECVFTQQDLRNKRYSTTYVEALQSQIRSLKEQLQILSSS 107
```

YDR272W GLO2 SGDID:S0002680, Chr IV from 1009004-1009828,

```
 Score = 52 (23.4 bits), Expect = 7.8, P = 0.9996
 Identities = 25/78 (32%), Positives = 28/78 (35%
Query: 11 TECVRVDKDCAYCTDEMFRDRRCNTQAELLAAGCQRESIVVMESSFQITEETQIDTTLR 69
          T C   D  C Y  D    D RC  T   L  AGC R      E    I     I  T+
Sbjct:118 TPCHTRDSICYYVKDPT-TDERCIFTGDTLFTAGCGRFFEGTGEE-MDIALNNSILETVG 175

Query:    70 RSQMSPQGLRVRLRPGEE 87
             R   S    + R+ PG E
Sbjct:   176 RQNWS----KTRVYPGHE 189
```

YGL116W CDC20 SGDID:S0003084, Chr VII from 289812-291644,

```
 Score = 55 (24.4 bits), Expect = 8.6, P = 0.9998
 Identities = 16/64 (25%), Positives = 32/64 (50%)

Query:38 ELLAAGCQRESIVVM---ESSFQITEETQI-DTTLRRSQMSPQGLRVRLRPGEERHFELE 93
         E++A G   E+ + +   E+ F++ E     +  +  SQ+SP G  +    G+E     +
Sbjct:494 EIVATGGNPENAISVYNYETKFKVAEVVHAHEARICCSQLSPDGTTLATVGGDENLKFYK 553

Query:94 VFEP 97
         +F+P
Sbjct:554 IFDP 557
```

YLR030W YLR030W SGDID:S0004020, Chr XII from 203291-204082,

```
 Score = 51 (23.0 bits), Expect = 9.8, P = 0.99995
 Identities = 11/30 (36%), Positives = 18/30 (60%)

Query:    65 DTTLRRSQMSPQGLRVRLRPGEERHFELEV 94
             +T+L  ++ S     V L+PGE+ H  LE+
Sbjct:   191 NTSLAENKRSSDSF-VSLKPGEDEHSPLEI 219
```

Hem12p [*Saccharomyces cerevisiae*]; gi|283290|pir||S23471 uroporphyrinogen decarboxylase (EC 4.1.1.37) - yeast (*Saccharomyces cerevisiae*); gi|3767|emb|CAA45253.1|Uroporphyrinogen decarboxylase [*Saccharomyces cerevisiae*]; gi|416894|sp|P32347|DCUP_YEAST Uroporphyrinogen decarboxylase URO-D) (UPD); gi|4776|emb|CAA79514.1| Uroporphyrinogen decarboxylase [*Saccharomyces cerevisiae*]; gi|798900|emb|CAA89078.1| Hem12p [*Saccharomyces cerevisiae*]

```
        Length = 362
```

```
 Score = 60 (26.2 bits), Expect = 2.5, P = 0.91
 Identities = 15/38 (39%), Positives = 22/38 (57%)

Query:    75 PQ--GLRVRLRPGEERHFELEVFEPLESPVDLYILMDF 110
             PQ  G+RV +  G+  HF     EPL +P DL  ++D+
Sbjct:    86 PQAMGMRVEMLEGKGPHFP----EPLRNPEDLQTVLDY 119
```

Appendix 5: Sequences of *P. sojae* compared with sequences from different eukaryotic organisms

Putative tyrosine kinase-like protein [*Dictyostelium discoideum*]

```
Score = 94.7 bits (234),  Expect = 1e-18
Identities = 52/128 (40%), Positives = 70/128 (54%), Gaps = 10/128 (7%)
Frame = +2

Query  11   WGAKVSDFGLSREKSVDETMSVTGTPLWLPPEMIRGERYTEKADVYSFGIVLAELDTRKI
190
            W  KV+DFGLS  +    TM+  GTP W  PE++R +RYTEKADVYSFGI+L E  TR+
Sbjct  526  WKVKVADFGLSTIEQQGATMTACGTPCWTSPEVLRSQRYTEKADVYSFGIILWECATRQD
585

Query  191  PYHDIKAKGARNKKVSGSTLMHMVAYENLRPSLSKNCMDSVRDLYKRCTSDDQSVRPTFE
370
            PY  I              ++  V  E +RP   K        L K C +++ S RPT E
Sbjct  586  PYFGIPP----------FQVIFAVGREGMRPPTPKYGPPKYIQLLKDCLNENPSQRPTME
635

Query  371  EIVQFLEN  394
            + ++ LE+
Sbjct  636  QCLEILES  643
```

***C. elegans* KIN-24 protein (corresponding sequence K07F5.4) [*Caenorhabditis elegans*]**

Hypothetical protein K07F5.4 - *Caenorhabditis elegans*

Tyrosine kinase family member (kin-24) [*Caenorhabditis elegans*]

```
Length=517
Score = 66.6 bits (161),  Expect = 8e-10
Identities = 37/95 (38%), Positives = 58/95 (61%), Gaps = 5/95 (5%)

Query  139  LFLEAAEGLRYLHEEIKLVHSNLKSDNILVTGDSRVKLTDFGLGVLALQDQAVQDKKFQE
318
            L ++AA G+RYLH++ K VH +L S N L++ D  VK+ DFGL     +DQ    +  +E
Sbjct  262  LLIDAARGMRYLHDK-KCVHRDLASRNCLISFDGIVKIADFGLSKTLEKDQKAFKEALKE
320

Query  319  --LGWRAPNCVQKKPFRRPSFQDDVYSFGLCVLDV  417
              L W AP C+Q++     S + DV++FG+ + +V

Sbjct  321  APLAWLAPECIQRE--SEFSTKTDVWAFGVVIFEV  353
```

Tyrosine-protein kinase Srms

Src-related kinase lacking C-terminal regulatory tyrosine and N-terminal myristylation sites [*Homo sapiens*]

```
          Length=488

Score = 59.3 bits (142),  Expect = 7e-08
Identities = 34/96 (35%), Positives = 50/96 (52%), Gaps = 2/96 (2%)
Frame = -2

Query  386  WTAPEVLDGRQYTPKADIYSFGVLLAQLATYECTSAEHSVMDDTEVPMLNNHKGSASGDA
207
            WTAPE  + R ++ K+D++SFGVLL ++ TY     E     +T   ++  ++      A
Sbjct  392  WTAPEAANYRVFSQKSDVWSFGVLLHEVFTYGQCPYEGMTNHETLQQIMRGYR--LPRPA
449

Query  206  EAPTPVRLLMFRCQAFQPEGRPTADELLEELHQIER  99
              P  V +LM  C    PE RP+   L E+LH I R
Sbjct  450  ACPAEVYVLMLECWRSSPEERPSFATLREKLHAIHR  485
```

Src-related kinase lacking C-terminal regulatory tyrosine and N-terminal myristylation sites (predicted) [*Rattus norvegicus*]

```
    Length=507

Score = 57.0 bits (136),  Expect = 3e-07
Identities = 34/98 (34%), Positives = 50/98 (51%), Gaps = 2/98 (2%)
Frame = -2

Query  386  WTAPEVLDGRQYTPKADIYSFGVLLAQLATYECTSAEHSVMDDTEVPMLNNHKGSASGDA
207
            WTAPE  + R ++ K+D++SFG+LL ++ TY     E     +T   +   ++      A
Sbjct  407  WTAPEAANYRVFSQKSDVWSFGILLYEVFTYGQCPYEGMTNHETLQQISRGYR--LPRPA
464

Query  206  EAPTPVRLLMFRCQAFQPEGRPTADELLEELHQIEREL  93
              P  V +LM  C    PE RPT   L E+L+ I R L
Sbjct  465  VCPAEVYMLMVECWKGSPEERPTFATLREKLNAINRRL  502
```

Tyrosine-specific protein kinase [*Mus musculus*]

```
          Length=496


Score = 55.8 bits (133),  Expect = 7e-07
Identities = 34/98 (34%), Positives = 50/98 (51%), Gaps = 2/98 (2%)
Frame = -2

Query  386  WTAPEVLDGRQYTPKADIYSFGVLLAQLATYECTSAEHSVMDDTEVPMLNNHKGSASGDA
207
            WTAPE  + R ++ K+D++SFG+LL ++ TY     E     +T   +   ++      A
Sbjct  396  WTAPEAANYRVFSQKSDVWSFGILLYEVFTYGQCPYEGMTNHETLQQISRGYR--LPRPA
453

Query  206  EAPTPVRLLMFRCQAFQPEGRPTADELLEELHQIEREL  93
              P  V +LM  C    PE RPT   L E+L+ I R L
Sbjct  454  VCPAEVYVLMVECWKGSPEERPTFAILREKLNAINRRL  491
```